Investigating the cellular functions of casein kinase 1 δ and ε through identification of interacting partners and substrates

by

Rodrigo Guillen

Dissertation

Submitted to the Faculty of the

Graduate School of Vanderbilt University

in partial fulfillment of the requirements

for the degree of

DOCTOR OF PHILOSOPHY

in

Cell and Developmental Biology

June 30, 2020

Nashville, Tennessee

Approved:

Kathleen L. Gould, Ph.D.

William P. Tansey, Ph.D.

David K. Cortez, Ph.D.

Marija Zanic, Ph.D.

Acknowledgements

First and foremost, thanks to my mentor, Dr. Kathy Gould, who struck a perfect balance of direct guidance and the freedom to pursue my own interests throughout my graduate career. I am grateful to Kathy for helping me develop my communication skills and emphasized the importance of story-telling in science. Beyond bench work and communication, Kathy was always supportive of my career development, giving me the opportunity to attend several extracurricular courses. Thank you!

I had the opportunity to meet many great people during my time in the Gould lab. A special thanks to MariaSanta Mangione and Christine Jones, the original members of 'OCD bay'. Thank you to Team CK1 members, Zac Elmore, Sierra Cullati and Janel Beckley. Lastly, thank you to all the other undergraduate, graduate and post-doctoral researchers that made the Gould lab a wonderful place to work – Chloe Snider, Alaina Willet, Nathan McDonald, Jun-Song Chen, Lipin Ren, Gabriele Juskeviciute, Macrin Wos, Rahil Bhattacharjee, Tony Rossi, Jitinder Singh Bisht, Josh Evers, Emma Stevens, and Eric Zhang.

I am grateful to my friends and family for their past and ongoing support. My parents taught me at a young age to pursue and enjoy learning. My siblings always supported me and were wonderful role models. Thank you to Christy King, my wife, for keeping me sane and giving me perspective throughout graduate school!

This work was supported by NIH grant Vanderbilt Initiative for Maximizing Student Diversity (R25 GM062459) and NIH grants R01 GM112989 and R35 GM131799 to K.L.G. Some experiments were aided with support from The VUMC Flow Cytometry Shared Resource (Supported by the Vanderbilt Ingram Cancer Center (P30 CA68485) and the Vanderbilt Digestive Disease Research Center (DK058404)).

Table of Contents

LIST OF TABLES

LIST OF FIGURES

Figure Page

LIST OF ABBREVIATIONS

CK1	Casein kinase 1
CDK	Cyclin-dependent kinase
mNG	monomeric NeonGreen
mVM	monomeric Venus-MAP
MAP	Multi-Affinity Protein
IDR	Intrinsically disordered region
GEF	Guanine nucleotide exchange factor
GAP	GTPase activating protein
MS	Mass spectrometry
LC-MS/MS	Liquid chromatography tandem mass spectrometry
Tfn	Transferrin
EGFR	Epidermal growth factor
NSAF	Normalized spectral abundance factor
CME	Clathrin-mediated endocytosis
iTRAQ	isobaric tagging for relative and absolute quantitation

CHAPTER 1

INTRODUCTION

Casein kinase 1 in the protein kinase superfamily tree

Cell viability requires regulated stimuli-responsive signaling pathways. Internal signaling pathways are the bases for biological processes necessary for cell viability. For instance, transitioning between cell-cycle stages or communication from the cell cortex to the nucleus in response to receptor-ligand signaling are dependent on different combinations of signaling pathways. Post-translational modifications (PTMs) modulate protein behavior along a signaling pathway [3-5]. Protein phosphorylation is an example of a reversible PTM in which the gamma phosphate of ATP is transferred enzymatically to a protein (Figure 1-1). The consequence of this type of PTM is a local electrostatic change on the surface of a protein, which can affect protein stability, localization, activity and protein-protein interactions [4, 6-8]. The importance of protein phosphorylation is exemplified by a recent report suggesting that nearly three-quarters of the human proteome is phosphorylated [9]. Deregulated protein phosphorylation can have detrimental effects on cells, potentially leading to cell death or tumorigenesis [10].

A phosphoryl group can be added to nine different amino acids: serine, threonine, tyrosine, histidine, lysine, arginine, asparagine, glutamine and cysteine [11]. The first residues discovered to be phosphorylated were serine and threonine, in 1932 and 1952, respectively [12, 13]. Their discovery partly benefitted from the methodology used to identify phosphorylated residues, which used partial acid hydrolysis. Serine and threonine are significantly acid stable while tyrosine is less so, and the other nine residues are not [14]. It took nearly thirty years to isolate phospho-tyrosine, which partially required a stroke of luck by way of aging buffers [15-17]. The buffers, which became more acidic, were favorable for separating phospho-serine, phospho-threonine, and phospho-tyrosine (pSer, pThr, pTyr). When referring to protein phosphorylation, it is

common to focus on pSer, pThr, pTyr because they have been the most highly characterized; however, phospho-histidine was discovered in the early 1960s and is reemerging as an avenue of research. Phospho-histidines (pHis), unlike pSer, pThr, pTyr, are acid-labile, making them very unlikely to withstand low-pH experimental conditions [18]. Interest in the prevalence of pHis, and the kinases and phosphatases responsible for its regulation, has reemerged with the development of an important tool that has assisted investigations into pSer, pThr, and pTyr: a pHis-specific antibody [19-21]. This tool has helped identify pHis proteins and some of the kinases responsible for pHis regulation [11].

Protein kinases are enzymes that catalyze the transfer of phosphate from an ATP molecule to their substrate (Figure 1-1). The human kinase superfamily of serine, threonine and tyrosine proteins kinases consists of over 500 members across 13 families, and encompasses 1.7% of the human genome [10]. It is of little surprise that nearly half of kinases are mapped to disease loci or cancer amplicons [10], and are major drug targets in combating human disease [22, 23].

Serine, threonine and tyrosine protein kinases share extensive sequence similarities within their catalytic domains. In fact, sequence conservation among kinases was used to develop oligonucleotide probes to identify protein kinases from cDNA libraries expressed in bacteria [24]. The catalytic domain can divided into eleven conserved subdomains interspersed by regions of low sequence conservation [25]. Subdomain I has a Gly-rich loop (G-X-G-X-X-G), while subdomain II contains an invariant lysine (in cAPK-α: Lys_{72}; Figure 1-1), both of which directly participate in binding and orientating ATP for successful phosphate transfer. [26]. Subdomain VI has two invariant residues (Asp_{166} and Asn_{171} in cAPK-α; Figure 1-1), while subdomain VII contains a highly conserved Asp-Phe-Gly triplet (Asp_{184}-Phe_{185}-$Glyc_{186}$ in cAPK-α). The Asp residues in subdomains VI and VII interact with ATP phosphate groups through Mg^{2+} salt bridges and function in phosphotransfer from ATP to a substrate. Subdomain VIII contains a highly conserved Ala-Pro-Glu triplet that assists in catalytic activity by stabilizing the structure of the kinase domain [27]. In proximity to subdomain VIII and the catalytic cleft is a conserved threonine important for catalytic activity. This threonine

is present in a loop (Th197 and Thr 161 in cAPK-α and Cdc2, respectively) outside of the catalytic cleft, and is referred to as the 'T-loop' [27]. T-loop phosphorylation significantly increases kinase activity *in vitro* and *in vivo* [28-30].

The eleven domains within the roughly 300 amino acids that constitute all Ser/Tthr/Tyr protein kinase catalytic domains are organized into a canonical structure consisting of an N-terminal lobe and a C-terminal lobe. The two lobes are composed primarily of beta-strands and alpha-helices, respectively (Figure 1-2). the catalytic cleft is located between the N- and C-lobes (Figure 1-2). Substrate access to the catalytic cleft is dependent on conformational changes in protein kinases that may arise from T-loop phosphorylation, binding to accessory proteins and target specificity. Some protein kinases require cyclic nucleotides such as cAMP for activity, other are activated by calcium and phospholipids; still others by calcium and calmodulin and many require additional subunits. For example, certain cyclin-dependent kinases require a transiently available subunit (a cyclin) for activity at specific times during the cell cycle.

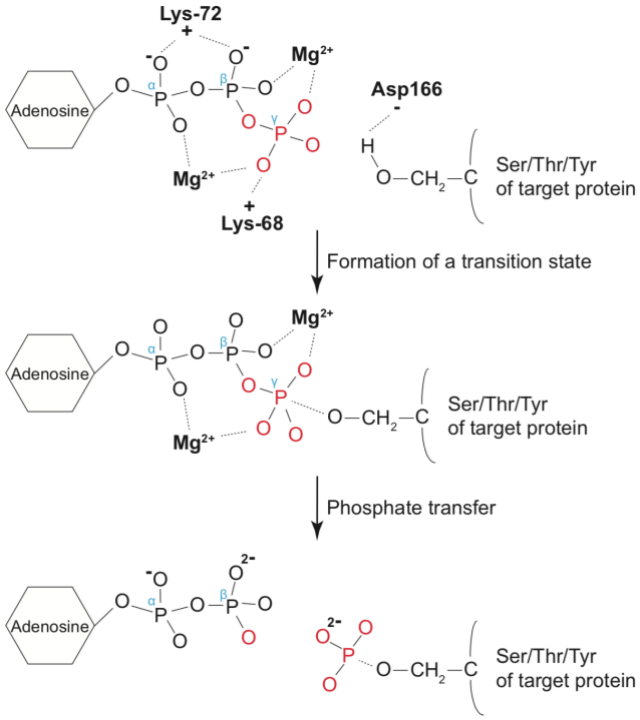

Figure 1-1: Phosphate transfer in a kinase reaction. Bold text refers to important ions and charged residues in the kinase domain. Charged residues relate to cAPK-α as an example. α, β, and γ relate to the position of the phosphate in the ATP molecule.

Sequence variations in Subdomains VI and VIII are important for determining the amino acid specificity of protein kinases. For serine/threonine kinases, a commonly found sequence between the invariant Asp and Asn residues in subdomain VI is Asp-Leu-Lys-Pro-Flu-Asn. This is in contrast to tyrosine kinases, which commonly have Asp-Leu-Arg-Ala-Ala-Asn or Asp-Leu-Ala-Ala-Arg-Asn. The amino-terminal side of Subdomain VIII has a conserved sequence in tyrosine kinases that is Pro-Ile/Val-

Lys/Arg-Trp-Thr/Met-Ala-Pro-Glu. This region is less conserved for serine/threonine kinases, but is often Gly-Thr-Ser-X-X-Try/Phe-X-Ala-Pro-Glu. These sequence preferences support conformations for transferring phosphate onto the appropriate side-chain residue.

As the number of identified and sequenced protein kinases increased, new sequence similarities emerged. Based on increased similarities, protein kinases are clustered into eight families [25, 31]. The topic of my dissertation work is a subset of the serine/threonine casein kinase 1 (CK1) family. CK1 enzymes were first identified based on their ability to phosphorylate the negatively charged substrate, casein, in vitro [32]. CK1 family members have a preference for substrates that contain a pre-phosphorylated or a cluster of negatively charged residues in the -3 position of the target serine or threonine [33, 34]. However, this preference is by no means absolute and there are examples of CK1 phosphorylating substrates that have not been primed or vary from the canonical motif, such as phosphorylation by CK1δ of p53 on Ser20 [35-37]. The only other large family of kinases that shares a preference for negatively charged substrates was named CK2. [38, 39]. However, CK1 and CK2 protein kinases form distinct families within the kinase superfamily and have limited sequence identity, significant structural differences, and non-overlapping substrates and functions.

The catalytic domain of CK1 enzymes is at their N-terminus; they all have a C-terminal tail extending from the catalytic domain that is predicted to be unstructured [25]. Only CK1 catalytic domain structures have been determined. The majority of the crystal structures are in complex with newly designed small molecules [40-46].

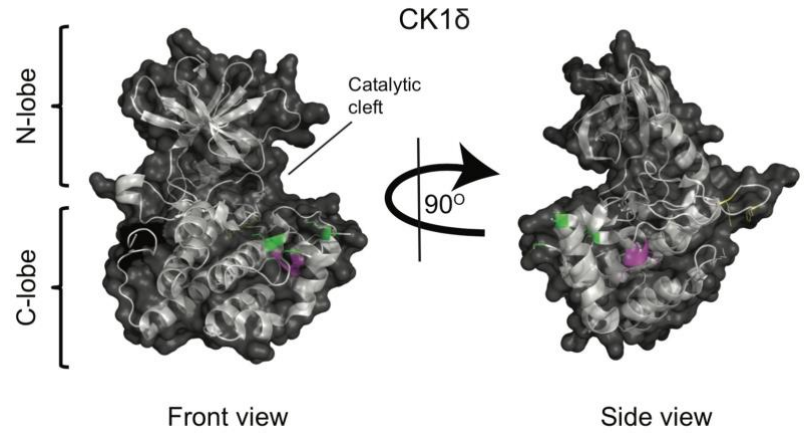

Figure 1-2: Crystal structure of CK1δ (amino acids 1-294) kinase domain. PDB ID number 5IH4 was used to visualize structure in Pymol. S-I-N residues in the C-lobe are in magenta. Residues corresponding to first anion binding site, Glyc215, Arg178, and Lys224, are in green. Residues corresponding to the second anion binding site, Arg157, His162, and Lys263, are in yellow.

However, there are two apo enzyme structures, one each of the mammalian CK1δ and CK1ε proteins [46-48].

The crystal structure of a truncated mammalian CK1 family member, CK1δ (amino acids 1-317), provided information about the kinase domain and C-terminal extension of CK1 enzymes. CK1δ was crystalized in the presence and absence of a phosphate analog, tungstate. The CK1δ structure was solved by using the structure of the *Schizosaccharomyces pombe* (*S. pombe*) CK1 family member Cki1∆298 as a search model [45, 48]. The resolved structures revealed four interesting characteristics about CK1 enzymes. First, the last 18 amino acids (aa 299-317) are unstructured. This led to the hypothesis that the entire C-terminus is unstructured, making it difficult to crystallize the full-length protein. Second, the substrate binding loop (amino acids 217-223) had poor electron density, suggesting it is a dynamic, flexible loop. The dynamic nature of this loop is of particular interest because it suggests the loop can take several conformations. If true, then the flexible loop could have an effect on kinase activity towards substrates. Third, there was high occupancy of a tungstate anion near the kinase active site, creating hydrogen bond interactions with Gly215, Arg178 and Lys224 (Figure 1-2, green residues). Importantly, a similar anion binding site was identified in the Cki1∆298 structure, suggesting the hydrogen bond is a common feature among CK1 family members [45]. This led to the hypothesis that the anion binding site relates to CK1's substrate recognition motif. Lastly, a secondary tungstate-binding site was identified, but with a lower occupancy rate. The secondary binding site interacts with Arg157, His162, and Lys263 (Figure 1-2, yellow residues) [48]. These sites are conserved among CK1 family members and are on the opposite side to the active site of the kinase. The presence of a tungstate ion in this location suggests that a phosphorylated residue binds to the back of the kinase domain. If true, this would also suggest that phosphate binding to the back of the kinase domain occurs in a more dynamic manner than the phosphate-binding at the substrate binding region. The two anion binding sites may represent important regulatory regions in the kinase domain of CK1.

A characteristic of CK1 enzymes that distinguish them from other protein kinase is the presence of a Ser-Ile/Val-Asn triplet in place of the canonical Asp-Pro-Glu sequence in subdomain VIII (Figure 1-2, magenta residues). The CK1 triplet exhibits the same conformation as the canonical triplet; however, with increased stability because of a hydrogen bond formed between the asparagine of the triplet and Arg198 and Asp199 [45]. This feature of the C-lobe was consistent among the many structures of CK1 enzymes that exist, whether bound or unbound to small molecules or substrates [40-46]. Whether or why there is a benefit to increased stability is unclear.

CK1 enzymes are active when produced in bacteria. Thus, they do not require additional subunits, or activation by small molecules or post-translational modifications. Unlike many kinases including cyclin-dependent kinase 2, CK1 does not require T-loop phosphorylation to become activated [27]. Taken together, these characteristics of CK1 have led to a popular idea that CK1 enzymes are constitutively active, if a primed substrate is available [49-51]. However, over the decades since their initial discovery, PTMs of CK1's non-catalytic C-terminal tail have emerged as regulators of CK1 activity.

The C-terminal domains of CK1 enzymes vary in length from 65-123 amino acids and sequence composition [52]. The C-terminal tail offers functional variability to family members through multiple mechanisms. First, sequence variability in the C-terminus differentiates between soluble (CK1α, CK1δ, CK1ε) and membrane-bound (CK1γ1-3) family members, and thus a way to determine their general localization patterns. The membrane-bound family members contain a prenylation motif in their C-terminus that is responsible for sequestering them to membranes [53-56]. Whether the C-terminus also influences the localization of soluble family members is an area of current investigation.

The C-termini of soluble CK1 enzymes are highly phosphorylated. The phosphorylation state of the tail was observed by comparing mock and phosphatase-treated full length protein with a C-terminal truncation [57, 58]. The difference in mobility shift on a polyacrylamide gel between untreated and phosphatase-treated recombinant protein is significantly less for C-terminal truncation mutants than for the full-length protein [57]. Further, phosphatase inhibitor treatment of cell lysates results in reduced mobility of soluble CK1 enzymes on polyacrylamide gels, indicating an increased

phosphorylation in cells [59]. This affect was not observed when the CK1 enzyme was mutated to inactivate the kinase, suggesting a cycle of *in vivo* autophosphorylation followed by phosphatase-dependent dephosphorylation [59]. In addition to auto-phosphorylation, the C-terminal tails are hypothesized to be phosphorylated by other kinases [57-59], offering another potential layer of regulation.

C-terminal phosphorylation inhibits CK1 kinase activity. The kinase domain alone, as well as full-length protein pre-treated with phosphatase, are more active towards *in vitro* substrates than their phosphorylated counterparts [57-61]. Further, partial proteolysis of the full-length enzyme that results in a loss of the C-terminal tail increases CK1's activity similar to phosphatase treatment. The similarity in activity between the two types of CK1 truncations suggests that there is a physical association between the phosphorylated C-terminal domain and the catalytic domain [60]. The second anion binding site observed in the CK1δ structure may pertain to binding a phosphorylated tail. Altogether, these studies led to a model in which a phosphorylated C-terminal tail binds to the kinase domain and blocks substrates from entering the active site, thus inhibiting CK1 activity [60]. Although this model has never been directly tested, it does stand in contrast to the view that CK1 is constitutively active. Further investigations are necessary to determine how activity of these enzymes are regulated in different biological contexts.

The focus of my thesis project has been to evaluate the binding partners and substrates of two of the three soluble mammalian CK1 enzymes, CK1δ and CK1ε, with a goal of determining whether they function in cell division. CK1δ and CK1ε have 98% identity in their kinase domain and 53% sequence identity in their C-terminus, making them the most closely related CK1 family members. In the next section of my introduction, I will describe what is known about the functional orthologs of CK1δ and CK1ε in the yeasts, *Saccharomyces cerevisiae* (*S. cerevisiae)* and *S. pombe*, that served as impetus for my studies and informed my approaches. This will be followed by a section introducing CK1δ and CK1ε, highlighting similarities and differences to their yeast orthologs.

S. cerevisiae Hrr25

Hrr25 (HO and radiation repair 25) is the single soluble *S. cerevisiae* CK1 enzyme. Hrr25 is considered to be a functional ortholog of CK1δ and CK1ε because its function can be compensated by the expression of human CK1ε, but not CK1α [62]. The *hrr25-1* mutant, which contains a transposon in the middle of the open reading frame of *hrr25*, was identified in a screen for mutants sensitive to X-rays [63], and subsequently to expression of an endonuclease or exposure to radiomimetic alkylating agents. The *hrr25-1* mutant strain exhibited a growth defect, were enlarged, and contained a primarily 2N DNA content suggesting a delay in passing through G_2- and M-phases of the cell cycle [63, 64]. A *hrr25Δ* mutant strain exhibited the same phenotypes as *hrr25-1*. These phenotypes could only be rescued an active Hrr25 enzyme [63].

There is limited information on why Hrr25 deficient cells are sensitive to DNA damage. However, there is evidence that Hrr25 positively affects transcriptional regulation of genes involved in DNA damage repair and its nuclear localization has Hrr25 in the right location to participate in transcriptional control. Hrr25 and the transcriptional co-activator Swi6 co-immunoprecipitate, and Hrr25 phosphorylates Swi6 *in vitro*. [65]. Swi6 forms two separate complexes. A complex with Swi4 activates transcription of genes necessary for transitioning from G_1-phase to S-phase. A different complex is formed with Mbp1 to transcribe proteins involved in DNA replication and DNA-damage repair [66, 67]. *swi6*Δ mutants are sensitive to DNA-damaging agents to a similar degree as *hrr25Δ* mutants. Additionally, both mutants (*swi6*Δ and *hrr25Δ*) have reduced gene expression of the small subunit of ribosome reductase (RNR) 2 & 3 [65]. Positively affecting RNR2 & 3 protein levels is consistent with a role DNA-damage repair because RNR2 & 3 expression increases upon activation of the DNA-damage checkpoint [68, 69]. Oddly, loss of Swi4, but not Mbp1, reduces RNR transcription [65], which is inconsistent with the reported roles of these Swi6-partners on gene expression. Further, overexpression of Swi4 rescued the reduced expression of RNR2 & 3 associated with loss of Hrr25 or Swi6. These results suggest a mechanism in which Swi6 phosphorylation by Hrr25 acts upstream of the Swi6/Swi4 transcriptional regulation of RNR genes. Whether Swi6 phosphorylation by Hrr25 affects Swi6/Swi4

complex formation and function remains to be determined. It seems unlikely that Swi6 is the only substrate of Hrr25 involved in DNA damage repair. It is also unclear if the functional relationship between Hrr25 and Swi6 directly or indirectly mediates DNA-damage repair. One possibility is that that Hrr25 phosphorylates Swi6 to mediate chromosome remodeling, allowing the DNA-damage-repair machinery to function properly. A more comprehensive study searching for Hrr25 substrates after treatment with DNA damaging agents would be informative in establishing its mode(s) of action in DNA metabolism.

A second function of Hrr25 is in the control of protein trafficking at various different locations. First, Hrr25 phosphorylates the vesicle-coat protein COPII at sites of macroautophagy [70], which depends on Hrr25's interaction with the Rab1 ortholog Ypt1. Second, Hrr25 localizes to the Golgi apparatus, where it co-localizes with early (Vrg4) and late (Sec7) Golgi markers to promote vesicle trafficking [71]. Hrr25 affects ER-to-Golgi vesicle trafficking by phosphorylating the coat protein Sec23p at the Golgi, ultimately promoting membrane fusion [71]. Lastly, Hrr25 is one of the initial proteins recruited to sites of clathrin-dependent endocytosis (CME) [72]. Hrr25 helps initiate endocytosis through its interaction with and phosphorylation of Ede1, the same protein that is partially responsible for Hrr25's localization to the site of cell division [72, 73]. The loss of Ede1 phosphorylation by Hrr25 results in a decrease in endocytic sites. Several other proteins involved throughout the many steps of endocytosis were tested in vitro to see if they also could be phosphorylated by Hrr25 and may be additional in vivo substrates [72]. Indeed, the broad localization pattern of Hrr25 across several classes of vesicles provides it the opportunity to affect trafficking at multiple points of protein trafficking.

Hrr25 localizes to two mitotic signaling platforms, the cell division site and the spindle pole body (SPB), which is the yeast equivalent of the mammalian centrosome. The division site is where an acto-myosin-based cytokinetic ring is formed for the purpose of physically divide the cell after chromosome segregation is complete. Localization of Hrr25 to the site of cell division requires synergy between Ede1 and

Cyk3, a mediator of cytokinesis [74-79]. What Hrr25 does at the cell division site is currently unknown.

Similar to other protein kinases involved in coordinating chromosome segregation and cytokinesis, Hrr25 localizes to the SPB. (Figure 1-2) [73, 80]. The SPB is a platform for the formation of the mitotic spindle, which is nucleated by the γ-tubulin ring complex (γ-TuRC). The *S. cerevisiae* γ-TuRC consists of fewer subunits than in higher eukaryotes, just two molecules of γ-tubulin and two γ-tubulin complex proteins (Spc97 and 98), and is termed the γ-tubulin small complex (γ-TuSC) [81, 82]. The γ-TuSC is composed of the *S. cerevisiae* γ-tubulin, Tub4, and two accessory proteins, Spc97 and Spc98. SPB localization of Spc97 and Spc98 is dependent on Tub4 [82]. At the SPB, Hrr25 interacts with and phosphorylates the Tub4 [73] on five residues localized on the interface of two γ-tubulin molecules. Mutating the five Hrr25-dependent phosphosites to alanine or phenylalanine (Tub4-5AP) led to loss of Spc97 and 98 from the SPB. Further, the *tub4-5AP* mutant displayed elongated and fragmented mitotic spindles [73]. Thus, CK1-mediated phosphorylation is key to Tub4 function in microtubule nucleation. Again, a comprehensive analysis of Hrr25 substrates via phosphoproteomics may reveal additional important targets of this enzyme in SPB-organized processes.

Hrr25 also plays important roles in meiosis [63, 64, 83, 84]. Meiosis is characterized by two rounds of chromosomal segregation and cytokinesis after a single round of DNA duplication. In meiosis 1, homologous chromosomes are segregated while the sister chromatids remain together, and in meiosis 2, sister chromatids are then separated. Accurate meiosis I requires that the centromeres of both sister chromatids be directed towards a single pole, as opposed to being bi-oriented as in meiosis II. Mono-orientation is achieved by

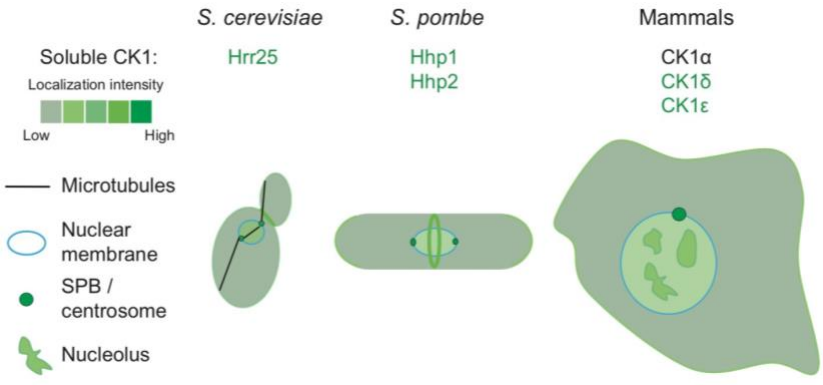

Figure 1-3: Localization pattern of soluble CK1 enzymes in *S. cerevisiae*, *S. pombe*, and mammals.

the monopolin complex (Mam1, Csm11 and Lrs4) that localizes to centromeres in meiosis I [85, 86]. Sister chromatids are also held together or “cohesed” by the cohesion complex, composed of Smc1, Smc3 and Rec8 subunits during meiosis. Cohesin is removed along chromosome arms in meiosis 1 and at the centromere in meiosis II, which is what allows the different forms of chromosomal segregation between the two meiotic stages. Removal of cohesion involves Rec8 proteolyis.

Hrr25 has several functions in yeast meiosis and hrr25 mutants fail at monopolar fusion, accurate chromosome segregation in meiosis II, and a failure to produce a spore membrane. First, Hrr25 appears to be a fourth integral component of the monopolin complex at centromeres in meiosis I. The N-lobe of the kinase is responsible for its association with Mam1, and is necessary for its localization to the centromere. Mam1 phosphorylation by Hrr25 promotes monopolar orientation of centromeres [64]. It is currently unknown if Hrr25 has other substrates located at the centromere in meiosis I.

Second, Hrr25, in coordination with Dbf4-dependent Cdc7 kinase, phosphorylates Rec8 along chromosome arms, promoting its cleavage during meiosis I [87]. Rec8 is also present at the centromere, but is protected from degradation by the shugoshin (Sgo)-protein phosphatase 2A (PP2A) complex [88] that counteracts Hrr25 activity towards Rec8. But whether it has additional substrates at the centromere is not known. Hrr25 appears diffuse across chromosomes, which is consistent with its role in Rec8 phosphorylation along chromosome arms [87].

Hrr25 also functions at the centromere during meiosis II where its phosphorylation of Rec8 is required for Rec8’s proteolysis by separase. Before separase can cleaves e Rec8, it must be activated by the APC_{Cdc20}.This event promotes sister chromatid separation. Failure to accomplish this goal explains why hrr25 mutant cells fail at this step of meiosis. Failure in meiosis II is hypothesized to cause failure of pro-spore membrane formation, resulting in loss of spore formation [64].

S. pombe Hhp1 and Hhp2

The *S. pombe* orthologs of Hrr25 (Hhp1 and Hhp2) were discovered on the basis of their sequence similarity to Hrr25 [89]. They were then each shown to rescue the growth defect and sensitivity to DNA-damaging agents of *hrr25*Δ cells, suggesting they

too are involved in DNA-damage repair [89]. Cell length phenotypes associated with loss of Hhp1 and Hhp2 are an indicator a role in DNA damage repair. *S. pombe* Cell length is an indicator of cell cycle staging. Cells increase in length during G2, reaching a length of ~12 μm [90]. Cells that affect entry into mitosis can stall in G2, resulting in elongated cells. For example, conditional depletion of Cdc25A, a positive mediator of Cdk1 activation, and thus mitotic entry, results in severely elongated cells[91] .

*hhp1*Δ mutant cells are elongated, and *hhp2*Δ are indistinguishable in length from wild-type. However, the double deletion mutant, *hhp1*Δ *hhp2*Δ, is more elongated than *hhp1Δ*, suggesting Hhp2 does contribute to the length phenotype and can perform some of the functions of Hhp1. *hhp1*Δ *hhp2*Δ cells are very slow growing, reminiscent of hhr25Δ, and are also temperature-sensitive [89]. Taken together, this indicates that Hhp1 and Hhp2 share largely overlapping, although not identical functions [89].

Hhp1/2 localization to the nucleus provides them with the opportunity to affect DNA-damage repair pathways. Hhp1/2 function redundantly in DNA damage repair resulting from UV and γ-ray exposure [89]. However, Hhp1/2 appear to have different responses to methylmethanosulfonate (MMS) treatment. *hhp1Δ* mutants, but not *hhp2Δ*, were sensitive to MMS, suggesting a role for Hhp1 in excision or recombination repair pathways. Furthermore, Hhp1/2 over-expression complement mutants that affect DNA repair and S-phase completion [92, 93]. Beyond the discovery and initial characterization of Hhp1/2, there have been no further publications directly investigating their role in DNA repair. Determining Hhp1/2 substrates in the process of DNA repair would advance our understanding of the similarities and differences between the enzymatic activity of these proteins.

Hhp1 and Hhp2 are enriched at the SPB [35, 61] where they directly interact with a SPB scaffolding protein, Ppc89, through a basic patch in the C-terminal lobe of their kinase domains (Figure 1-4) [61]. AT the SPB, these enzymes modulate the onset of cytokinesis, keeping this process coordinated with chromosome segregation.

In *S. pombe*, cytokinesis is triggered by the septation initiation network (SIN). The Plk1 ortholog, Plo1, is responsible for activation of SIN signaling [94]. Upon entry into mitosis, Plk1 is recruited to SPBs and binds Sid4, one of the two major scaffolding

proteins of the SIN [95]. Their interaction sets off a kinase cascade that leads to communication between the SPB and cytokinetic ring to coordinate chromosome segregation and cytokinesis. In the presence of a mitotic arrest resulting from depolymerization of the microtubule cytoskeleton, *S. pombe* deploy two parallel checkpoints. The spindle-assembly checkpoint, which monitors the attachment between chromosomes and microtubules, is mediated by the E3 ubiquitin ligase APC/C [96-101]. The second checkpoint consists of inactivation of the SIN by an E3 ubiquitin ligase Dma1 [102, 103]. Under microtubule stress, Dma1 is recruited to the SPB, where it ubiquitinates Sid4, which blocks Sid4-dependent recruitment of Plk1 [35, 95]. Sid4 phosphorylation is necessary for its interaction with Dma1. Hhp1/2 are responsible for initiating Dma1 recruitment by phosphorylating Sid4 on S275 and T278 [35]. Binding between Ppc89 and Hhp1/2 at the SPB places Hhp1/2 in proximity to Sid4, allowing for SIN signaling at the onset of microtubule stress. Failure to recruit Hhp1/2 to SPBs through the use of Ppc89-binding mutants results in failure to inhibit the [61].

It is unclear what drives Hhp1/2 localization to the nucleus and division site. Additionally, Hhp2 localizes to cell tips [61, 88]. Similar to the Elmore et. al. study, sequence and structural comparisons between Hhp2 and the membrane-localized CK1 family member Cki2 may shed light on surface residues responsible for their localization pattern. Loss of the palmitoylation sequence in Cki2 results in a strikingly similar localization pattern to Hhp2 [61]. The biggest difference in Cki2 being no SPB

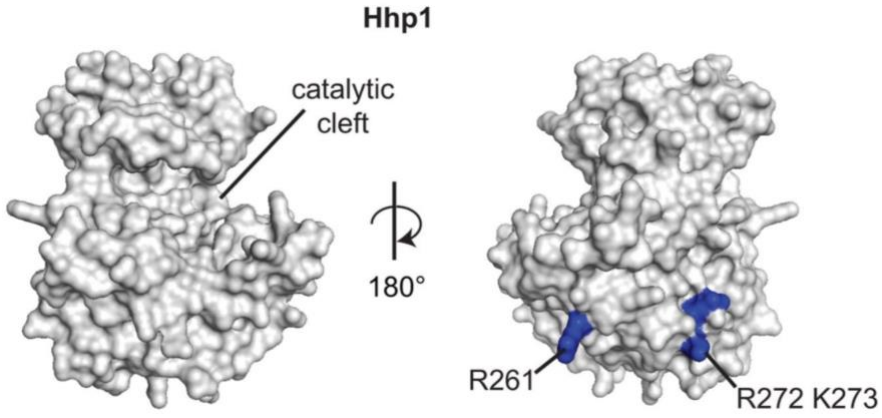

Figure 1-4: Basic patches in the C-lobe of Hhp1 are critical for SPB localization. Homology model of Hhp1 catalytic domain generated from Phyre$_2$ software and visualized with MacPymol. Residues critical for Hhp1 SPB localization are in blue. Adapted from *Elmore et. al.* MBoC (2018).

localization. Therefore, there must exist one or more patches in the kinase domain of CK1 family members that are responsible for their nuclear and tip localization.

Hhp1/2 are functionally similar to Hrr25 in meiosis. Both enzymes are involved in phosphorylating Rec8 for the purpose of targeting it to be cleaved by separase [88]. Similar to their role in DNA-damage repair, Hhp1 and Hhp2 have varying abilities to phosphorylate Rec8 and rescue Rec8-dependent growth retardation. Importantly, targeted over-expression of Hhp2 to centromeres results in Rec8 cleavage, even in the presence of Sgo-PP2A [88]. The data suggests that the balance between Hhp1/2 and Sgo-PP2A protein levels mediates Rec8 phosphorylation, and thus whether it is target for cleavage. Hhp1/2 have similar localization patterns in meiosis, although Hhp1 appears to have a more pronounced cytoplasmic localization than Hhp2 [88].

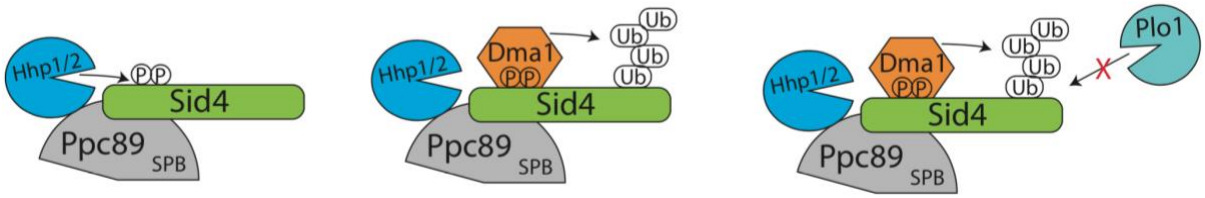

Figure 1-5: Cartoon representation of Hhp1/2 function in mitotic checkpoint signaling. Microtubule stress results in Hhp1/2 phosphorylation of Sid4, leading to Dma1 recruitment and ubiquitination of Sid4. Plo1 localization to the SPB is inhibited.

Mammalian CK1δ and CK1ε

The closely related CK1δ and CK1ε were first discovered from different tissues. The sequence of CK1δ, along with CK1α, CK1γ and the bovin-specific isoform CK1β, were first isolated from cDNA purified from bovine brain samples [104], and the 49 kDa protein was subsequently purified from rat testis [32]. Two years later, a human placental cDNA library was used to purify and characterize CK1ε [105]. Like *S. pombe* Hhp1/2, CK1δ and CK1ε (hereafter referred to as CK1δ/ε) but not the third soluble CK1 isoform, CK1α, rescue the growth defects of hrr25Δ cells, indicating that they are the functional orthologs of Hrr25 and of Hhp1/2 [89, 105]. Consistent with a role in proliferation, small molecular inhibitors with the greatest

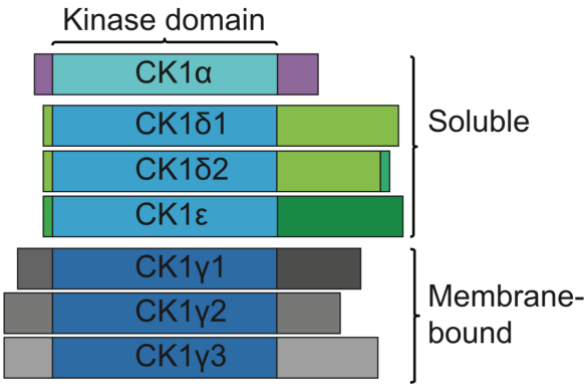

Figure 1-6. Casein kinase 1 protein family domain layouts. CK1 family members have 58-99% sequence identity in their kinase domain and. The greatest degree of sequence variability is in their N- and C-termini. Family members can be divided into soluble

degree of targeting specificity towards CK1δ/ε have an anti-proliferative effect on tissue cultured cells [106]. Further, CK1δ deletion in mice results in organismal death in the perinatal period of development [107]. CK1δ/ε share the majority of their substrates and interacting partners [108-111], which led to a hypothesis that they largely play redundant functions. Similar to their yeast orthologs, CK1δ/ε function in a variety of cellular processes, such as DNA-damage repair, ribosome biogenesis and cell cycle control [83, 112-115]. Further, CK1δ/ε function in tissue development pathways, such as Wnt and HIPPO signaling.

Like Hrr25, CK1δ/ε function in multiple signaling networks that impact gene transcription [49, 107, 111, 116, 117]. There are at least three pathways in which CK1δ/ε function. First, CK1δ/ε coordinates with GSK3 to phosphorylate the transcriptional coactivator YAP, which activates the HIPPO pathway [111]. Second, CK1δ/ε have multiple functions in the canonical Wnt pathway. In the absence of Wnt ligand, cytoplasmic β-catenin protein levels are kept low through association with a degradation complex. The complex consists of axin, adenomatous polyposis coli (APC), and the enzymes GSK3β and protein phosphatase 2A (PP2A). Phosphorylated β-catenin is recognized by the F-box protein β-TrCP, which ubiquitinates β-catenin, resulting in its degradation. These events are also mediated by axin and APC phosphorylation. In a simplified Wnt signaling model, extracellular Wnt ligand binds to a receptor complex composed of Frizzled (Fz), disheveled (Dvl) and lipoprotein receptor-related protein 5/6 (LRP5/6). Receptor-ligand binding results in its interaction with axin, thus relieving β-catenin from its association with the degradation complex. Intracellular levels of β-catenin are then stabilized, resulting in its cytoplasmic accumulation and nuclear import. Once in the nucleus, β-catenin associates with the TCF family of transcription factors, promoting expression of Wnt target genes [118]. Wnt signaling functions in embryonic development to establish cell polarity, dorsal axis formation, and tissue patterning [118-120].

CK1 family members have both positive and negative roles in Wnt signaling. In neurites, the centrosomal localization of CK1δ promotes Wnt3A-dependent neurite development [121], which is predicted to be dependent on phosphorylation of Dvl-2/3.

However, although CK1δ/ε are known to activates the Wnt pathway through phosphorylation of Dvl [122, 123], Dvl-2/3 phosphorylation at the centrosome has not been demonstrated. Increased expression of CK1ε and Dvl has a synergistic effect on axis duplication and expression of Wnt-activated genes in *Xenopus* embryos [116, 124]. CK1δ/ε are also believed to negatively regulate the pathway through phosphorylation of axin and β-catenin [125]; The exact roles of each of CK1δ/ε is not clearly understood due to overlapping substrates and the presence of multiple substrates within a given cellular process.

CK1δ/ε-dependent regulation of circadian rhythm is a third example of a role for these enzymes in transcription control. At the core of the circadian rhythm pathway are the transcriptional co-activators, CLOCK and BMAL1 [126]. CLOCK and BMAL1 form a heterodimer to bind DNA promotor regions and start transcription of a family of genes that include their regulators, Period (*Per1-3*) and Cryptochrome (*Cry1* and *Cry2*). Increased transcription and subsequent translation leads to an accumulation of these proteins in the cytoplasm, formation of heterodimers, and their association with CK1δ/ε [127-130]. CK1δ/ε-dependent phosphorylation promotes Per/Cry nuclear entry and cytoplasmic degradation, with the majority of the phosphosites present on the Per protein [117, 131-134]. Nuclear entry of Per/Cry results in their association with CLOCK/BMAL1 and repression of CLOCK/BMAL1-dependent gene expression [126, 135]. This results in the reduction of *Per* and *Cry* gene expression; thus, Per and Cry negatively regulate their own expression. The period length of a circadian rhythm depends on the duration of transcriptional and translational production of *Per* and *Cry* genes, and their negative feedback of CLOCK/BMAL1 activity. CK1δ/ε activity establishes period length of the circadian clock by mediating the timing of nuclear entry and degradation of Per and Cry proteins [107, 133]. Interestingly, the Tau mutation in CK1ε (R178C), loss of function mutation in CK1δ (T44A), or the loss of a single phosphosite in Per2 (S226G) results in reduced period length [136-139]. This is in contrast to targeted inactivation of CK1δ/ε or loss of the enzymes in mice, which results in an increase in the period length [107, 140-142]. These differences may be due to effects of inhibiting one CK1 enzyme versus both. Further, Per protein is more heavily

phosphorylated than its partner, Cry, suggesting a greater degree of complexity in phosphoregulation. The functional consequence of Per2 phosphorylation by CK1δ/ε has most closely been studied, where it CK1δ/ε are known to target multiple residues.

The precise mechanism of CK1δ/ε in multisite phosphorylation of Per2 has only recently been elucidated. CK1δ2, the shorter transcript of *CSNK1D*, and CK1ε are more efficient at priming Per2 for sequential, multi-site phosphorylation than CK1δ1 [143]. This is of particular importance because, aside from this most recent study, there is limited information on the differences between *CSNK1D* splice variants. Future work investigating the functional differences between CK1δ1, CK1δ2 and CK1ε in the circadian clock would be beneficial to our understanding of the CK1 family. Similar to their role in Wnt signaling, it is unclear whether CK1δ/ε localization, beyond the cytoplasm and nucleus, is important for its role in circadian rhythm control.

Although the roles of CK1δ/ε are best understood in the context of circadian rhythm and Wnt signaling, they are likely underappreciated or overlooked in other cellular contexts. For instance, CK1δ/ε localize to the acentriolar spindle pole and meiotic spindle in meiosis [144]. While CK1ε appears to associate with the meiotic spindle throughout the process, CK1δ concentrates on the meiotic spindle only during meiosis II, suggesting their localization is differentially regulated in meiosis. Their localization to spindles in meiosis may be a general characteristic of CK1δ/ε, given that CK1δ localizes to the mitotic spindle in somatic cells [145] and CK1ε localizes to kinetochore microtubules in prophase of mitosis [146], and both enzymes localize to the centrosome throughout the cell cycle. Their presence at meiotic and mitotic spindles and spindle-poles may signify a general function in microtubule or cytoskeletal dynamics, as well as their functional importance in cell cycle control.

CK1δ/ε function in cell-cycle regulation by controlling entry into mitosis [114]. Mitotic entry depends on a shift in balance of Cdk1 phosphorylation. Prior to G_2/M, Cdk1 is phosphorylated and thus deactivated by Wee1 kinase. Mitotic entry requires deactivation of the Cdk1 negative regulator Wee1[147-150]. Wee1 deactivation allows Cdc25 phosphatase to alleviate the inhibitory phosphorylation on Cdk1, while cyclin-activating kinase (CAK) phosphorylates and activates Cdk1 [151]. CK1δ promotes

Wee1 degradation at the G_2/M transition through direct phosphorylation of Wee1 [114]. CK1ε, on the other hand, affects entry into mitosis by promoting Cdk1 activation through phosphorylation of its positive regulator, Cdc25A. Because of these reported roles in mitotic entry, approaching investigations of CK1δ/ε function in mitosis with protein degradation is not ideal. These investigations were performed with the use of small molecular inhibitors that target CK1δ/ε and, therefore, it is unknown if both enzymes are able to phosphorylate Wee1 and Cdc25A. Instead, it would be better to start by determining and validating CK1δ/ε substrate phosphosites. This would be followed up by determining the importance of phosphorylation on the substrates' function, if one is known.

Summary

Because important cell-cycle proteins localize to and function at the centrosome [152-159], I hypothesized that the centrosomal localization of CK1δ/ε positioned them to have a significant role in cell-cycle signaling. The absence of tools to directly visualize CK1 enzymes *in vivo*, along with the development of CRISPR/Cas9 gene editing, motivated me to produce gene-edited cell lines to visualize endogenous CK1δ/ε. The construction of these lines, their characterization, and their use in identifying CK1δ/ε binding partners are described in Chapter II. In chapter III, I describe my efforts to identify CK1δ/ε substrates that relate to the localization of CK1δ/ε to centrosomes. Chapter IV describes future investigative routes that could be taken to understand each data-set (interactors and substrates) individually and in relation to each other.

Chapter 2

CRISPR-mediated gene targeting of CK1δ/ε leads to enhanced understanding of their role in endocytosis via phosphoregulation of GAPVD1

(Guillen, RX, Beckley, JR, Chen, JS, and Gould KL. (2020). *Sci Rep*. 2020 Apr 22; 10(1):6797. doi 10.1038/s41598-020-63669-2)

Introduction

The casein kinase 1 (CK1) family of serine/threonine protein kinases is evolutionarily conserved from yeast to human [160]. Characterized by a conserved catalytic domain, CK1 enzymes vary in the length and sequence of their non-catalytic C-termini [161]. CK1s typically recognize substrates with acidic motifs N-terminal to phosphorylation sites and tend to generate clusters of consecutive phosphoserines on their substrates [162].

Seven CK1 family members exist in humans (α, α2, δ, ε, γ1-3). CK1α, CK1α2, CK1δ and CK1ε are soluble, while CK1γ1-3 attach to cell membranes via C-terminal prenylation [53, 54, 163, 164]. Though the four soluble CK1s are highly related, CK1δ and CK1ε (hereafter referred to as CK1δ/ε) have the greatest degree of sequence identity within their kinase domains, function in similar biological pathways, and share interacting partners and substrates [108-110, 111 , 128, 146, 160, 165]. In particular, CK1δ/ε have well-characterized functions in circadian rhythm, ribosome biogenesis, and are involved in endocytosis [72, 83, 131, 160, 166]. However, the full complement of CK1δ/ε-interacting partners, substrates, and functions is still unknown.

In this study, we used CRISPR/Cas9 technology to individually tag CK1δ and CK1ε at their endogenous loci, allowing us to visualize their localization at endogenous protein levels, purify them, and identify associated proteins. Mass spectrometry (MS) analysis identified 181 interacting proteins, the vast majority of which co-purified with both enzymes. GAPVD1, a guanine nucleotide exchange factor (GEF) that is involved in endocytosis [167], was one of the most prevalent interacting partners. GAPVD1 contains a GAP-like domain and a GEF domain at its N- and C-termini, respectively,

that are separated by a predicted intrinsically disordered region (IDR). GAPVD1 is reported to function in insulin-stimulated glucose intake by acting as a GAP towards two small GTPases, TC10 [168] and Ras [167], and as a GEF towards Rab5A and Rab31 [168-170]. Disruption of the *Caenorhabditis elegans* GAPVD1 ortholog, RME-6, reduced the internalization of bovine serum albumin, while also reducing the volume of vesicles containing Rab5 [171]. Furthermore, knock-down of GAPVD1 from HeLa cells results in reduced internalization of transferrin (Tfn) and epidermal growth factor receptor (EGFR) [172], and the loss of the *Drosophila* ortholog of GAPVD1 results in decreased FITC-albumin intake in nephrocytes.[173]. Similar defects in nephrotic function were found in humans with homozygous GAPVD1 mutations [173]. An association between GAPVD1 and CK1δ/ε was identified previously, also through affinity purifications and MS analysis [128, 146], but the functional relevance of this interaction has not been previously reported.

Here, we demonstrate that GAPVD1 is not only associated with CK1δ/ε but is also a very good substrate, containing ~38 CK1 phosphosites within its IDR. Eliminating these phosphorylation sites inhibits GAVD1's endocytic function while a phosphomimetic version of GAPVD1 functions normally. Thus, our results indicate that one way in which CK1δ/ε modulates endocytosis is through phosphoregulation of GAPVD1.

Results

Characterization of CK1δ/ε gene-edited HEK293 cells

We used a single round of CRISPR/Cas9-mediated gene editing to individually tag endogenous CK1δ and CK1ε with the multifunctional Venus-MAP (VM) that contains a Flag-streptavidin-His_6 insert into a loop of the Venus protein [174] or mNeonGreen (mNG) [175] in HEK293 cells (Figure 2-1A, B). CSNK1E encodes a single CK1ε isoform, while CSNK1D encodes two CK1δ isoforms that differ in their C-terminus due to differential splicing [146]. The longer CK1δ form was tagged. In both cases, sequences encoding the tags were placed between the final coding exon and 3' UTR (Figure 2-1A). We verified that all alleles in the selected clones had been modified to produce CK1δ-VM, CK1ε-VM, CK1δ-mNG, or CK1ε-mNG by PCR amplifications of

1000 base-pair regions flanking the insert sites of VM or mNG (Figure 2-1B). Using antibodies that recognize CK1δ or CK1ε, we confirmed that the desired tagging had occurred by immunoblotting whole cell lysates (Figure 2-1C).

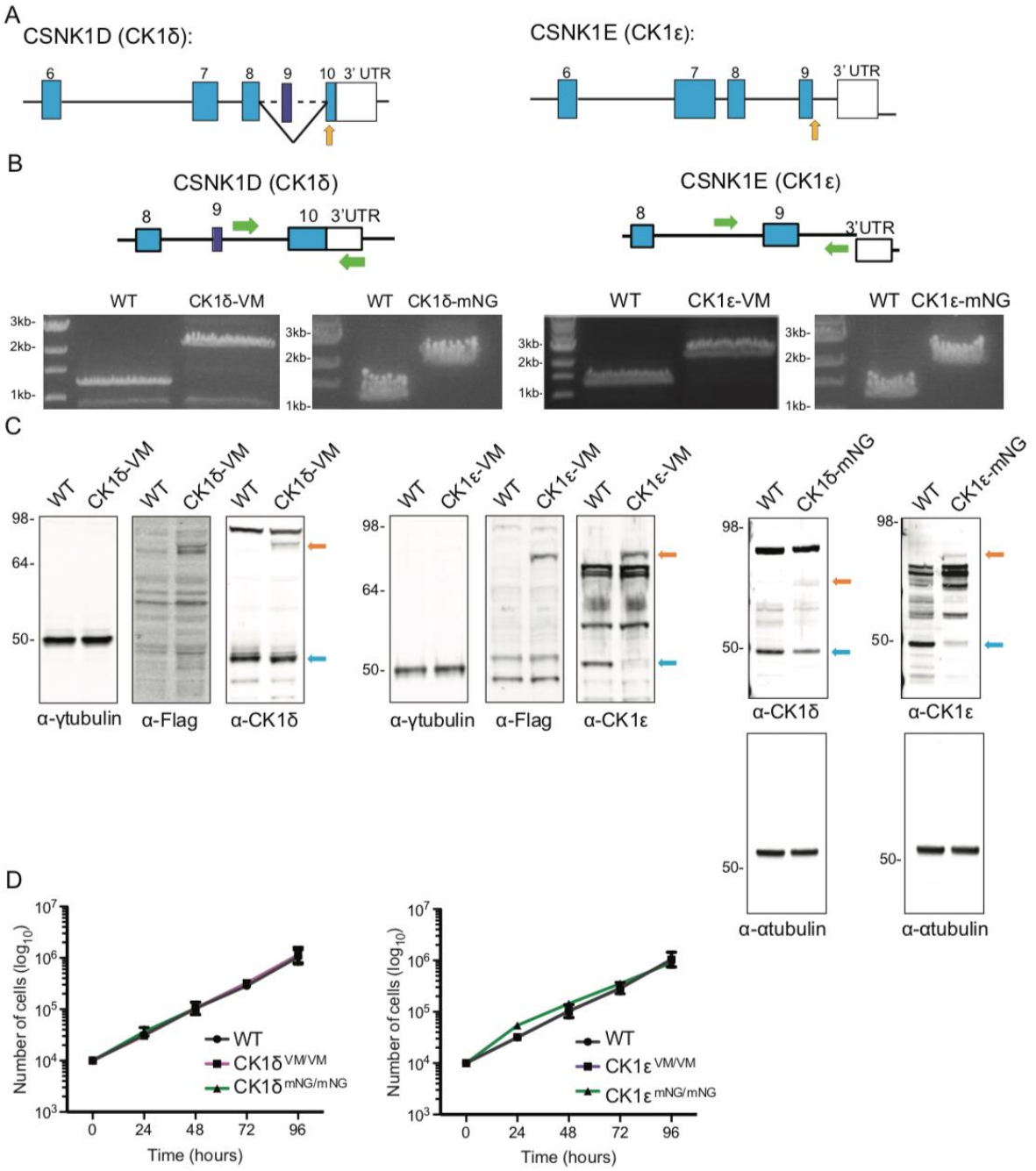

Figure 2-1: CRISPR gene-editing of CK1δ and CK1ε. (A) Cartoon representation of the 3'ends of the CK1δ (CSNK1D) and CK1ε (CSNK1E) genes. The orange arrows point to the positions where gRNAs were designed to target Cas9 for gene editing. Numbers correspond to exons. (B) PCR verification of cell lines with endogenously tagged
CK1δ/ε variants. Green arrows indicate positions of primers used to verify insertion of tags by PCR analysis. (C) Immunoblot analyses of whole cell lysates (WCLs) from wildtype (WT) and CK1δ/ε-VM cells with anti-γ-tubulin or anti-α-tubulin (loading control), anti-Flag or anti-CK1δ/ε antibodies. Orange arrows indicate fluorescent fusion proteins. Blue arrows indicate untagged proteins. (D) Proliferation assays of WT HEK293 and CK1δVM/VM, CK1δmNG/mNG, CK1εVM/VM and CK1εmNG/mNG cell lines.

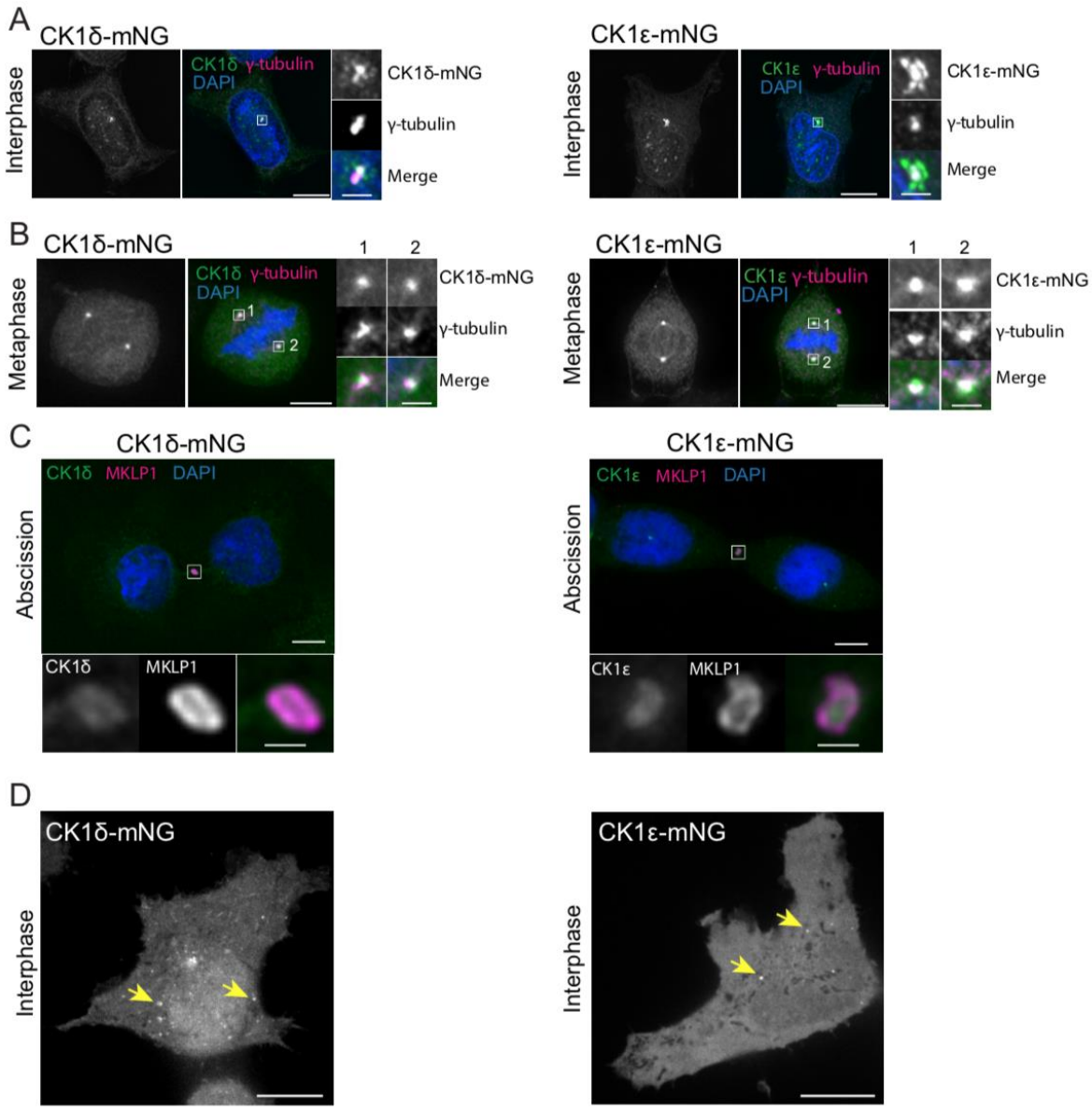

Figure 2-2. Intracellular localization of endogenous CK1δ-mNG and CK1ε-mNG. (A-C) Representative images of fixed HEK293 cells at indicated cell cycle stages producing CK1δ-mNG or CK1ε-mNG stained with (A) DAPI and anti-γ-tubulin, (B) DAPI and anti-γ-tubulin, or (C) DAPI and anti-MKLP1 antibodies. Scale bars, 10 μm. Insets correspond to centrosomes in A and B or the midbody in C. Scale bars, 0.5 μm. (D) Representative single z-sections of live-cell images of HEK293 CK1δ-mNG and CK1ε-mNG cells. Yellow arrows indicate examples of vesicle-like structures Scale bars, 10 μm.

Because deletion of mouse CSNK1D results in embryonic lethality [107, 166], we examined whether tagging CK1δ or CK1ε impaired cell proliferation. We found that there was no change in the rate of cell proliferation of homozygous $CK1\delta_{VM/VM}$, $CK1\varepsilon_{VM/VM}$, $CK1\delta_{mNG/mNG}$, or $CK1\varepsilon_{mNG/mNG}$ HEK293 cell lines (Figure 2-1D).

Fixed-cell imaging showed diffuse and punctate localization of both CK1δ-mNG and CK1ε-mNG in the cytoplasm, and diffuse localization in the nucleus of interphase cells (Figure 1A). Prominent localization to the centrosome was detected throughout the cell cycle (Figure 1A-D), similar to previous observations based on overexpression of the tagged enzymes in a variety of cell lines [61, 121, 146, 176]. In addition, we detected these enzymes at the site of abscission marked by MKLP1 staining, a location not previously reported (Figure 1C). By live cell imaging, many of the cytoplasmic puncta of CK1δ-mNG and CK1ε-mNG (Figure 1A and D) were mobile (Movie S1). Given the known role of CK1δ/ε in endocytosis [72], at least a portion of these moving puncta are likely to be endocytic vesicles.

Identification of CK1δ/ε-interacting partners in HEK293 cells

We used the cell lines producing CK1δ-VM and CK1ε-VM to identify CK1δ/ε interacting proteins. CK1δ-VM and CK1ε-VM (or VM protein alone as a negative control) were each purified in duplicate from asynchronously growing or mitotic cells, and the purifications were analyzed by liquid chromatography-tandem mass spectrometry (LC-MS/MS). Proteins identified in the VM-only sample (Supplementary Table 1A) were excluded from the list of potential CK1δ/ε interactors. The resulting list of candidate interactors for each CK1 enzyme was filtered further by considering only those proteins identified by a minimum of 10 total spectral counts in each purification. Next, a normalized spectral abundance factor (NSAF) was calculated for each protein [177] which takes into account the total spectral count and size of each identified protein in relation to the entire data set. Using these criteria, 181 proteins co-purified with either CK1δ or CK1ε (Supplementary Table 1B). Interestingly, 118 proteins, including all of the most abundant proteins, were found in both the CK1δ-VM and in CK1ε-VM purifications, indicating that these enzymes have many interacting partners in common (Supplementary Table 1C). The proteins unique to either enzyme purification were of low abundance and the majority of these were found in CK1δ purifications (51 versus 30) (Supplementary Tables 1D and 1E). Additionally, there was significant overlap between the identified proteins from asynchronous and mitotic cells that co-purified with CK1δ-VM and CK1ε-VM (Supplementary Table 1B), indicating that the primary

interacting partners of CK1δ and CK1ε are consistent throughout the cell cycle, or that we failed to capture more labile interactions that distinguish CK1δ/ε functions at different cell cycle stages.

As expected from the pleiotropic functions assigned to CK1δ/ε [108, 165, 178], the proteins associated with CK1δ/ε are involved in an array of biological processes including protein transport, circadian rhythm, DNA repair, and cell division (Figure 2-3A). Although the most striking localization of endogenously tagged CK1δ/ε enzymes during all stages of the cell cycle is to the centrosome (Figure 2-2A, B), centrosomal scaffolding proteins were not among the most abundant interacting proteins, and we did not identify the previously reported centrosomal anchor of CK1δ, AKAP450 [179]. A significant subset of co-purifying proteins localize to endosomes and the Golgi apparatus, indicative of the involvement of CK1δ/ε in vesicular trafficking (Figure 2-3B) [72, 172]. Indeed, one of the most abundant CK1δ/ε interacting proteins was GTPase-containing and VPS9 domain-containing protein 1 (GAPVD1) (Figures 2-3C and 2-3D).

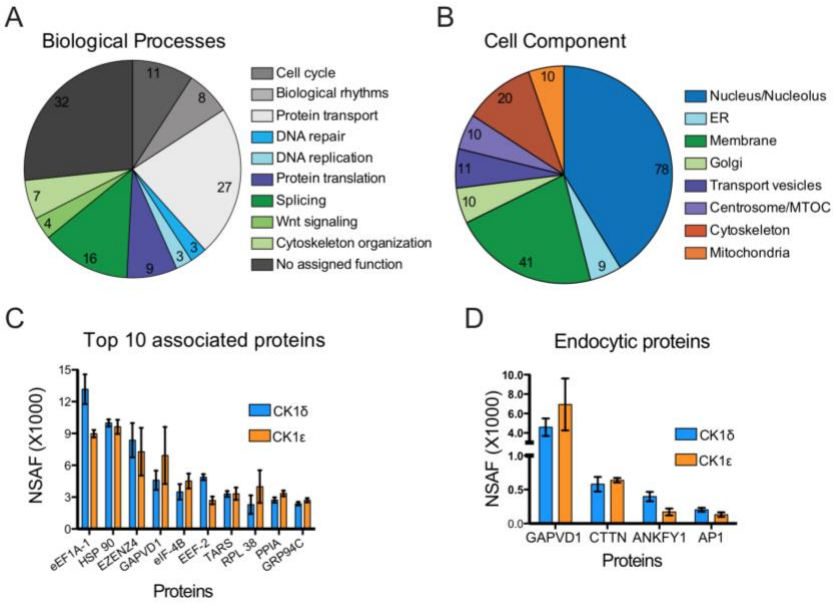

Figure 2-3**:** Analysis of CK1δ/ε interacting proteins. (A) Pie chart depicting the number of associated proteins with a gene-ontology (GO) annotation [1, 2] that function in general cellular processes. Note that this chart includes 120/181 of the associated proteins. (B) Pie chart indicating the number of associated proteins with a GO annotation for localization to a specific cellular compartment. (C) The mean NSAF scores for the top ten proteins identified in four affinity purifications each of CK1δ and CK1ε. (D) NSAF values of the four identified proteins with a GO annotation for function in endocytosis.

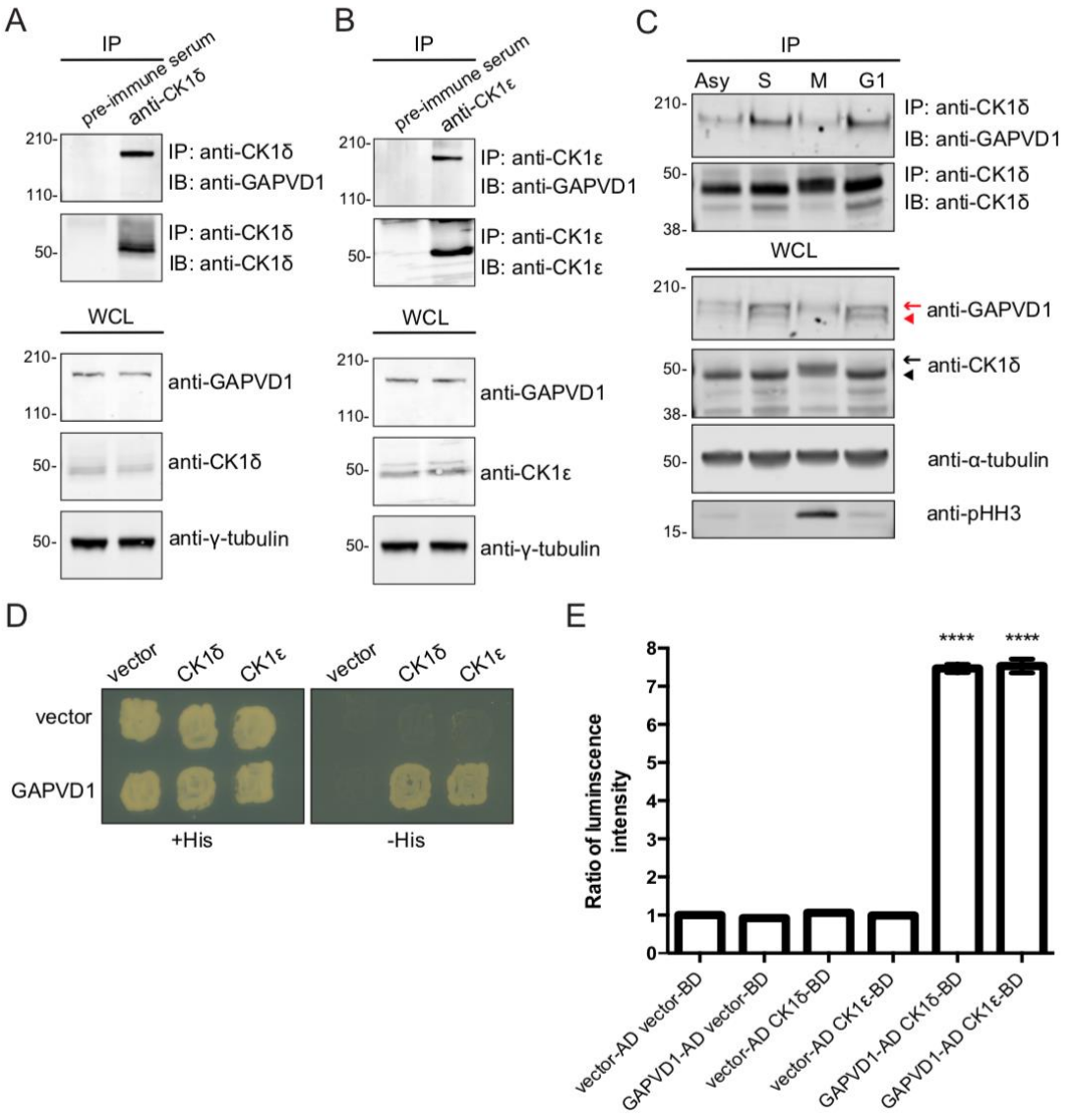

Figure 2-4: CK1δ/ε interact with GAPVD1 throughout the cell cycle. (A and B) Immunoblots of the indicated proteins from whole cell lysates (WCL) or immunoprecipitates (IPs) of CK1δ (A) or CK1ε (B) from HeLa cell lysates. (C) Immunoblots of the indicated proteins from WCL (bottom panels) or IPs of CK1δ/ε from asynchronously (Asy) growing HeLa cells or HeLa cells synchronized in S-phase (S), metaphase (M), or G_1-phase (G1). The black arrow and arrow-head indicate phosphorylated and dephosphorylated CK1δ/ε, respectively. pHH3, phosphohistone H3; a marker of mitotic cells. The red arrow and arrow-head indicate phosphorylated and dephosphorylated GAPVD1, respectively. (D) Yeast-two-hybrid showing direct interaction between GAPVD and CK1δ and CK1ε as indicated by growth on -His plates. (E) Bar graphs show β-galactosidase activity of the indicated bait and prey plasmids tested for growth in D (represented as ratio to empty bait and prey luminescence intensity). Each assay was performed in triplicate. ****, $p<0.001$ determined using a one-way ANOVA followed by Tukey's posthoc test. ns, not significant. Error bars represent SEM.

To validate this interaction in another cell line, we switched to HeLa cells for ease of cell cycle synchronization and assaying endocytosis. We found that GAPVD1 co-immunoprecipitated with CK1δ/ε from HeLa cell lysates when CK1δ/ε were isolated with polyclonal antibodies specific to CK1δ (Figure 2-4A) or CK1ε (Figure 2-4B). Because our MS results indicated that GAPVD1 is associated with CK1δ/ε in both asynchronous and mitotically arrested cells, we tested whether any changes in their interaction occurred during the cell cycle. Congruent with the MS results, GAPVD1 and CK1δ co-immunoprecipitated from cells arrested at multiple cell cycle stages (G1, S and M) (Figure 2-4C). Mitotic cells were validated by the presence of phosphohistone H3 and

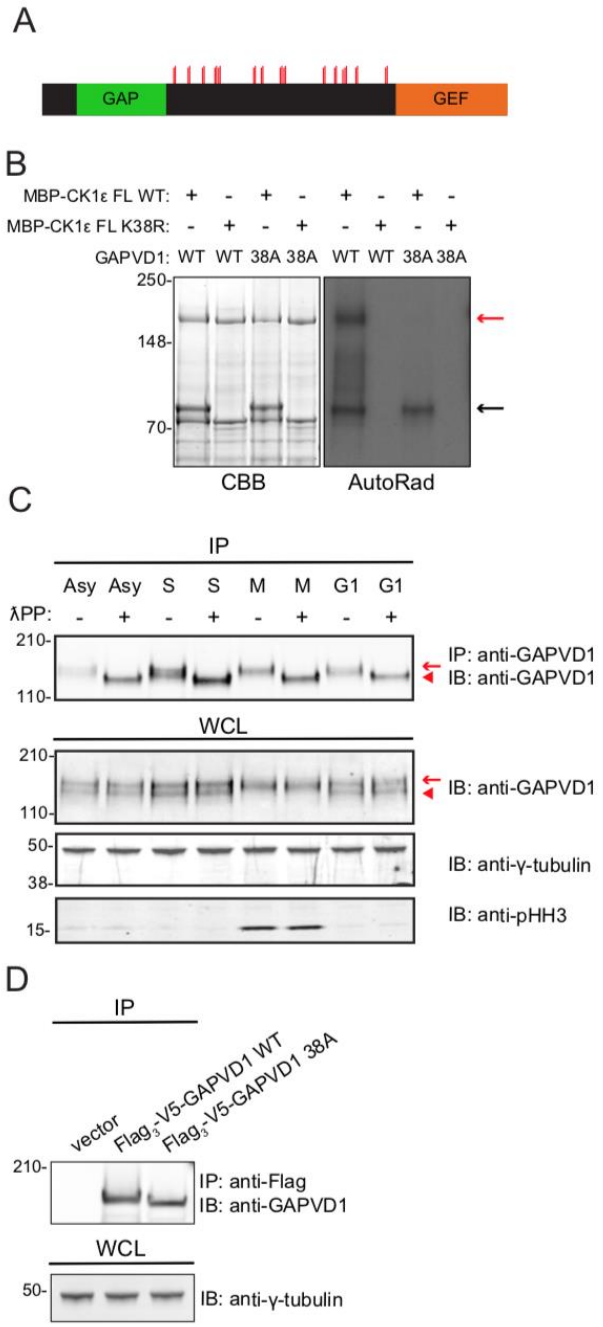

Figure 2-5**:** GAPVD1 is a substrate of CK1ε. (A) Cartoon representation of GAPVD1 protein domains. Green relates to the GAP domain, orange relates to the GEF domain. Red lines correspond to positions of serine or threonine residues that are mutated to alanine in the GAPVD1 38A mutant. (B) In vitro kinase assays of recombinant MBP-CK1ε WT and K38R (kinase-dead) detected by Coomassie brilliant blue (CBB) staining of SDS–PAGE gels, with GAPVD1 WT and 38A as substrates. Phosphorylated GAPVD1 was detected by autoradiography (AutoRad). Black arrow indicates autophosphorylation of MBP-CK1ε. Red arrow indicates GAPVD1. (C) Immunoblots of WCLs and IPs of GAPVD1 from asynchronously (Asy) growing HeLa cells or HeLa cells synchronized in S-phase (S), metaphase (M), or G_1-phase (G1). IPs were treated (+) or not (-) with lambda phosphatase (λPP) and blotted with the indicated antibodies. Red arrow and arrow-head indicate phosphorylated and dephosphorylated GAPVD1, respectively. pHH3, phosphohistone H3; a marker of mitotic cells. (D) Immunoblots of IPs from HeLa GAPVD1$^{-/-}$ cells transfected with vector only or vector expressing $Flag_3$-V5-GAPVD1 or $Flag_3$-V5-GAPVD1-38A.

interestingly, CK1δ appeared to be hyperphosphorylated at this stage (Figure 2-4C). In addition, GAPVD1 and CK1δ/ε interact in a yeast-two hybrid assay, suggesting that aGAPVD1 and CK1δ/ε may directly interact (Figure 2-4D, E).

GAPVD1 is a CK1δ/ε substrate in vitro

We next examined if GAPVD1 is a substrate of CK1δ/ε. Our MS experiments and those of other labs [180-183] revealed that GAPVD1 is highly phosphorylated, predominantly in the IDR, and most of the phosphorylation sites match the consensus motif for CK1δ/ε [33, 34, 184].

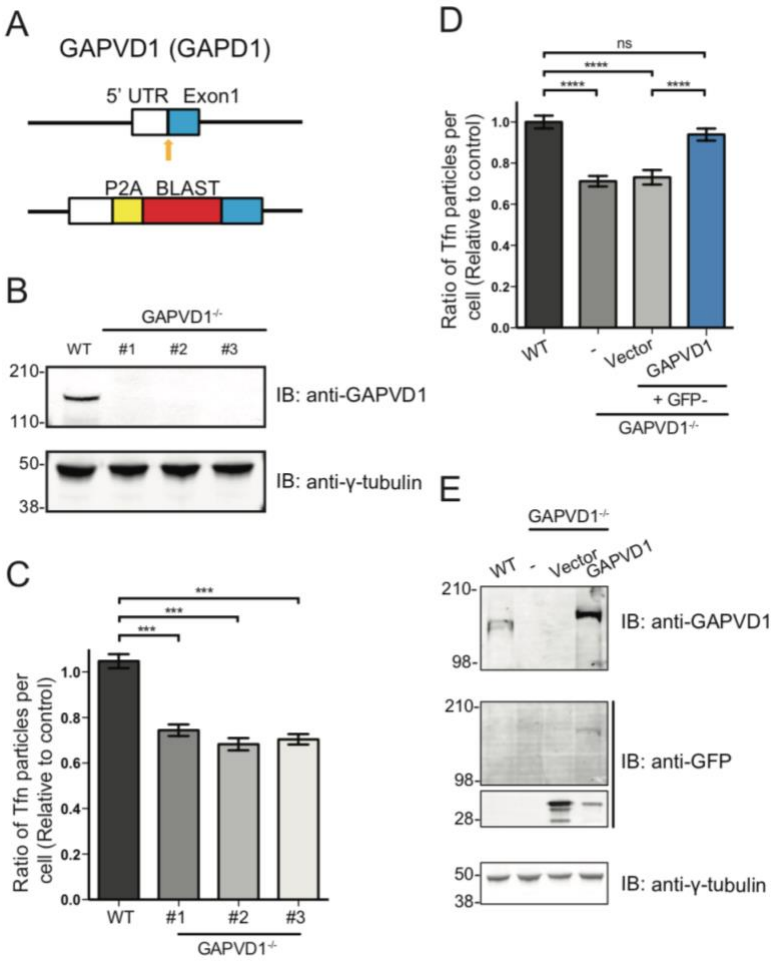

Figure 2-6: GAPVD1 promotes endocytosis. (A) Cartoon representation of the 5'end of the GAPVD1 (GAPD1) gene and the repair plasmid that disrupts GAPVD1 expression. The orange arrow points to the position where a gRNA was designed to target Cas9 for gene editing. Numbers correspond to exons. BLAST: Blasticidin; P2A: ribosomal skip sequence. (B) Immunoblots of WCLs from WT and GAPVD1$^{-/-}$ cells (#1-3) with anti-GAPVD1 and anti-γ-tubulin (loading control) antibodies. (C) Quantification of Alexa 594-coupled Tf uptake in HeLa WT and GAPVD1$^{-/-}$ cells. (D) Quantification of Alexa 594-coupled Tf uptake in HeLa WT and GAPVD1$^{-/-}$ cells transfected with GFP-C2 vector or GFP-GAPVD1. For C and D, the mean and standard error of the mean (SEM) from 4 independent experiments (n ≥ 40 cells per experiment) are presented as the ratio to control. ***, p <0.005, ****, p < 0.001, p values determined using a one-way ANOVA followed by Tukey's posthoc test. ns, not significant. (E) Representative immunoblot of WCLs from cells in D.

Our LC-MS/MS analyses of CK1δ/ε-VM purifications identified six sites of GAPVD1 phosphorylation on CK1δ/ε consensus sites (Supplementary Table 1F). However, our experimental method did not include a phosphopeptide enrichment step, limiting our ability to identify the full cohort of phosphorylated residues. For this GAeson, we mutated all 38 serine and threonine residues to alanine in the IDR of the protein that fit

the consensus motif for CK1δ/ε and were identified using MS, either by us or others [181, 185, 186] (Figure 4A). We found that wildtype recombinant MBP-CK1ε but not a kinase-dead MBP-CK1ε phosphorylated the wildtype GAPVD1, but not GAPVD1-38A (Figure 4B). Consistent with the cumulative MS data detecting 38 phosphorylated residues clustered in the IDR of GAPVD1, and similar to the 'strings' of serines and threonines phosphorylated in other substrates [162], we found that mutating only the subset of the 38 sites identified in our purifications (*S566, S569, S740, S742, S746, S747, S902, S903)* did not eliminate CK1ε-mediated phosphorylation of GAPVD1 in vitro (data not shown).

As expected for a highly phosphorylated protein, GAPVD1 immunoprecipitates treated with lambda phosphatase migrated faster on SDS-PAGE than untreated immunoprecipitates, irrespective of cell cycle stage (Figure 4C). Mitotic cells were validated by blotting with antibodies to phosphohistone H3 (Figure 4C). When transiently transfected into HeLa cells, immunoprecipitated, and analyzed by immunoblotting, $Flag_3$-V5-GAPVD1-38A migrated faster than $Flag_3$-V5-GAPVD1 WT, consistent with the loss of phosphorylation in vivo (Figure 4D).

GAPVD1 phosphorylation promotes endocytosis

GAPVD1 has reported roles in fluid-phase and receptor-mediated endocytosis and CK1δ/ε are also required for efficient Tfn and EGFR internalization [72, 172], an endocytic role conserved with the CK1δ/ε ortholog Hrr25 in *Saccharomyces cerevisiae* [72]. Thus, we established cell lines in which we could test the effect of CK1 on GAPVD1 function. The GAPVD1 gene was disrupted in HeLa cells using CRISPR/Cas9-mediated gene editing (Supplementary Figure 2A). The consequent loss of all copies of GAPVD1 from three independently isolated cell lines was validated by immunoblotting (Supplementary Figure 2B). To confirm that loss of GAPVD1 resulted in a defect in endocytosis, the internalization of Tfn conjugated to Alexa-594 (Tfn-594) was assayed in GAPVD1$^{-/-}$ cells as previously described [187]. In all three GAPVD1$^{-/-}$ cell lines, we detected a reduction in the internalization of Tfn-594, consistent with a general endocytic defect (Supplementary Figure 2C). Furthermore, the observed endocytic

defect could be rescued by re-introducing GAPVD1 (Figure 5B and Supplementary Figures 2D, E).

We next asked if phosphorylation at CK1 sites modulates GAPVD1's role in endocytosis by transfecting into the GAPVD1$^{-/-}$ cell lines WT GAPVD1, the 38A mutant of GAPVD1, or a mutant of GAPVD1 in which the 38 phosphosites were replaced with aspartic acid residues (38D), and then measuring either Tfn uptake as described above or Epidermal Growth Factor (EGF) uptake as described previously [172] (Figure 5). Although expressed to an equivalent level as WT, the 38A mutant of GAPVD1 did not rescue the endocytosis defects of GAPVD1$^{-/-}$ cells (Figure 5B-D). In contrast, GAPVD1-38D did rescue the endocytic defects of these cells (Figure 5B-D). These results indicate that GAPVD1 phosphorylation by CK1δ/ε promotes endocytosis.

Discussion

The full complements of interacting partners and substrates of CK1δ/ε have not been well defined. Although this study is not the first to investigate the localization or interactome of CK1δ/ε [128, 146], we are the first to use CRISPR/Cas9 gene editing to tag and purify these endogenous enzymes, which alleviates any issue that could arise from overexpression studies. We confirmed all previous noted localization patterns for CK1δ/ε (centrosome, nucleus, cytoplasm) [165] and discovered that CK1δ/ε also localize to the midbody. In addition to identifying known interacting partners involved in biological rhythms, such as Period protein 1 and 2 [127, 128, 131, 138], we identified additional interacting proteins involved in other biological processes that CK1δ/ε are involved in, such as endocytosis. Twenty-seven of the identified proteins are involved in protein transport, with four having roles specific to endocytosis. Although CK1δ/ε and their *Saccharomyces cerevisiae* homolog, Hrr25, have been shown to localize to sites of clathrin-mediated endocytosis (CME) [72] and loss of CK1δ or CK1ε significantly reduces passive and ligand-stimulated CME [72, 172], CK1 substrates involved in CME have only been identified in yeast [72]. Our analysis has shown that CK1δ/ε phosphorylation of GAPVD1 is key to its role in CME. In addition to GAPVD1, our list of interacting proteins contains good candidates for additional endocytic CK1δ/ε substrates

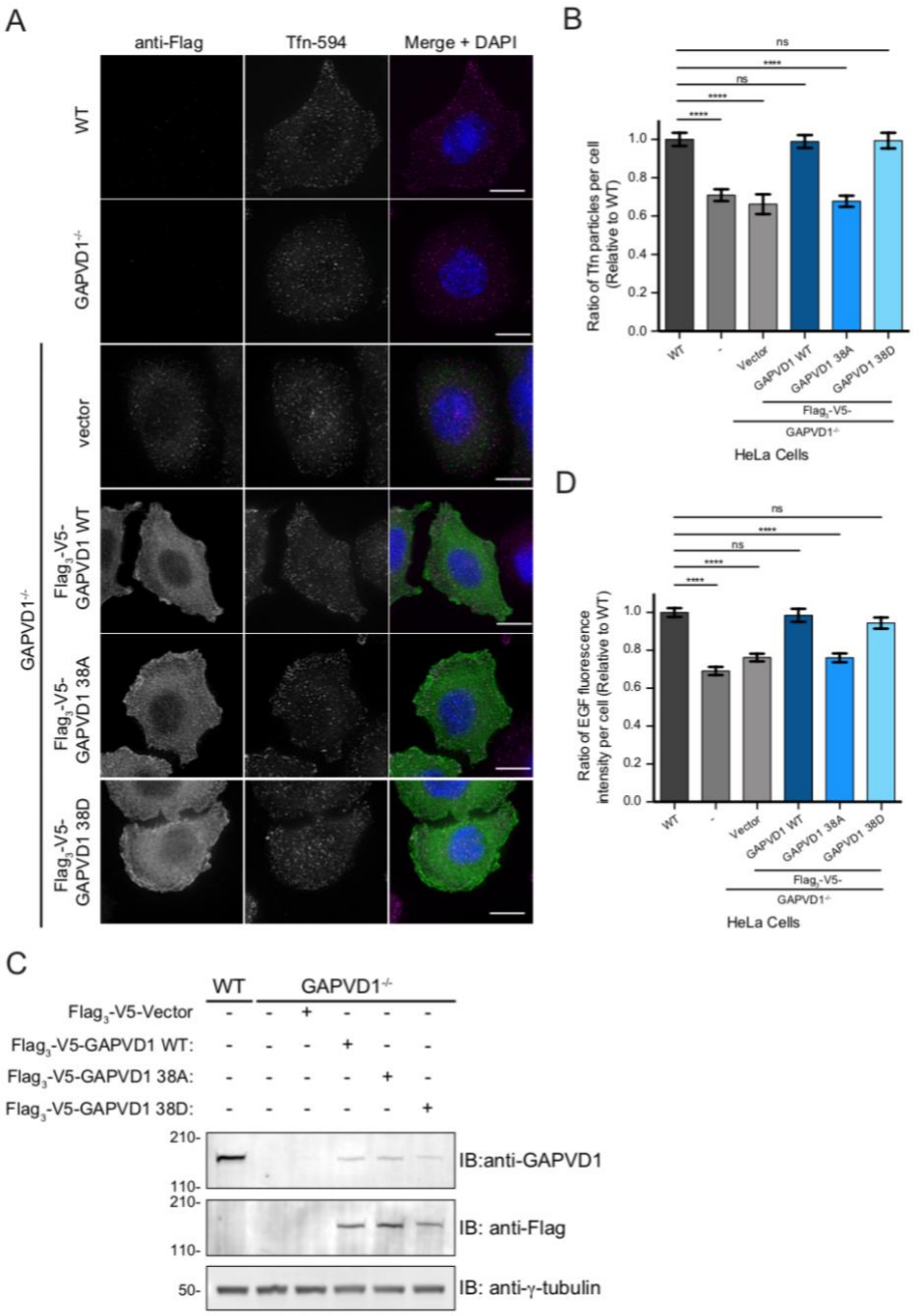

Figure 2-7: GAPVD1 phosphorylation promotes endocytosis. (A) Representative images of HeLa WT and GAPVD1$^{-/-}$ cells incubated with Tfn-594 in an endocytosis assay. Scale bar 10 µm. (B) Quantification of Alexa 594-coupled Tfn uptake in HeLa WT and GAPVD1$^{-/-}$ cells transfected with Flag$_3$-V5 plasmids. The mean and SEM from 3 independent experiments (n ≥ 40 cells per experiment) are presented as a ratio to control. (C) Immunoblots of whole cell lysates from the experiments in A and B. (D) Quantification of Alexa 488-coupled EGF uptake in HeLa WT and GAPVD1$^{-/-}$ cells transfected with Flag$_3$-V5 plasmids. The mean and SEM from 3 independent experiments (n ≥ 40 cells per experiment) are presented as a ratio to control. In B and D, ****, $p < 0.001$, p values determined using a one-way ANOVA followed by Tukey's posthoc test. ns, not significant.

in human cells. Indeed, our study provides a plethora of information for further study of the involvement of CK1δ/ε in multiple biological processes.

The most striking localization of endogenously tagged CK1δ/ε enzymes during all stages of the cell cycle is to the centrosome. Due to the many contributions of the centrosome to mitosis [188, 189], we sought to identify the interacting partners of CK1δ/ε not only in asynchronously growing cells but also in mitotic cells but centrosomal proteins were surprisingly not abundant co-purifying proteins. One potential explanation for this result is that CK1δ/ε centrosomal localization may be very dynamic, and transient interactions are difficult to detect by co-purification approaches. Another unexpected result from our MS data is that there were few co-purifying proteins specific to either asynchronous or mitotic samples, which might indicate either that interaction partners do not change appreciably during the cell cycle or that we failed to capture more labile interactions that distinguish CK1δ/ε functions at different cell cycle stages.

Similar to other substrates of CK1δ/ε [162], there are many sites of phosphorylation on GAPVD1. The 38 CK1 consensus phosphorylation sites are clustered in the IDR of GAPVD1 similar to the ‘strings’ of serines and threonines phosphorylated in other substrates [162]. Many questions remain about GAPVD1 phosphorylation including whether all of these sites need to be phosphorylated in order to support GAPVD1 function in endocytosis. It also remains to be determined whether there is a specific order in which phosphorylation of GAPVD1 occurs and whether some sites are more prevalent or important than others. Though the GAPVD1 GEF domain has been shown to bind Rab5 via yeast two-hybrid [171] and act as a GEF toward Rab5A in vitro [167], GEF or GAP activity of purified full-length GAPVD1 has never been reported nor has it been shown to interact directly with another protein. Thus, it will also be interesting to determine how phosphorylation impacts GAPVD1 function, whether by stimulating its GEF domain, modulating the function of its GAP-like domain, and/or influencing other reported interactions [169, 170, 173].

While no other kinase has been shown to phosphorylate and regulate GAPVD1 function, other GAPVD1 phosphosites have been identified in phosphoproteomic

screens that fit Cdk1, p38 and PKA consensus motifs [181, 185, 186]. CK1δ/ε phosphorylation of GAPVD1 may thus be dependent upon and is likely coordinated with phosphorylation by other kinases as in the case for YAP in the Hippo pathway [111].

Accession #	Gene name	Accession #	Gene name
A9X7H1		B4DY72	
B4DMA2		P61289	PSME3
B7Z697		P08758	ANXA5
B4DPU3		B7Z602	
Q14C86	GAPVD1	Q8N752	CSNK1A1L
P23588	EIF4B	B4E1G2	
D6R9F8	TARS1	O15534	PER1
Q53RC5	DKFZp547I014	O75821	EIF3G
P78371	CCT2	P23381	WARS1
E5RI05	ANXA6	Q9BRS2	RIOK1
P62937	PPIA	B7Z525	
E7ESK7	YWHAZ	E7ERJ7	PABPC1
Q58FF2	GRP94c	Q01518	CAP1
P63173	RPL38	P17980	PSMC3
Q99417	MYCBP	Q6ZRV2	FAM83H
Q75MM1	WUGSC	P05023	ATP1A1
P50991	CCT4	Q9UKK9	NUDT5
O14744	PRMT5	B4DRH6	
Q59ET3		Q9P2F5	STOX2
Q5S4N1		B4DHQ3	
B4DHR1		Q4J6C0	PPM1B
Q9UG54	MAP3K7	P24752	ACAT1
P16949	STMN1	Q96AG4	LRRC59
Q59GR8		Q5W0B1	OBI1
Q15750	TAB1	Q14247	CTTN
Q8WWY3	PRPF31	P17812	CTPS1
Q9BQA1	WDR77	B4DMF5	
E9PFF2	TKT	Q13547	HDAC1
Q9BUA3	SPINDOC	O43852	CALU
A8MXB7	SNX24	P48444	ARCN1
Q8TC76	FAM110B	P33992	MCM5

P22626	HNRNPA2B1	Q16526	CRY1
Q15208	STK38	D6W539	HADHB
Q13162	PRDX4	P55060	CSE1L
P98175	RBM10	Q9Y6Y0	NS1
Q9Y657	SPIN1	Q59F66	
B4DM33		Q9UNZ2	NSFL1C
B3KPZ8		Q9Y2H1	STK38L
E9PQD7	RPS2	O75874	IDH1
E5RHC1	PPP2CB	Q13310	PABPC4
Q53R94	RTN4	Q16630	CPSF6
B5MDF5	RAN	Q9Y4E8	USP15
O43143	DHX15	P36871	PGM1
Q49AN0	CRY2	Q06210	GFPT1
P35813	PPM1A	Q9H4A4	RNPEP
Q9Y295	DRG1	Q9UNF1	MAGED2
Q9P2R3	ANKFY1	Q6U8A4	
Q01804	OTUD4	Q9Y2W1	THRAP3
Q6UWP8	SBSN	O15055	PER2
O15397	IPO8	Q7L014	DDX46
Q9BXP5	SRRT	Q96QK1	VPS35
B4DWX6		E7EVA0	MAP4
Q9Y678	COPG1	Q92620	DHX38
Q99613	EIF3C	P26358	DNMT1
O60664	PLIN3	Q7Z6Z7	HUWE1
Q08211	DHX9	Q9UQ35	SRRM2
Q08554	DSC1	Q14004	CDK13
Q9NYF8	BCLAF1	E9PRY8	EEF1D
P12036	NEFH	Q14008	CKAP5

Table 2-1. Proteins identified in both CK1δ and CK1ε MAP purifications

Accession #	Gene name	Accession #	Gene name
D6RD83	HNRNPD	Q10567	AP1B1
E7EPA1	PRPSAP2	Q9C0C9	UBE2O
P62316	SNRPD2	Q86XP3	DDX42
P60891	PRPS1	Q9UPT6	MAPK8IP3
P09104	ENO2	Q9BSJ8	ESYT1
Q3MHV2	RPLP0	O95163	ELP1
P67809	YBX1	O60610	DIAPH1
Q99497	PARK7	O75694	NUP155
P39687	ANP32A	Q13464	ROCK1
B7Z213			
P43487	RANBP1		
P52565	ARHGDIA		
Q9UIS4	SNRPB		
O43809	NUDT21		
Q5JYR7	RPN2		
Q02878	RPL6		
P22061	PCMT1		
Q15417	CNN3		
Q14558	PRPSAP1		
Q8WUA2	PPIL4		
P07339	CTSD		
Q96P63	SERPINB12		
Q59EH7			
P60228	EIF3E		
Q9P258	RCC2		
P25685	DNAJB1		
Q9BT78	COPS4		
P55010	EIF5		
P49189	ALDH9A1		
O15355	PPM1G		
Q5T5C7	SARS1		
Q13835	PKP1		
A8MXP9	MATR3		
O60749	SNX2		
Q9UQE7	SMC3		
Q15459	SF3A1		
Q8NB74			
Q4VCS5	AMOT		
O00267	SUPT5H		
O60763	USO1		
Q9P1Y5	CAMSAP3		

Table 2. Proteins identified only in CK1δ MAP purifications

Accession #	Gene name
P01040	CSTA
P63167	DYNLL1
Q5T3N1	ANXA1
P62269	RPS18
P42766	RPL35
P04792	HSPB1
A4D1G5	LOC392748
P61254	RPL26
A0PJ72	ABCF1
P80723	BASP1
P05783	KRT18
P30040	ERP29
P31947	SFN
P02545	LMNA
P31327	CPS1
P20042	EIF2S2
Q7Z7G8	VPS13B
P00966	ASS1
B3KXN5	
P42765	ACAA2
P35237	SERPINB6
Q6NWZ1	CKAP4
Q9P270	SLAIN2
E9PMS6	LMO7
O75330	HMMR
Q16513	PKN2
P78344	EIF4G2
Q9NZM1	MYOF
Q15149	PLEC
Q09666	AHNAK

Table 2-3. Proteins identified only in CK1ε MAP purifications

Amino Acid	Site	Best Ascore	Delta Asy	Delta Asy	Delta Mit	Delta Mit	Epsilon Asy	Epsilon Asy	Epsilon Mit	Epsilon Mit
66	S66	100% (51.96)								2
390	T390	100% (88.98)		1	4	5				16
566	S566	100% (22.45)		1		1				1
569	S569	100% (17.94)				3				3
740	S740	100% (26.83)		1						2
742	S742	100% (39.76)		1		2	1			7
746	S746	99% (24.11)			1	1				19
747	T747	81% (15.91)								12
902	S902	100% (33.98)	8	4	9	10	4	3	6	21
903	S903	100% (54.03)	1	2	8	5		1	1	5
946	S946	70% (11.10)			1				1	
1019	S1019	100% (87.75)		1	2			2	2	3
1023	S1023	100% (1,000.00)				3				1
1096	S1096	100% (65.25)			3	6			1	5
1103	S1103	89% (12.42)							2	1
1105	S1105	100% (28.70)		1		4			1	3
1130	S1130	100% (76.61)		2	2	1				6
1133	S1133	100% (84.74)			1					1

Table 2-4. GAPDV1 phospho-sites identified from MAP purifications

CHAPTER 3

Identifying CK1δ/ε substrates

Introduction

Casein kinase 1 (CK1) is a family of serine/threonine protein kinases conserved from yeast to mammals that function in a variety of cell-signaling pathways. The CK1 family is comprised of six members that can be divided into those that are soluble (CK1α, CK1δ and CK1ε) and those that are membrane-bound (CK1γ1-3) [3]. All six family members have a N-terminal catalytic domain and a C-terminal tail. The catalytic domains share a high degree of sequence similarity, and the C-terminal tails are of varying length and sequence composition. Of the soluble family members, CK1δ and CK1ε share the greatest degree of sequence identity, with 99% sequence identity in their catalytic domain and 53% identity in their C-termini. This sequence similarity between CK1δ and CK1ε may translate to functional redundancy. Indeed, CK1δ and CK1ε have redundant substrates and functions in circadian rhythm, Wnt signaling, Hippo signaling, ribosome biogenesis, and p53 stability [4-8]. Although there has been extensive research on specific CK1δ and CK1ε targets in a variety of pathways, whether they have important mitotic substrates has not been reported.

CK1δ/ε localize to mitotic structures from which spatial and temporal control of mitosis are coordinated [9-11]. CK1δ/ε localize to the major microtubule-organizing center, the centrosome, throughout mitosis, as well as the regenerating nucleus during telophase [12]. Additionally, we have reported their localization to the midbody, while others have identified its interaction with midbody-localized proteins during the abscission process [13]. Further, CK1ε is reported to localize to kinetochore microtubules in prophase [12]. Taken together, this localization pattern raises the possibility that these enzymes function in the control of mitotic processes, including cell division.

To deepen our understanding of potential CK1δ/ε roles in mitosis, I employed a combination of cell cycle synchronization, small molecule inhibitor treatment and

isobaric tags for relative and absolute quantification (iTRAQ)-based, large-scale phospho-proteomics to identify CK1δ/ε substrates. We identified 175 potential substrates, the majority of which can be assigned to specific cellular functions.

Results

We used three small molecule inhibitors of CK1δ/ε in our experiments. We chose PF-670 because it has been previously used to inhibit CK1 enzymes in studies of circadian rhythm and Wnt signaling [14-18]. We also used SR-1277 and SR-3029, inhibitors with increased specificity towards CK1δ/ε [19, 20]. To determine appropriate inhibitor concentrations to use in our phosphoproteomics experiments, we tested a wide range of each for anti-proliferative activity. Cell numbers were determined after three days of continuous DMSO or inhibitor treatment. SR-1277 and SR3-3029, but not PF-670, had anti-proliferative activity, with EC50s of 44 nM and 89 nM for SR-1277 and SR-3029, respectively. These values were similar to what was previously reported for their activity on human melanoma A375 cells (Figure 1A) [19, 20]. Because loss of CK1δ/ε activity has an anti- proliferative effect on cells [19, 21], we chose to use the highest concentration from our experiment (1 μM).

To increase the probability of identifying CK1δ/ε mitotic substrates, HeLa cells were first arrested in S-phase through a sequential thymidine-aphidicolin block [22], released into inhibitor-free media for a period of 10 hours, and then treated for 30 minutes with DMSO, 1 μM PF-670, 1 μM SR1277 or 1 μM SR-3029 (Fig 1B). Using this synchronization protocol, the mitotic index of the cell populations prior to lysis was ~35%, a value that has been observed previously with this method [23]. Cells were then lysed, their proteins were digested with trypsin, and the peptides were labeled with one of four isobaric tags. The four samples were combined, phosphopeptides were enriched using TiO_2 resin, and the mixture was analyzed by LC-MS/MS. mass spectrometry (Figure 1B).

Candidate CK1δ/ε substrates were determined by identifying phosphopeptides with greater-than-or-equal to 1.5-fold reduction in inhibitor-treated samples compared to the DMSO-control sample. We identified 2292 phosphopeptides, corresponding to 627 proteins, with a minimum 1.5-fold reduction in at least one of the inhibitor-treated

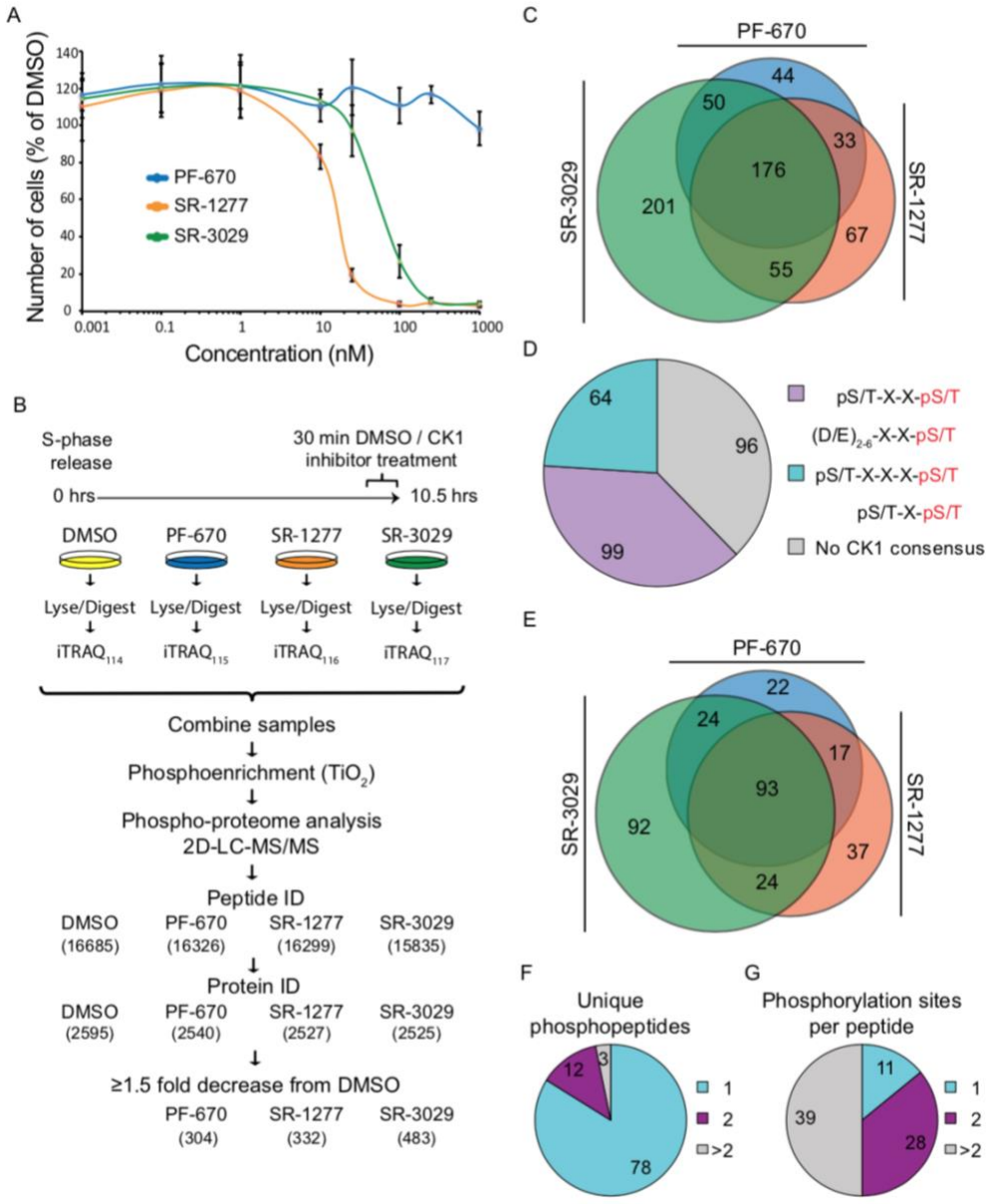

Figure 3-1: Mass spectrometry analysis of CK1δ/ε substrates **A**. Cell proliferation assay in which cells were treated with DMSO, PF-670, SR-1277, or SR-3029 at varying concentrations for 3 days. CK1δ/ε inhibitor-treated cell populations were compared to DMSO-control samples at each concentration. **B**. Graphical representation of the phosphoproteomics procedure. Cells were treated with DMSO or 1 μM of one of the three CK1δ/ε inhibitors. Numbers refer to phosphopeptide or protein identifications. **C**. Venn diagram of the number of proteins identified with reduced phosphorylated peptides compared to DMSO for each inhibitor. **D.** A Pie chart depicting the proportion of phospho-peptides with a ≥1.5-fold decrease in all inhibitor-treated sampled compared to DMSO-control samples with the canonical CK1 consensus motif, a small variation to the motif, or does not fit the motif. **E**. Venn diagram of the number of proteins identified with reduced phosphorylated peptides compared to DMSO for each inhibitor with the canonical CK1 consensus motif or a small variation to the motif. **F**.A Pie chart depicting the proportion of proteins where 1, 2 or >2 unique phospho-peptides were identified. **G**. A Pie chart depicting the number of phospho-residues identified in proteins where a single unique phospho-peptide was identified.

samples. We first considered further only those proteins whose phosphopeptides were identified as reduced in all three inhibitor-treated samples (Figure 1C), which brought the list down to 257 phosphopeptides (Table S1), corresponding to 176 proteins (Table S2). CK1δ/ε recognize substrates with acidic motifs N-terminal to phosphorylation sites (pS/T-X-X-S/T or $(D/E)_{2-6}$-X-X-S/T) and often generate stretches of phosphoserines on their substrates [24-26]. A phosphorylation site matching a CK1 consensus was identified in 98 phosphopeptides (Figure 1D). An additional 64 phosphopeptides varied from the canonical motif by a single residue (pS/T-X-X-X-S/T or pS/T-X-S/T) (Figure 1D). These 162 phosphopeptides comprised 110 unique phosphopeptides and corresponded to 75 proteins (Figure 1E and Table S3). In addition to the 162 phosphopeptides, we found reductions in a significant number of phosphopeptides with a phosphorylated tyrosine or phosphorylated serine/threonine followed by a proline at the +1 position. These identifications suggest that inhibition of CK1δ/ε for 30 minutes likely affects downstream tyrosine and proline-directed kinases.

We further considered the 75 proteins (Table S3) most likely to be substrates of CK1δ/ε in the overlap of inhibitor-treated samples (Figure 1E). A single unique phosphopeptide was identified in ~75% of these proteins (Figure 1F). Two or greater-than two unique peptides were identified in 17% and 6% of the putative substrates, respectively, with Ki67 covered by 13 unique phosphopeptides (Figure 1G). Consistent with CK1δ/ε's tendency to phosphorylate multiple closely spaced residues on their substrates [24], 53% of the single unique phosphopeptides were identified with >2 phosphoresidues (Figure 1F). An additional 16 potential protein substrates were identified by considering phosphopeptides that have signal reductions in the three inhibitor-treated samples across multiple peptides (Table S3).

A subset of the putative substrate list (73/93) is associated with gene ontology terms relating to a wide range of biological processes (Fig 2A). These include processes in which CK1δ/ε are known to participate in, such as biological rhythms, endocytosis, and DNA repair [27-29]. Localization information is available for a different subset of candidate substrates (73/93). The wide range of localization patterns of

A.

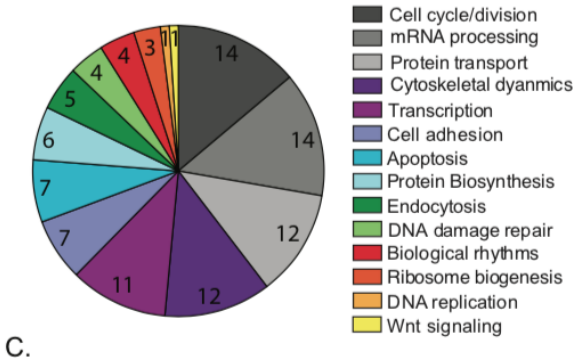

B.

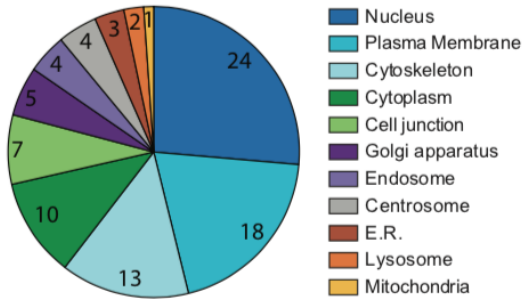

C.

		Ratio of DMSO:Inhibitor		
Gene	Protein	PF670	SR1277	SR3029
Cell cycle/division				
CSPP1	Centrosome and spindle pole-associated protein 1	3.814	4.938	3.561
SHRM3	Protein Shroom3	3.969	3.417	2.635
NPM1	Nucleophosmin	1.552	1.777	4.903
STMN1	Stathmin	1.632	2.958	1.720
DNA damage repair				
XRCC1	X-ray repair complementing defective repair in Chinese hamster cells 1	2.146	3.794	2.333
ERCC6	DNA excision repair protein ERCC-6	1.584	DIV/0	1.705
MDC1	Mediator of DNA damage checkpoint protein 1	DIV/0	DIV/0	DIV/0
Cytoskeletal dynamics				
LIMA1	LIM domain and actin-binding protein 1	2.599	2.346	2.335
CTTN	Src substrate cortactin	DIV/0	DIV/0	DIV/0
DNHD1	Dynein heavy chain domain-containing protein 1	4.001	2.955	DIV/0
Protein Transport				
GAPVD1	GTPase activating protein and VPS9 domains 1	1.565	1.775	2.335
SLC35A2	UDP-galactose translocator	3.593	2.937	2.746
ANXA4	Annexin	2.370	1.665	2.692
Transcription				
BACH1	Transcription regulator protein BACH1	3.772	3.042	3.653
YAP1	Transcriptional coactivator YAP1	2.830	2.690	3.210
SLTM	SAFB-like transcription modulator	2.830	2.690	2.281
Ribosome biogenesis				
RPLP2	60S acidic ribosomal protein P2	2.044	1.807	1.871
POP1	Ribosomal protein, large, P0	1.675	3.412	2.592
CK1δ	Casein Kinase 1 δ	2.509	2.365	1.724

Figure 3-2: Analysis of CK1δ/ε substrates **A.** Pie chart depicting the gene-ontology (GO) annotation [1, 2] for 73/93 candidate substrates. **B**. Pie chart depicting the gene-ontology (GO) annotation for intracellular localization for 73/93 of the putative substrates. **C**. A table of potential CK1δ/ε substrates identified in the iTRAQ dataset.

putative substrates (Fig 2B) is consistent with the broad localization and many known functions of CK1δ/ε [30-32]. Figure 2C lists the most abundant hits from three of the largest gene ontology groups (transcription, cell cycle/division, and protein transport) and three other gene ontology groups relating to processes in which CK1δ/ε arereported to function (DNA damage repair, cytoskeletal dynamics and ribosome biogenesis) [6, 33-35].

Of the 93 proteins identified as putative CK1δ/ε substrates, only five (YAP, TOP2β, GAPVD1, and CK1δ itself) were previously reported to be substrates [5, 36-38]. CK1δ/ε are both known to autophosphorylate and there is evidence that they each autophosphorylate multiple sites in their C-termini [36, 39]. We identified a single C-terminal phosphopeptide (GAPVNIsSsDLTGR) of CK1δ that fits a variant CK1 consensus (pS/T-X-S/T, Table S2).

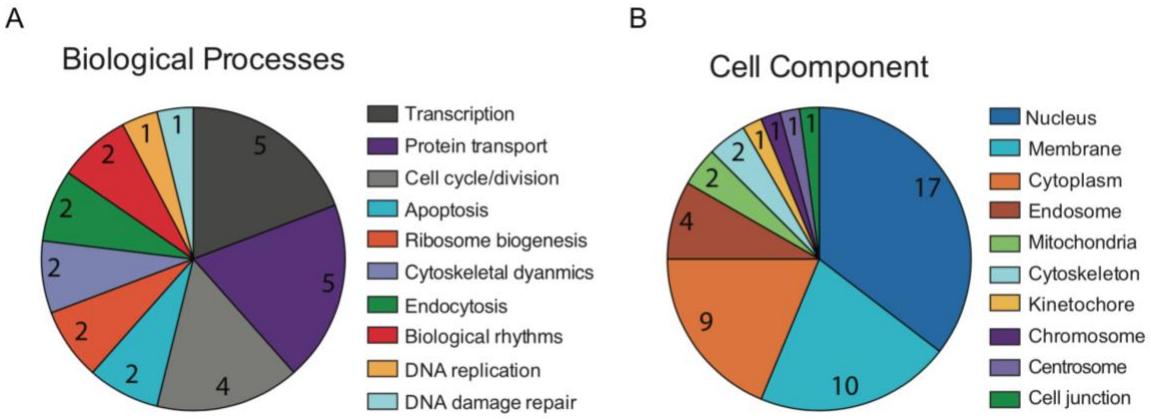

Figure 3-3: Analysis of CK1δ/ε putative substrates identified only in SR-1277-traeted samples A. Pie chart depicting the gene-ontology (GO) annotation for 21/37 candidate substrates. B. Pie chart depicting the gene-ontology (GO) annotation for intracellular localization for 35/37 of the

Three potential substrates identified by multiple phosphopeptides containing multiple phosphosites (cortactin, GAPVD1, and NPM1) were also identified in CK1δ/ε interaction screens [12, 40]. The GAPVD1 phosphosites were validated as bonafide CK1δ/ε phosphosites previously. GAPVD1 phosphorylation by CK1δ/ε inhibits endocytosis in interphase HeLa cells.

The three small molecule inhibitors we used do not have the same degree of specificity towards CK1δ/ε. Though PF-670 has been used extensively to study CK1 function [14-18], *in vitro* it significantly inhibits other kinases including p38 mitogen-

activated protein (MAP) kinase, epidermal growth factor receptor, and MAP kinase 8 [16, 19]. While SR-1277 and SR-3029 have greater specificity than PF-670 and similar IC_{50} values for inhibition of CK1δ/ε in *in vitro* kinase assays, SR-1277 inhibits still fewer off target kinases than SR-3029 at a 10 μM concentration [19]. The possibility of off-target inhibition by PF-670 in particular led us to consider further those phosphopeptides reduced in the SR-1277-treated sample alone or that were reduced in both the SR-1277-treated and SR-3029-treated samples. The 56 phosphopeptides that were reduced when cells were treated with either SR-1277 or SR-3029 corresponded to 24 proteins (Table S3). Like proteins identified in the full overlap (Figure 2A), these potential substrates are associated with several processes known to involve CK1 enzymes such as cell cycle/division, DNA repair and ribosome biogenesis; the majority of them localize to the nucleus (Table S3). An additional 37 proteins can be considered putative CK1δ/ε substrates if we consider phosphopeptides with a reduction in just the SR-1277-treated sample ('Only SR-1277' list) (Table S4). A subset of this list (21/37) can be categorized in the same set of GO annotations as the previous lists (Figure 3A & B). Importantly, another previously verified CK1δ/ε substrate [41], TOP2A, was identified by using this criterion (Table S4). Three phosphosites were identified on a single peptide of TOP2A (Table S3), two of which fit the variant CK1δ/ε consensus motif.

Discussion

Although there are many reported CK1δ/ε substrates that function in a wide range of biological processes [3, 42, 43], there has been no previous large scale phosphoproteomic analysis of its substrates. Here, we employed a combination of cell synchronization, small molecule inhibitor-treatment and large-scale mass spectrometry to more comprehensively identify CK1δ/ε substrates. Depending upon the stringency of our analysis (candidates identified by treating cells with one, two, or three CK1δ/ε inhibitors), we identified up to 621 potential new substrates, and additional phosphorylation events that are dependent on CK1δ/ε activity. Our data suggest that several previously identified CK1δ/ε interacting partners are substrates of these enzymes. We confirmed that CK1δ is autophosphorylated *in vivo* and identified sites of

autophosphorylation. Our list of putative CK1δ/ε substrates provide an abundance of opportunities to study CK1δ/ε functions in the cell cycle.

One caveat in the interpretation of our phosphoproteomic data set is that some phosphopeptides were only detected in the DMSO-treated sample. This could mean one of two things. First, those peptides may become dephosphorylated during CK1δ/ε inhibition, which would make them very strong candidate substrates. Alternatively, phosphopeptides may not have been detected in the inhibitor-treated samples due to stochastic sampling variation, resulting in false positive substrate identifications. The use of three inhibitors and our focus on overlapping results reduces somewhat this technical consideration.

Several putative substrates identified in our phosphoproteomic screen have not previously been identified as CK1δ/ε substrates, but function in pathways that are known to contain validated CK1δ/ε substrates. For example, CK1δ/ε-dependent phosphorylation mediates the nuclear export of eukaryotic translation initiation factor 3A [44]. Although we did not identify EIF3A, EIF3B, D, & G were identified as putative CK1δ/ε substrates (Table S1). Similarly, promyelocytic leukemia protein (PML) was identified as a putative substrate in each of the inhibitor-treated samples, and is reported to function in the same DNA-damage response pathway as CK1δ/ε [45]. PML is reported to protect p53 from MDM2 inhibition by facilitating p53 phosphorylation on Thr18 [46]. CK1δ/ε interact with PML and p53 in response to DNA damage[45], and CK1δ/ε inhibition significantly reduces phosphorylation of p53 on Thr18. However, inhibition was achieved through treatment with IC126, which inhibits many off-target kinases[19], and negatively affects microtubule polymerization [47, 48]. In addition to PML, we identified TP53BP1, a p53 effector binding partner [49], in the list of proteins with a reduction in phosphorylation in just the SR-1277 sample.

The soluble CK1 ortholog in *Saccharomyces cerevisiae,* Hrr25, and *Schizosaccharomyces pombe*, Hhp1 and Hhp2, have roles in mitosis and meiosis, in addition to roles in endocytosis, ribosome biogenesis, and DNA repair [29, 34, 50-54]. Hrr25, Hhp1 and Hhp2 localize to the major microtubule organizing center of the cell, the spindle-pole body (SPB), and the site of cell division [50, 52]. These three sites

require extensive reorganization of cytoskeletal components. Several putative substrates fall into the category of proteins involved in cytoskeletal dynamics, such as stathmin and CSPP1 [55-57], providing the possibility that CK1δ/ε, like their yeast ortholog, are important for microtubule dynamics in mitosis.

It is clear that their localization to the SPB is functionally important for mitosis, but it is still unclear what function their activity has at the site of division. Whether CK1δ/ε function in a similar manner to Hrr25 and Hhp1/2, in nucleation of the mitotic spindle or control of mitotic exit, is currently unknown Further, we identified two components (Cdc27 and ANAPC4) of the E3 ubiquitin ligase anaphase-promoting complex (APC).

Accession #	Gene name	Identified phosphosites
Q9UQ35	SRRM2	S1379s S1378s S2365s S351s S353s S2272s T2316t T2275t S2280s T2289t T384t T400t S317s S323s T318t S322s S323s
Q09666	AHNAK	S212s S216s S5752s S5763s S5752s S5763s T5845t S5749s S5762s S5780s T5798t
P06748	NPM1	S106s S112s S217s S125s S254s
Q59HH7	XRCC1	T212t S213s T216t S218s T229t S233s S234s S237s S240s S243s T533t T537t S539s
Q9H6F5	CCDC86	S80s S91s S110s S113s S102s Y109y S50s T42t S91s S18s S21s S47s
A0A024QZJ7	CCDC6	S240s S244s S351s S352s S359s S367s T349t Y356y T376t
P49792	RANBP2	T19t S21s S2526s T2613t T2153t T2160t T1396t S1400s
A0A024RAY2	KRT18	S7s S15s S18s S30s S31s S34s
A0A024R8A2	GAPVD1	S566s S569s S757s S758s S761s T762t
B2RTY4	MYO9A	S266s S293s S294s S1362s S1363s S1364s
Q53HG7	CTTN	T399t T411t Y421y T401t S405s S418s
P29590	PML	S485s S502s S518s S527s S530s
P98164	LRP2	S3281s Y572y T583t T585t Y586y
Q9NYV4	CDK12	S681s S685s S382s S383s
Q9UJ94	LINC00527	T70t S104s
Q8WXI7	MUC16	T9325t S9329s S9330s S9331s T9333t S9334s S9341s S9345s T9347t S9348s
C9JWU6	OPN4	T14t T22t S38s S12s S35s S37s
B4DQZ7		S380s S383s S384s S386s T388t S392s
A4D2J9	CAMK2B	T320t T325t S327s T328t T333t
Q86UK0	ABCA12	S721s T724t S731s Y738y T740t
Q6XUX3	DSTYK	S716s Y720y Y722y S726s S727s
Q6ZN14		T108t S110s S112s S116s T117t
Q8WWY3	PRPF31	S445s S446s S450s S451s T455t
Q86WJ6	HCN1	T646t S651s S652s T654t
A0A0D9SEY1	MAP4K4	T576t S579s S580s S585s
A0A0C4DH71	PIGP	S5s T6t S7s S19s
B1AN92	EIF4G3	S9s S12s T14t T20t

Table 3-1: Putative substrates identified in each of the inhibitor-treatment samples

Accession #	Gene name	Identified phosphosites
Q14663	KBF2	S116s S134s S150s T156t
Q53GA4	PHLDA2	S138s S141s S144s T151t
B5MBZ0	EML4	S906s T908t T910t S914s
Q01167	FOXK2	S369s S373s S392s S398s
Q14676	MDC1	S963s S964s S988s S990s
Q9BU23	LMF2	S678s S682s S686s S699s
A0A024R821	EIF3B	S152s S154s S164s
Q9Y4M6	DKFZp434F222	S118s T121t S124s
Q8IWJ2	GCC2	T1381t S1384s T1388t
Q8IWY7	TTBK2	S665s S667s S668s
O14867	BACH1	T241t S244s S245s
B4DE15	SLC35A2	T314t S317s S321s
Q9NPI6	DCP1A	T309t S315s S319s
A0A024R9W5	HUWE1	S3919s T3924t T3927t
Q5T011	SZT2	S2116s Y2127y S2132s
Q52S25	HLA-B	S48s Y51y T55t
A0A024RA38	KBTBD2	T11t Y13y S16s
J3KPF3	SLC3A2	S37s, T39t S41s
L8EBH8	C18orf34	S4s S17s S19s
P43403	ZAP70	Y178y S179s T183t
Q96M86	DNHD1	T3967t S3970s S3974s
Q14511	NEDD9	S296s S298s T332t
Q13596	SNX1	S32s S39s T41t
Q70Z35	PREX2	Y502y T506t Y507y
Q9HCI5	MAGEE1	T270t S271s S277s
B4DDR8	MED24	S326s S353s T364t
O15371	EIF3D	T526t S528s S529s

Table 3-1: Putative substrates identified in each of the inhibitor-treatment samples

Accession #	Gene name	Identified phosphosites
E9PRY8	EEF1D	T563t S578s
Q9H501	ESF1	S657s S663s
A0A024R168	NR4A3	T266t S282s
Q6NZI2	CAVIN1	S202s S203s
A0A024RBS2	RPLP0	S304s S307s
E9PAV3	NACA	S2029s T2037t
Q03468	ERCC6	S429s S430s
Q9Y3F4	STRAP	S335s S338s
A0A024RCA7	RPLP2	S102s S105s
Q1MSJ5	CSPP1	S95s T98t
A0A087WYR8	CDH23	T1307t T1312t
Q9Y664	KPTN	S26s T45t
Q86TC9	MYPN	T251t S255s
A0A0B4J1V8	PPAN-P2RY11	S238s S240s
Q8TF72	SHROOM3	Y344y S348s
Q07889	SOS1	S1136s S1137s
Q9H2B4	SLC26A1	S578s T580t
E9PAU2	RAVER1	S724s S728s
Q6V1P9	DCHS2	S1737s T1741t
Q6LES2	ANXA4	S60s T61t
A0A024R5D9	SF1	S80s S82s
Q9H736		S118s T149t
Q59GS5	Pxn	S176s T193t
A7LNJ1	SLC20A1	T422t S432s
H7BYT1	CSNK1D	S382s S384s
Q96CE4 P50406	STMN1 HTR6	S16s S25s S249s S252s
Q96A49	SYAP1	S269s
B7Z8Q2		S204s
B2RDQ3		S26s
Q53GG0	LIM1A	S374s
Q9Y2V2	CARHSP1	T50t
Q92616	GCN1	T1631t
Q6P2E9	EDC4	S725s
Q86YB2	DHX8	T78t
G5E9U6	FKBP1B	S30s
O00264	PGRMC1	S181s
Q3KQU3	MAP7D1	T600t

Table 3-1: Putative substrates identified in each of the inhibitor-treatment samples

Accession #	Gene	Identified phosphosites
H3BSD9	MYO7B	Y21y S24s S30s
Q6YHK3	CD109	S1044s T1047t T1049t Y1051y T1054t
Q8WWI1	LMO7	T956t S960s S988s S991s S873s
P78332	RBM6	S912s T923t
Q5JTH9	RRP12	S1080s
P02545	LMNA	S615s
A0A024R3W7	EEF1B2	S106s
A0A0A0MTS7	TTN	S125s
J3KP11	CACNA1E	T1063t T1064t S1066s S1082s T1083t
Q8N412	STPG2	S25s Y26y T53t S57s
B3KWL5		S36s T38t S44s T54t
A0A024R8R6	CDR2L	S304s S308s
Q8WUA2	PPIL4	S178s
Q9UJX5	ANAPC4	S779s
E9PJ14	ING4	T41t S43s
P07814	EPRS1	T868t S891s
Q99618	CDCA3	S29s T37t S43s S31s S44s S199s S209s
P18858	LIG1	S141s T233t
Q14181	POLA2	S126s T130t S141s S150s S154s
Q9NQS7	INCENP	T298t S312s S314s
O76021	RSL1D1	T465t S467s S469s
Q12888	TP53BP1	S1426s S1430s
Q9H3S7	PTPN23	S1123s S1133s

Table 3-2: Putative substrates identified in the SR-1277 and SR-3029-treated samples

Accession #	Gene names	Identified phosphosites
Q7Z5J8	ANKAR	S436s Y438y T446t Y448y
Q86VR2	FAM134C	S435s T440t S433s S436s
Q96NM8		S143s T144t S146s S148s
P30260	CDC27	T356t S369s
A0A0C4DGZ0		S1864s
A0A087X1R1	SMTN	S411s T414t
Q8N6T3	ARFGAP1	S155s S160s
A0A024RA42	BZW2	S412s S414s
A8K6X9		T925t
B4DEE7	CIAO3	T164t
A0A087WXU3	ESYT2	S755s S758s
Q7Z4Q2	HEATR3	T228t S239s S242s S243s
P42331	ARHGAP25	S395s S398s T409t
Q96I05	SPOCD1	T336t
A0A024R2M0		T557t S563s S565s S566s
Q5VTM2	AGAP9	Y349y S363s Y367y
A0A024R9J3	COLEC10	Y198y S202s
Q5JPT6	GIG10	S509s S511s
P20700	LMNB1	T575t
P25874	UCP1	S218s T227t S231s S243s
Q9UPT8	ZC3H4	T1106t S1108s
Q4KMP7	TBC1D10B	T135t S141s T152t T154t
Q12802	AKAP13	S2749s T2750t T2753t
Q86XP3	DDX42	S111s
Q9NYF8	BCLAF1	T42t S44s
Q53EU0	Kaput	T398t S406s
O75155	CAND2	T112t T122t S124s T128t

Accession #	Gene names	Identified phosphosites
P20020	ATP2B1	S1257s
Q8N8N7	PTGR2	T317t S331s S350s
A0A024R2W3	PRKAR2A	S78s S80s
Q8WYP3	RIN2	Y881y T894t S895s
Q562F6	SGO2	S1239s T1243t
A0A024R233	TJP2	S398s S400s
Q5JSH3	WDR44	S470s S471s
P11388	TOP2A	S1387s
O60832	DKC1	S451s S453s S455s
Q9NR30	DDX21	S171s S173s

Table 3-3: Putative substrates identified only in the SR-1277-treated sample

CHAPTER 4

CK1δ/ε inhibition affects multiple cellular processes

Introduction

Members of the casein kinase 1 (CK1) family were some of the first protein kinases identified to modify proteins through the catalytic transfer of phosphate [1]. However, all family members were not identified until the early-to-mid nineties [2-5]. Members of the CK1 family are segregated by their localization pattern. In mammals, CK1γ1-3 localize to membranes, while CK1α, CK1δ and CK1ε are soluble and localize throughout the cell. In Chapter 2, I showed that endogenous CK1δ and CK1ε are enriched in the nucleus and centrosome, and therefore are in optimal positions to influence cell cycle progression.

The multiple and apparently overlapping or redundant roles of CK1δ and CK1ε, including in the Wnt and circadian clock pathways [6, 7], make it difficult to tease apart specific functions using siRNA or shRNA knockdown. These methods require incubation periods that are several cell cycles long, which can result in indirect consequences that elicit confounding phenotypes. Furthermore, knockdown efficiency can be heterogeneous within a population of cells, and this issue becomes more complex when moving from knockdown of one protein to the simultaneous knockdown of two proteins.

Small molecule inhibitors are an alternative tool for determining the effect of proteins, particularly those with enzymatic function, like kinases and phosphatases. They are effective in much shorter times, and their use provides increased certainty that an entire population of cells are uniformly affected. However, similar to shRNA and siRNA treatment, a shortcoming of small molecule inhibition is the possibility of off-target effects. Early CK1δ/ε inhibitors required high concentrations and had significant off-target effects, such as binding tubulin and disrupting microtubule nucleation [8, 9]. Small molecule inhibitors directed towards CK1δ/ε have become increasingly specific *in vitro* [10, 11], providing greater confidence that only CK1δ/ε are affected *in vivo*.

Recently developed Scripps inhibitors inhibit far fewer off-target kinases and have low IC_{50} values for CK1δ/ε [10].

To investigate whether CK1δ/ε activity is important for mitosis and/or the cell cycle at large, I used small molecule inhibitors and imaging techniques to analyze a set of molecular components involved in the cell cycle. I observed both mitotic defects and increased DNA damage in cells treated with CK1δ/ε inhibitors. The accumulation of DNA damage is likely due to CK1δ/ε functioning in a DNA damage repair pathway activated by DNA replication stress.

Results

Long-term CK1δ/ε inhibition results in mitotic defects

To investigate whether CK1δ/ε function in mitosis, I inhibited the enzymes for varying periods of time in HeLa and RPE-1 cells, 8-16 hours, and analyzed the cells' mitotic structures. First, an asynchronous cell population was treated with CK1δ/ε-inhibitors (0.5 μM SR-1277 or SR-3029) for the duration of a single doubling time (experimentally determined to be 16 hours; Figure 4-5A). Small molecule inhibition of CK1δ/ε resulted in 7-fold and 50-fold increases of mitotic cells with misaligned and unaligned chromosomes, respectively (Figure 4-5A & 5B). Additionally, there was a 6-fold increase of mitotic cells exhibiting multipolar spindles (Figure 4-5D). This phenotype is reminiscent of a mitotic spindle pole cohesion defect [12-15], suggesting CK1δ/ε may be involved in keeping the spindle pole intact. Because of the similarity in phenotype between cells treated with SR-1277 and SR-3029, only SR-3029 was used to test this possibility. Following the same protocol as previously described, I assayed for the presence of the centriolar marker centrin1 at spindle poles of multipolar spindles. SR-3029-treated cells with multipolar spindles had a significant increase in the percentage of poles with no centrioles and a similar decrease in poles with two centrioles (Figure 4-5E). This defect was observed in both HeLa and RPE-1 cells treated with SR3029, suggesting this is a general effect associated with CK1δ/ε inhibition. These initial experiments also led to the observation that SR3029-treated cells had mitotic spindles with less γ-tubulin at their spindle poles (Figure 4-5G). These results lead me to hypothesize that reduced γ-tubulin at the spindle poles affects spindle pole cohesion by

reducing the amount of force that the centrosome can sustain during chromosome congression [14]. To test this hypothesis, a CENP-E inhibitor was used to alleviate

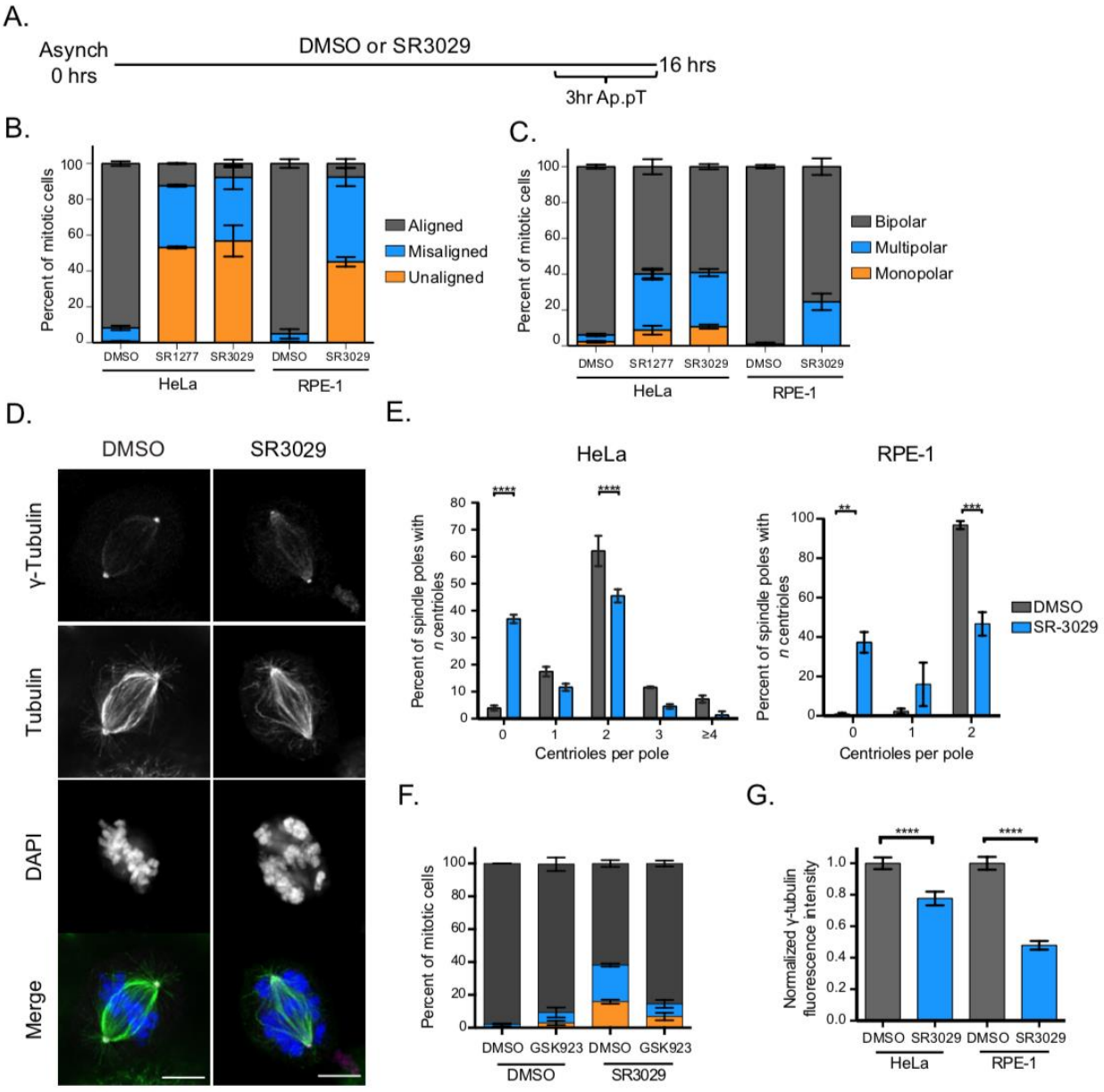

Figure 4-1. CK1δ/ε inhibition results in multipolar spindles, defects in chromosome alignment, and centrosome cohesion defects. A. Asynchronous HeLa cells were treated with CK1δ/ε inhibitors (0.5 μM SR-1277 and SR-3029[3]) or vehicle control (DMSO) for 16 hours. For the last three hours, cells were treated with APC/C inhibitors to arrest cells in metaphase. Cells were fixed and stained with α-tubulin and phospho-histone H3 or centrin and γ-tubulin. B. Percent of metaphase HeLa and RPE-1 cells with aligned, misaligned and unaligned chromosomes. Presented are representative cells with aligned, misaligned and unaligned chromosomes. C. Percent of metaphase HeLa and RPE-1 cells with bipolar, multipolar and monopolar spindles. D. Presented are representative cells with multipolar spindles. E. Percent of poles in multipolar spindles from HeLa and RPE-1 cells that contain 0, 1, 2, 3, or ≥4 centrioles. Representative multipolar spindles with different number of centrioles at spindles poles. ns = not significant. F. Percent of metaphase HeLa and RPE-1 cells with bipolar, multipolar and monopolar spindles after treatment with DMSO or SR3029 and DMSO of GSK923 (A CENP-E inhibitor) G. γ-tubulin fluorescence intensity after treatment with DMSO or SR3029 in HeLa and RPE-1 cells. Scale bar is 10 μm.* = p<0.05, ** = p<0.001, *** = p<0.005, **** = p<0.0001

some of the force imposed by the kinesin on the spindle pole to help mediate chromosome congression. Simultaneous inhibition of CK1δ/ε and CENP-E resulted in a significant decrease, and near rescue, of the multipolarity defect that results from CK1δ/ε inhibition (Figure 4-1F). These data provide the first evidence that CK1δ/ε function in promoting spindle-pole integrity in mitosis by promoting centrosome stability, and thus allowing the centrosome to handle forces necessary for chromosome congression.

Because long-term inhibition may present secondary phenotypes, I sought to understand the effects of CK1δ/ε inhibition within a shorter temporal scale. Treatment of asynchronous cells with DMSO or SR3029 was reduced to eight hours. Furthermore, instead of immunofluorescent analysis, I analyzed live HeLa cells expressing GFP-tubulin and H2B-mCh using a spinning disc confocal microscope. I analyzed cells that were about to enter or had just entered mitosis, as determined by a combination of the two fluorescent signals. None of the DMSO-treated cells showed significant chromosome misalignment, multipolarity or spindle-pole cohesion defects. However, all of the SR3029-treated cells analyzed showed signs of chromosome misalignment once cells entered mitosis (Figure 4-6A). Additionally, half of the cells became multipolar within the duration of imaging and showed signs of spindle pole cohesion defects (Figure 4-6A), similar to our immunofluorescence results (Figure 4-5E). As expected, those cells that had the most severe chromosome alignment defects did not exit mitosis, and either died or exceeded the duration of imaging (Figure 4-6B). These results indicate that inhibition of CK1δ/ε during S/G_2-phases of the cell cycle has an effect on the subsequent mitosis. We sought to determine if any of the observed mitotic defects arise when CK1δ/ε are inhibited as cells enter mitosis.

Short-term CK1δ/ε inhibition disrupts chromosome alignment in metaphase

To determine if the observed mitotic defects are a direct or indirect consequence of inhibiting CK1δ/ε activity, I treated cells with DMSO or SR-3029 for a shorter period of time (3 hours). I synchronized cells in S-phase using a sequential thymidine/aphidicolin block and release protocol [16]. After synchronization, cells grew uninhibited for seven hours. This was followed by inhibition of the APC/C in combination with DMSO or SR-

3029 for three hours (Figure 4-3A). Cells treated with SR-3029 displayed significant increases in misaligned and unaligned chromosomes (Figure 4-3B & C). The unaligned chromosome phenotype was less severe in cells treated with a CK1δ/ε inhibitor during entry into mitosis than cells treated for the duration of a single cell cycle. These results suggest that CK1δ/ε activity is critical for proper chromosome alignment as cells enter mitosis. In cells treated with SR-3029, there was no increase in multipolar cells and a negligible increase in the percentage of poles with no centrioles (Fig 4-3D). These two phenotypes are likely indirect consequences from inhibition of CK1δ/ε.

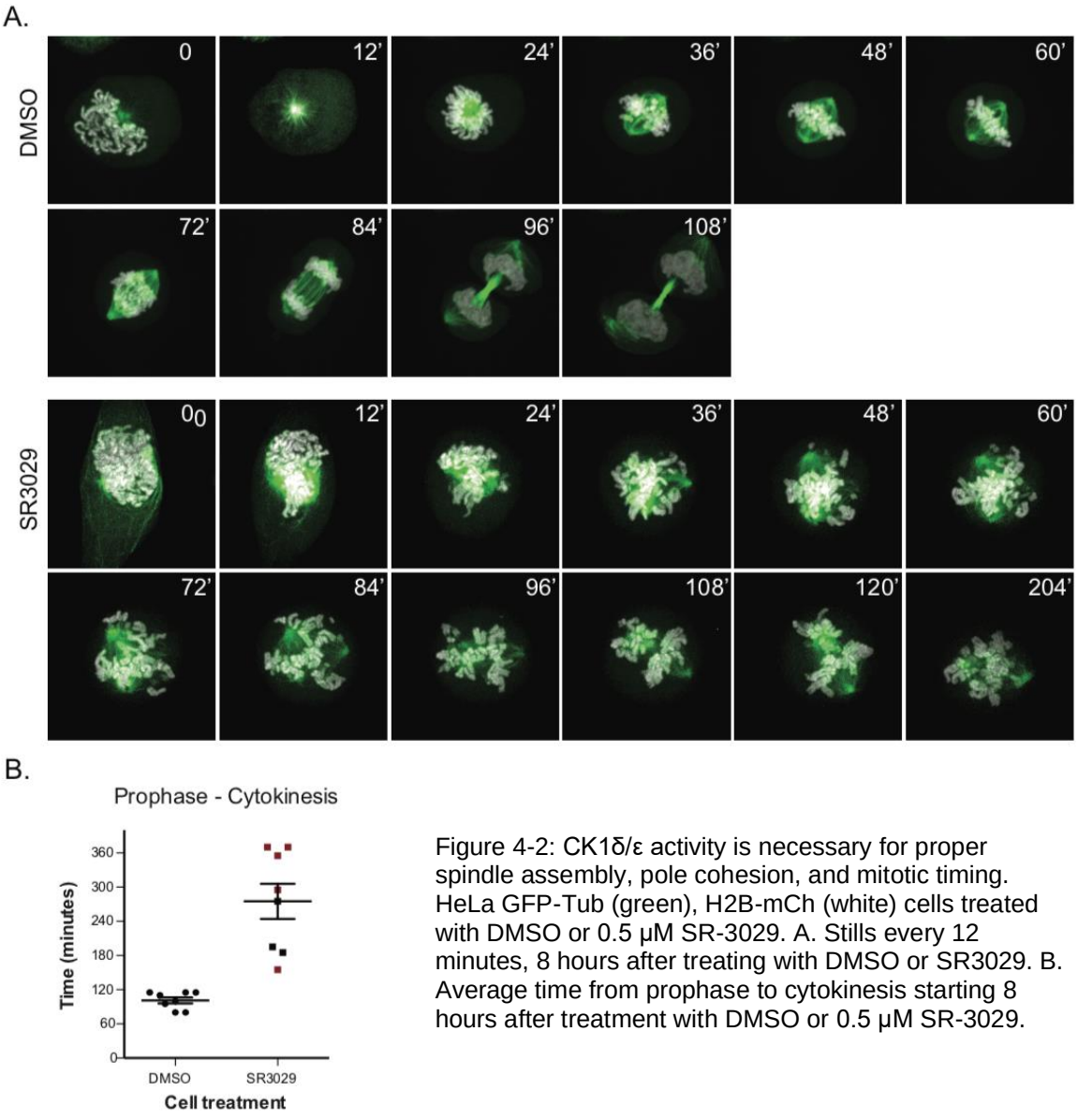

Figure 4-2: CK1δ/ε activity is necessary for proper spindle assembly, pole cohesion, and mitotic timing. HeLa GFP-Tub (green), H2B-mCh (white) cells treated with DMSO or 0.5 μM SR-3029. A. Stills every 12 minutes, 8 hours after treating with DMSO or SR3029. B. Average time from prophase to cytokinesis starting 8 hours after treatment with DMSO or 0.5 μM SR-3029.

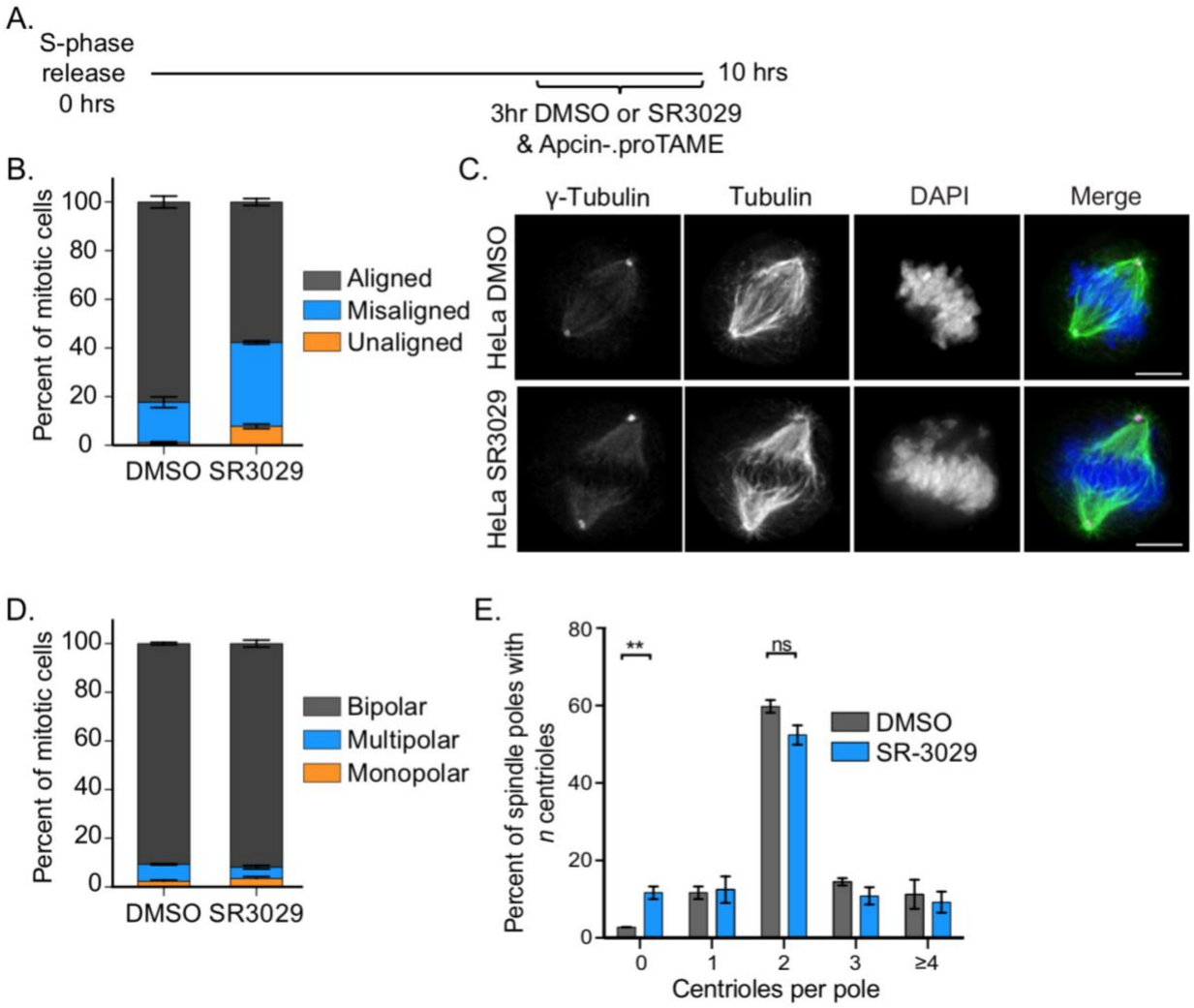

Figure 4-3. CK1δ/ε inhibition results in defects in chromosome alignment A. Schematic of synchronization protocol. 0.5 μM were treated with CK1δ/ε inhibitors (SR-1277 and SR-3029[3]) or vehicle control (DMSO) and with APC/C inhibitors to arrest cells in metaphase for three hours. Cells were fixed and stained with α-tubulin and phospho-histone H3 or centrinle and γ-tubulin. B. Percent of metaphase HeLa cells with aligned, misaligned and unaligned chromosomes. C. Representative metaphase cells. Scale bar = 10 μm D. Percent of metaphase HeLa cells with bipolar, multipolar and monopolar spindles. E. Percent of poles in multipolar spindles from HeLa that contain 0, 1, 2, 3, or ≥4 centrioles. Representative multipolar spindles with different number of centrioles at spindles poles. ns = not significant. * = $p<0.05$, ** = $p<0.001$, *** = $p<0.005$, **** = $p<0.0001$.

γH2A.X levels gradually increases over time as a result of CK1δ/ε inhibition

While conducting the previous experiments, I noticed cell populations treated with CK1δ/ε inhibitors were sparser than those treated with DMSO. Initial characterization of the Scripps inhibitors concluded that CK1δ/ε inhibition has an anti-proliferative effect on A375 cells [10]. These results are consistent with results from three previous publications. First, CK1δ$^{-/-}$ mice do not survive past perinatal stage 8 [17]. CK1ε

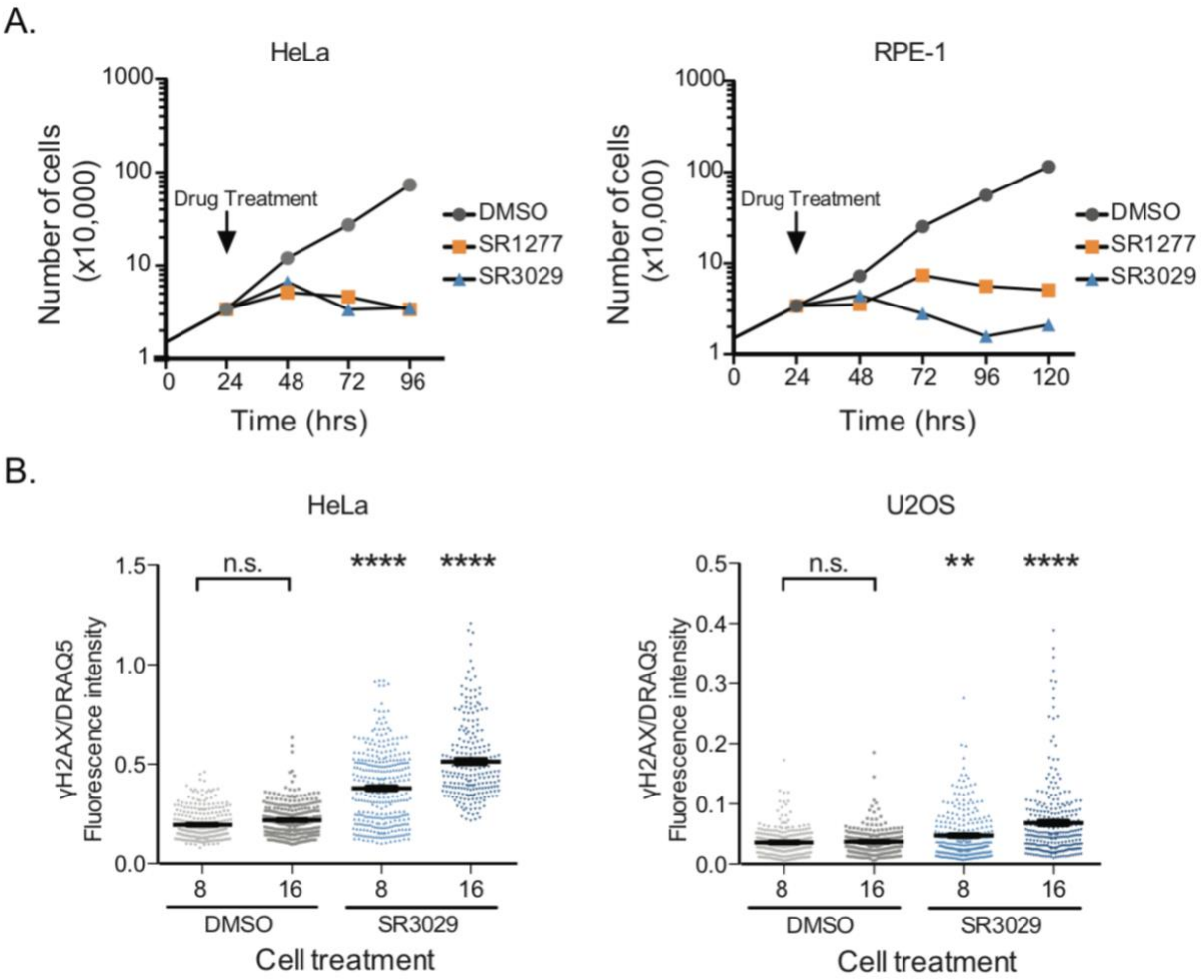

Figure 4-4. CK1δ/ε inhibition results in an accumulation of DNA damage A. Growth assays of HeLa and RPE-1 cells treated with DMSO and CK1δ/ε inhibitors. Cell number was counted every 24 hours. B. Asynchronous populations of HeLa and U2OS cells were treated with CK1δ/ε inhibitor for 8 or 16 hours. Cells were fixed and stained for DNA (DRAQ5) and γH2AX. The average fluorescence intensity ratio of γH2AX to DRAQ5 in nuclei were measured. ** = P<0.01, **** = P<0.0001

depletion in tissue culture cells results in cell death [18]. Lastly, CK1δ$^{-/-}$ mouse fibroblasts have an increase in γH2A.X levels [19], suggesting it has a function in DNA damage repair. Further, their function in cell survival is consistent with growth defects observed in yeast *hrr25Δ* and *hhp1Δ /hhp2Δ* mutants [20, 21]. To begin investigating how CK1δ/ε promote DNA damage repair, I performed similar experiments to those previously mentioned using the CK1δ/ε inhibitors. HeLa and RPE-1 cells treated with SR-1277 and SR-3029 for 3-4 days showed a significant drop in proliferation, similar to what has been observed previously (Figure 4-4A). I next tested whether CK1δ/ε

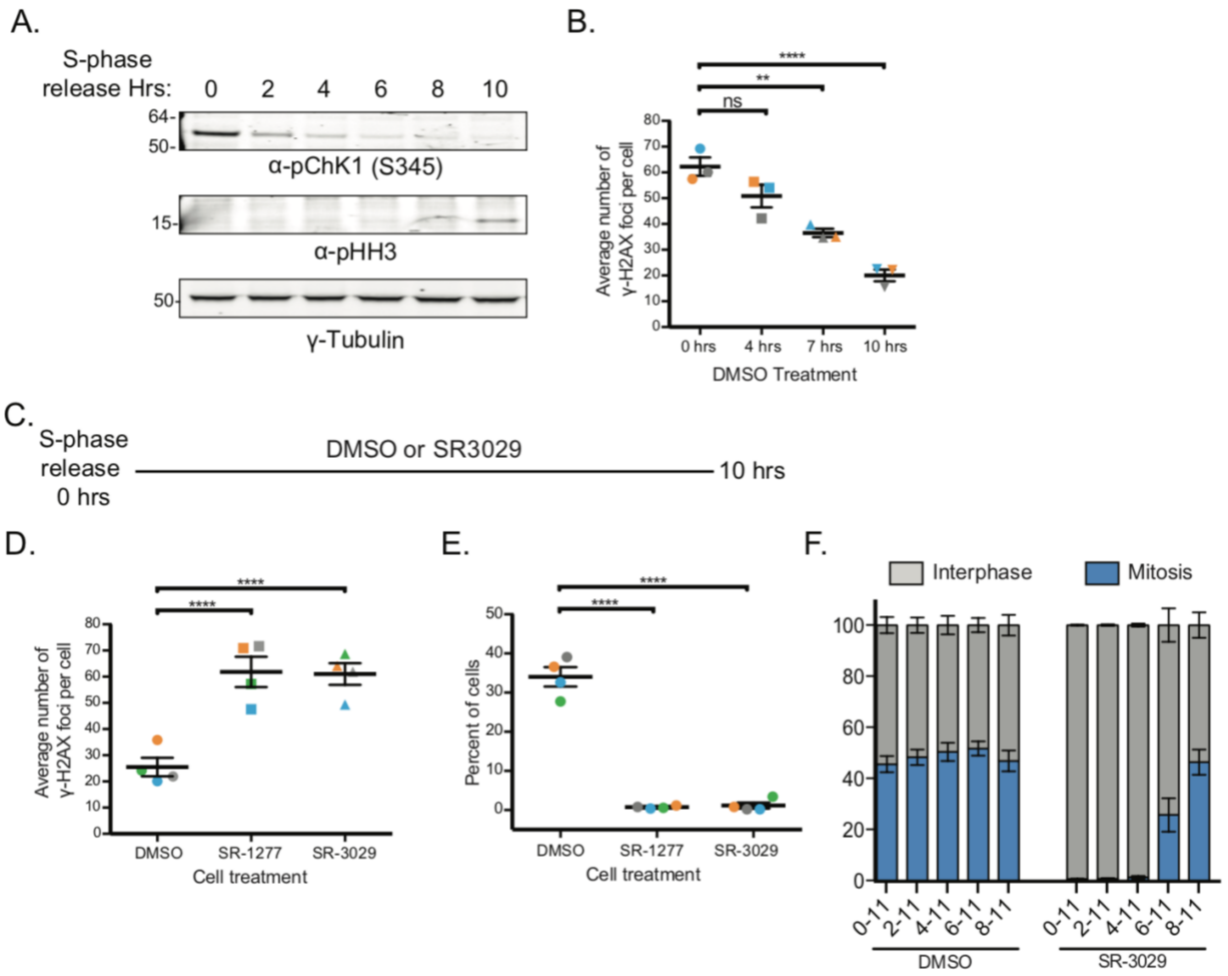

Figure 4-5. CK1δ/ε function in DNA damage repair resulting from replicative stress. A. Immunoblots of HeLa WCL arrested in S-phase or released from S-phase and collected in two-hour increments. Membrane was plotted with antibodies directed to phospho-Chk1, pHH3 and gamma-tubulin. B. Cells were synchronized and released into S with DMSO. Cells were fixed and stained right after release, 4, 7, and 10 hours after release. The average number of γH2AX foci per cell were measured. C. Experimental procedure utilized for D and E. D. The same experiment was conducted, but cells were treated with CK1δ/ε inhibitors or vehicle control for 10 hours after release. E. The mitotic index was measured for each group. F. Percent of cells in interphase and mitosis for samples treated for the indicated time frames after release from an S-phase arrest. ** = P<0.01, **** = P<0.0001

inhibition affects γH2A.X levels. I treated HeLa and U2OS cells with DMSO or SR-3029 for 8 or 16 hours. Both cells gradually accumulated γH2A.X fluorescence intensity, indicating an accumulation of DNA damage (Figure 4-4B).

CK1δ/ε activity promotes DNA damage repair

To test if CK1δ/ε are involved in DNA repair, I began by studying the kinetics of DNA damage repair following release from S-phase (Figure 4-5A-F). CK1δ/ε inhibition blocked DNA-damage repair, as evidenced by the persistence of γH2A.X foci, which

resulted in a near complete inhibition of mitotic entry (Figure 4-5D & E). Cells released from an S-phase arrest prior to CK1δ/ε inhibition gradually entered mitosis after the 6-hour time-point (Figure 4-7F) and at this time point, γH2A.X foci are near their lowest levels, indicating resolved DNA damage (Figure 4-7B). These data suggest CK1δ/ε activity is necessary for DNA-damage repair.

Discussion

Multipolar mitotic spindles generally arise through one of two mechanisms. One is through the presence of supernumerary centrosomes, resulting from centriole over duplication or cytokinesis failure [13, 22]. A second is through spindle-pole shearing, resulting from early centriole disengagement or loss of spindle-pole integrity [13, 23, 24]. The observed mitotic defects associated with long-term CK1δ/ε inhibition are reminiscent of the last example. The mechanism by which loss of spindle-pole integrity leads to spindle multipolarity is not well understood, but multiple pathways likely feed into this function. One pathway involves Plk1-dependent phosphorylation of a centrosome satellite protein, Kizuna [12]. Plk1 and centrosome satellite proteins are important for γ-tubulin localization to the centrosome [25, 26]. A second pathway involves phosphorylation of ch-TOG and TACC3 by Aurora-A and integrin-linked kinase [27, 28]. Similar to my results, loss of spindle-pole integrity can be rescued by inhibiting spindle-assembly motors. Spindle-pole integrity resulting from dynein light-intermediate chain depletion was rescued by inhibiting Eg-5 [15]. Defects associated with CLASP1/2 depletion were rescued by inhibition of CENP-E. My results suggest CK1δ/ε activity feeds into one of these pathways to promote spindle-pole integrity.

The spindle pole integrity defect is likely a consequence of CK1δ/ε activity in S-phase. CK1δ/ε activity is necessary to resolve DNA damage resulting from replication stress. As a result, the DNA damage checkpoint is activated and stalls the G_2/M transition. One critical process that occurs during this period is centrosome maturation, resulting in restructuring centrosomal scaffolding proteins and an increase in γ-tubulin protein levels at the centrosome [29, 30]. CK1δ/ε inhibition may disrupt these processes by stalling cell cycle progression, increasing the likelihood of defects as time passes. Many cell-cycle proteins localize to the centrosome [31-35]. It is possible that CK1δ/ε

activity directly or indirectly promotes their centrosomal localization or just signaling as a consequence of stalling DNA damage repair.

My data suggest CK1δ/ε have a more direct function in promoting chromosome alignment in metaphase than spindle polarity or spindle-pole integrity. This would be consistent with CK1ε localization to the kinetochore[36]. Although I did not observe this localization pattern in Chapter two, it may be transient and require live cell imaging to observe. These results are also consistent with identification of several centromere and kinetochore localized candidate substrates from Chapter three.

Soluble yeast CK1 orthologs were first characterized for their role DNA damage repair. My results are consistent with previous conclusions that CK1δ/ε function in DNA damage repair, indicating this is an important function of soluble CK1 family members. It is still unclear whether CK1δ/ε function directly or indirectly in DNA damage repair, but my data suggests they are necessary for DNA repair before cells enter mitosis. My data also leaves open the possibility that CK1δ/ε function in G_2 to promote entry into mitosis, independent of any DNA repair function.

CHAPTER 5

Conclusions and future directions

Chapter Summaries

Casein kinase 1δ and casein kinase 1ε (CK1δ/ε) are serine/threonine protein kinases that function in a wide variety of biological processes. They have the greatest degree of sequence similarity among CK1 family members and are predicted to have largely redundant functions. Although there have been hundreds of publications on their importance in cellular processes, a precise characterization of their interacting partners and substrates has not been undertaken. In the previous chapters, I presented the production of tools and implementation of experiments to probe the localization, interacting partners, and substrates of CK1δ/ε.

In Chapter two, I identified the proteins that co-purify with CK1δ/ε. This was accomplished by producing cells in which CK1δ and CK1ε were endogenously tagged with a fluorescent protein containing a multi-affinity purification epitope. I identified GAPVD1 as a major interacting partner of both CK1δ/ε throughout the cell cycle. GAPVD1 was determined to be phosphorylated by CK1δ/ε, and this phosphorylation was necessary for GAPVD1's function in promoting endocytosis. The cellular tools I produced also allowed me to visualize the localization patterns of endogenous CK1δ/ε for the first time. By knowing their interacting partners, as well as having an accurate grasp of their localization pattern, we have the opportunity to begin asking questions regarding what is necessary for CK1δ/ε localization and function.

In Chapter three, I identified CK1δ/ε substrates using a combination of cell synchronization, small molecule inhibition and quantitative phosphoproteomics. The primary goal was to determine mitotic substrates of CK1δ/ε, but we likely identified substrates important in other cell cycle phases. Three small molecular inhibitors were used to maximize the likelihood of identifying authentic substrates. Putative substrates will be prioritized for future experiments based on the samples in which they were identified. The top priority will be those identified in all three inhibitor-treated samples,

followed by the identification in the two Scripps inhibitor samples, and then in just the SR-1277-treated sample.

Collectively, my projects produced two catalogues of proteins that will provide additional insights into CK1δ/ε functions. It will be important to validate interacting partners and substrates, and determine how their association with CK1δ/ε affect the cellular functions in which CK1δ/ε are involved. It is also of great interest to me to determine how the interacting proteins and substrates relate to each other through CK1δ/ε.

The importance of CK1δ/ε localizations

Chapter two describes the localization pattern of CK1δ/ε throughout the cell cycle. My initial interest was in determining how CK1δ/ε localize to the centrosome. This interest was primarily fueled by CK1δ/ε enrichment to the centrosome in overexpression models, as well as the importance of the centrosome as a signaling hub [2-6]. After producing tools to visualize the localization of endogenous CK1δ/ε, it became clear that their localization pattern is much more complicated and dynamic than previously described [7]. They are consistently in the nucleus, at the cell periphery and in dynamic puncta (Figure 2-2), suggesting their localizations are more similar to the yeast orthologs, Hrr25 and Hhp1/2, than we had previously understood. The localization of a protein is often important for its function in a specific cellular process. My hypothesis that this is true for CK1δ/ε stems from two observations in the literature. First, CK1δ is reported to accumulate in the nucleus after DNA damage [8], suggesting its change in localization is functionally relevant to DNA damage repair. Second, Hhp1/2 protein levels at the SPB increase after mitotic stress [9]. The SPB localization of Hhp1/2 is necessary for inhibiting downstream signaling for cytokinesis, but it is unclear if the increase in protein levels is required. To understand the localization pattern of CK1δ/ε under homeostatic and stressed conditions, it will be imperative to determine the proportion of CK1δ/ε at different locations in the cell. The most accurate method for making this determination would be to endogenously tag different cell cycle markers in the CK1δ/ε$_{mNG/mNG}$ cell lines, and use imaging approaches to measure the amount of CK1δ/ε at these locations. For instance, a CK1δ/ε$_{mNG/mNG}$ cell line with γ-tubulin tagged

with a red fluorescent protein could be used in combination with Hoechst staining to compare CK1δ/ε-mNG abundances in the nucleus with those at the centrosome. DIC imaging could be incorporated to delineate the entire cell, allowing us to determine the fractions of CK1δ/ε-mNG in the nucleus and at the centrosome compared to their overall cellular levels. This analysis could be performed at different stages of the cell cycle and during different stress conditions. Of particular interest to me is to determine if CK1δ/ε behave in a similar manner as Hhp1/2 (e.g. accumulate at centrosomes) under conditions of mitotic stress.

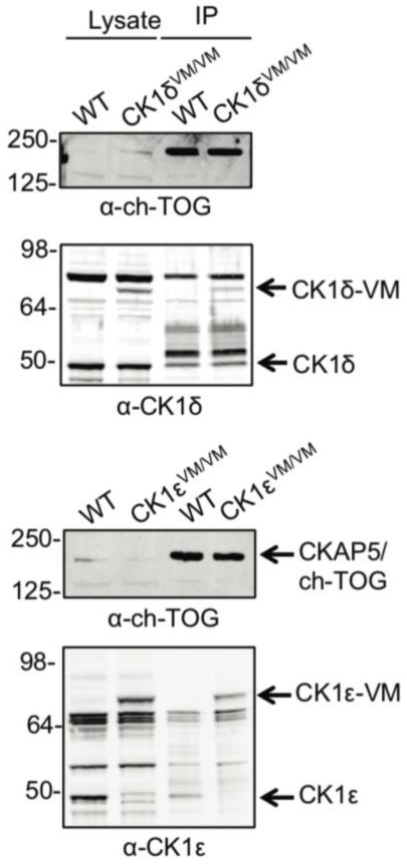

Figure 4-1. ch-TOG interacts with CK1δ/ε. Immunoprecipitation of CKAP5 from HEK293 CK1δ$_{VM/VM}$ and HEK293 CK1ε$_{VM/VM}$ cells. Whole cell lysates and IP samples are blotted with GAPVD1, CK1δ/ε, or CK1ε antibodies.

To our surprise, we did not find a single core centrosomal protein (Cep), or AKAP450 [10], in our search for CK1δ/ε interacting partners. Although we did not identify a canonical centrosomal anchoring protein, we did identify ch-TOG, a microtubule-binding protein. ch-TOG functions in microtubule polymerization at the centrosome in interphase, and spindle pole and kinetochore during mitosis, making it very important for microtubule-based transport, mitotic spindle assembly and chromosome segregation [11-13]. ch-TOG contains five microtubule-binding domains and a C-terminal coiled-coil domain responsible for localizing it to the centrosome [12]. CK1δ/ε co-immunoprecipitated with ch-TOG from HEK293 lysates when ch-TOG was isolated using a commercially available antibody (Figure 4-1). Future experiments should focus on determining the nature of their interaction. Does ch-TOG target CK1δ/ε to the centrosome, and, if so, is their interaction direct? If their interaction is direct, what are the residues on CK1δ/ε that are responsible for their interaction? A CK1δ/ε centrosome-targeting mutant would be an excellent tool

for investigating the importance of CK1δ/ε localization to the centrosome. Further, do CK1δ/ε affect ch-TOG localization or function through their interaction, and is ch-TOG a CK1δ/ε substrate? A long-term direction would be to endogenously tag ch-TOG with a fluorescent protein in unmodified cell lines, as well as in cell lines where CK1δ, CK1ε, or both enzymes are knocked out. These cells would be used to monitor ch-TOG localization, and be compared to the effect of inhibiting CK1δ/ε with small molecule inhibitors.

An open question that arose in Chapter two was whether CK1δ/ε affects any catalytic function of GAPVD1. The GAP and GEF domains have been reported to have function as individual recombinantly produced domains [14], but neither GAP nor GEF activity has been demonstrated using full-length GAPVD1. Further, the full-length protein, as well as individual GAP or GEF domain deletion mutants, are unstable when expressed in mammalian cells or bacteria. This made it technically impossible to perform GAP and GEF assays, and to determine whether CK1δ/ε phosphorylation affected those activities. Future experiments would focus on producing and purifying recombinant GAPVD1 from insect cells. This approach may be more suitable for isolating a more stable protein. Another possibility is that GAPVD1 stability is increased when phosphorylated. This stems from our observation that all of the CK1δ/ε-dependent phosphosites are located in a region of GAPVD1 that is predicted to be intrinsically disordered (Figure 2-5A) and GAPVD1 is consistently phosphorylated throughout the cell cycle (Figure 2-5C). To test if phosphorylation is important for producing a stable recombinant protein, GAPVD1 and CK1δ/ε could be co-expressed in insect cells or bacteria. If both approaches are successful, purified GAPVD1 (unphosphorylated and phosphorylated) would be used to test if phosphorylation affects its GAP and/or GEF function.

Whether the interaction between CK1δ/ε and GAPVD1 functions in biological processes aside from endocytosis is an area of interest. GAPVD1 was implicated in the circadian rhythm pathway through its participation in a complex containing CK1δ, Per and Cry; Per1 & 2 and Cry1 & 2 were present in both our CK1δ and our CK1ε purifications [1]. Importantly, three Per complexes were identified in the aforementioned

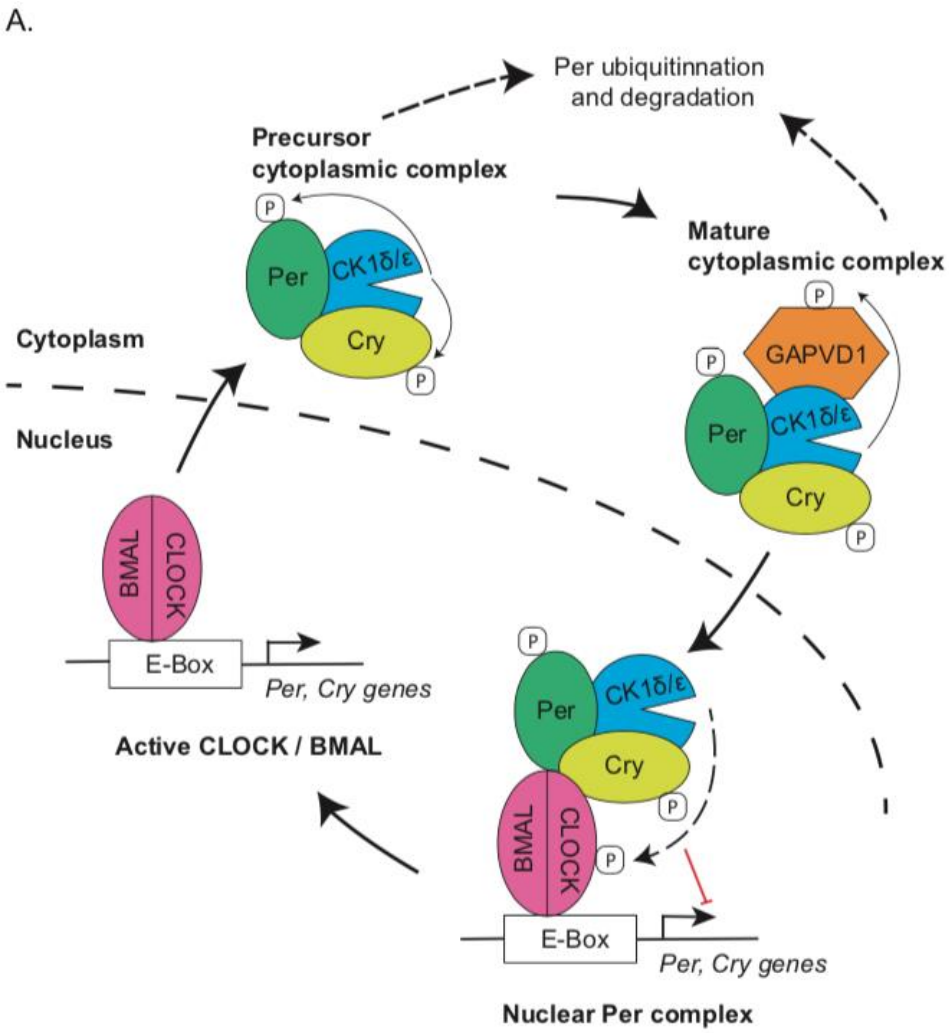

Figure 4-2: GAPVD1 participates in the circadian rhythm pathway. A. Model of circadian clock complexes. Adapted from [1]. Dashed arrows indicate untested pathways B. Growth assay of HeLa WT and GAPVD1$^{-/-}$ #1-3. Each color corresponds to an individual experiment.
* = $p<0.05$, ** = $p<0.001$, *** = $p<0.005$

study; one in the nucleus and two in the cytoplasm. CK1δ was identified in all three complexes, while GAPVD1 was identified in the larger cytoplasmic complex, which was referred to as the Mature Cytoplasmic Per complex (Figure 5-2A) [1]. GAPVD1 depletion from mouse fibroblasts resulted an increase in circadian period, similar to small molecule inhibition of CK1δ/ε [1, 15-17]. However, the mechanism by which GAPVD1 functions in the control of circadian rhythm is an open question. My preliminary data regarding the effect of GAPVD1 loss on the cell cycle suggests it is important for cell cycle duration (Figure

5-2B). The increase in doubling time would be consistent with the relationship between circadian rhythm proteins and the cell cycle machinery that affects cell-cycle timing [18-21].

Several experiments can be conducted to determine how GAPVD1 feeds into the circadian clock. Because GAPVD1 is only present in a mature cytoplasmic Per complex [1] and it is most notably known for its function in protein trafficking, one hypothesis is that GAPVD1 functions to transport the Per complex to the nucleus. Wild-type and GAPVD1$^{-/-}$ HeLa cells could be used to determine the proportion of Per and Cry proteins in the nucleus versus the cytoplasm. If GAPVD1 affects their transport to the nucleus, then you would expect to see a reduction in Per and Cry protein levels in the nucleus. It is likely that this effect could only be detected within a specific window of time in the circadian clock and cell cycle. Therefore, GAPVD1 production could be knocked out in mouse reporter fibroblasts [1] to assess whether it functions in delivering a mature Per complex to the nucleus. These same cell lines can be used to determine if loss of GAPVD1 affects the composition of the cytoplasmic Per complex. Each *Per* and *Cry* gene could be modified to produce a protein tagged with Venus-MAP in wild-type and GAPVD1$^{-/-}$ cells. These cell lines would then be used to purify Per-VM and Cry-VM from cytoplasmic extracts, followed by mass spectrometry to determine the associated proteins. These experiments could be taken a step further and use iTRAQ-based phosphoproteomics to have a quantitative readout of protein levels from each sample. If an effect on cytoplasmic Per complex formation or transport to the nucleus is observed, the GAPVD1$^{-/-}$ cells could then be used to re-introduce wild-type and the phospho-mutants to determine if CK1δ/ε phosphorylation is important for GAPVD1 function in the circadian rhythm pathway. The most accurate assessment would be made by making GAPVD1-positive stable cell lines in the GAPVD1$^{-/-}$ background, allowing you to have a homogenous population of cells.

CK1δ/ε mitotic substrates

We have only begun to scratch the surface in determining CK1δ/ε mitotic substrates. Those proteins identified as putative substrates in all three inhibitor-treated

samples should be the top priority for future work. Analysis would begin by using lysates from cells treated or not with CK1δ/ε inhibitor to probe for phospho-shifts on polyacrylamide gels. I have begun by examining CK1δ itself. CK1δ clearly decreases in mobility during mitosis (Figure 5-3). The decreased mobility is partially eliminated by inhibiting CK1δ/ε, suggesting that CK1δ is autophosphorylated or phosphorylated in trans by CK1ε in M phase (Figure 4-3). A post-doctoral fellow in the Gould lab, Dr. Sierra Cullati, is currently identifying all of the autophosphorylation sites on Hhp1/2 and CK1δ/ε using *in vitro* assays. Future work could combine our efforts to determine the importance of CK1δ autophosphorylation in mitosis, and other biological processes. An undergraduate student in the lab, Eric Zhang, assisted me in producing multiple CK1δ$^{-/-}$ U2OS cell lines (data not shown). These cells could be used to re-introduce wild-type and CK1δ phospho-mutants to evaluate protein mobility at different stages of the cell cycle. The three phospho-sites identified on CK1δ in Chapter 3 have been tested by Sierra and verified as autophosphorylation sites (data not shown). However, they were not the full complement of sites. The 3A phospho-mutant and a phospho-mutant with the full complement of sites mutated to alanine would be used in future experiments to determine which sites are important for a change in protein mobility in mitotic samples. The mutant with the greatest effect could then be used to evaluate if CK1δ autophosphorylation is important for chromosome alignment in mitosis, as seen in Chapter 4 (Figure 4-3B).

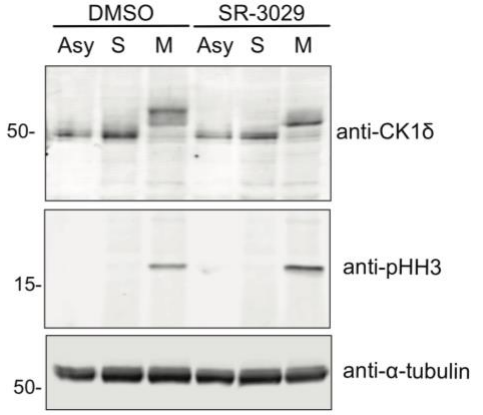

Figure 5-3: CK1δ is autophosphorylated in mitosis. Immunoblots of WCLs of CK1δ, pHH3, and α-tubulin from asynchronously growing (Asy) WT HeLa cells or HeLa cells synchronized in S-phase (S) and metaphase (M). 1 μM SR-3029.

A parallel approach would be to create CK1δ/ε C-terminal truncation mutant cell lines. Because the C-terminal tails of CK1δ/ε are autophosphorylated and targeted by other kinases, this would have a more global effect on CK1δ/ε function. However, this approach would be worthwhile for two reasons. First, CRISPR/Cas9 could be used to introduce a stop codon at the end of the kinase domain of each enzyme; therefore,

ell

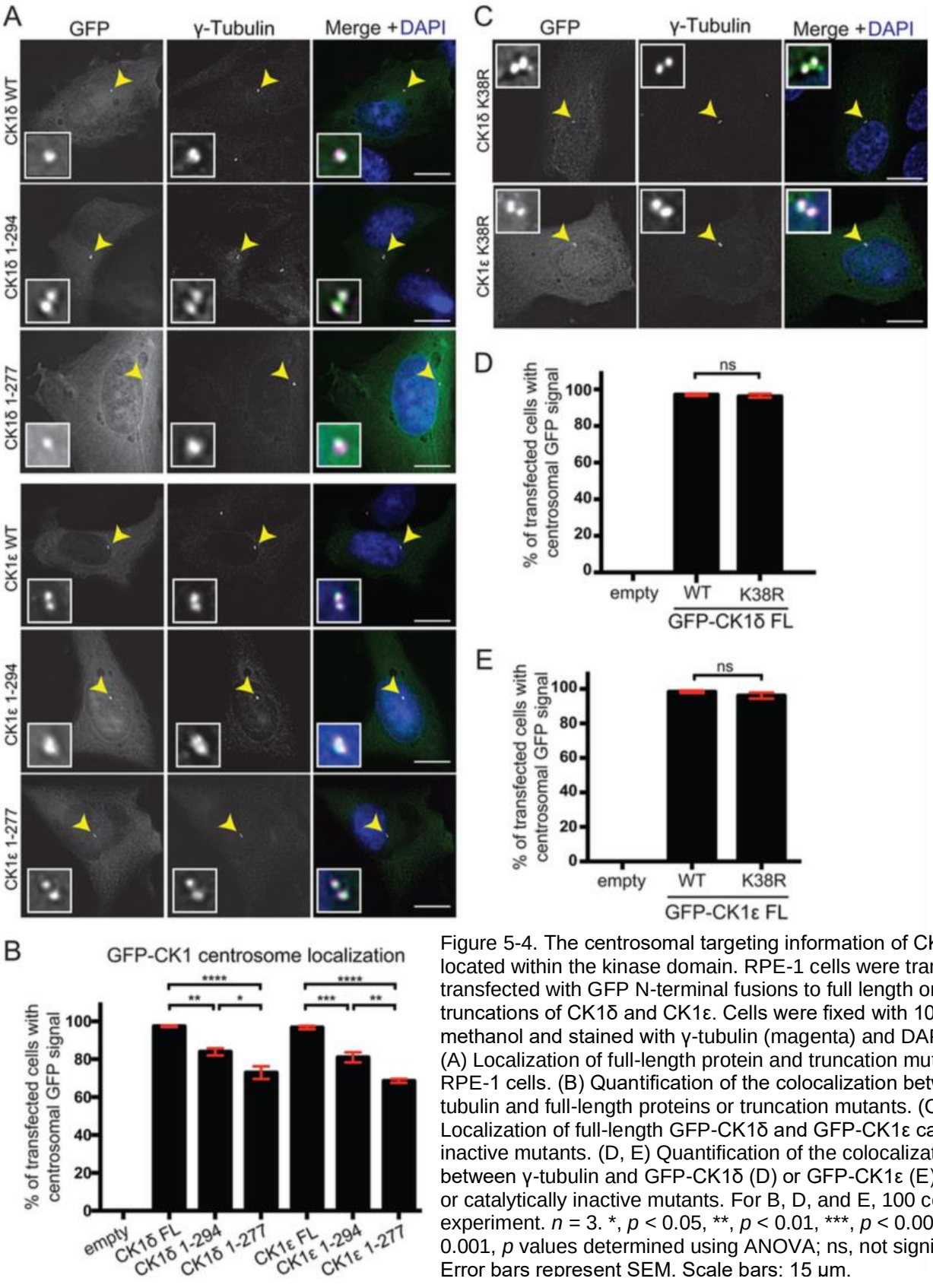

Figure 5-4. The centrosomal targeting information of CK1δ/ε is located within the kinase domain. RPE-1 cells were transiently transfected with GFP N-terminal fusions to full length or truncations of CK1δ and CK1ε. Cells were fixed with 100% methanol and stained with γ-tubulin (magenta) and DAPI (blue). (A) Localization of full-length protein and truncation mutants in RPE-1 cells. (B) Quantification of the colocalization between γ-tubulin and full-length proteins or truncation mutants. (C) Localization of full-length GFP-CK1δ and GFP-CK1ε catalytically inactive mutants. (D, E) Quantification of the colocalization between γ-tubulin and GFP-CK1δ (D) or GFP-CK1ε (E) wild type or catalytically inactive mutants. For B, D, and E, 100 cells per experiment. $n = 3$. *, $p < 0.05$, **, $p < 0.01$, ***, $p < 0.005$, ****, $p < 0.001$, p values determined using ANOVA; ns, not significant. Error bars represent SEM. Scale bars: 15 μm.

lines could be used to provide qualitative differences with the autophosphorylation mutant, providing insight into how other kinases affect CK1δ/ε function. Lastly, these cells could be used to determine if endogenous CK1δ/ε depend on their C-termini for their localization pattern. Most importantly, to the centrosome. Hhp1/2 kinase domains alone localize to the SPB, indicating they do not require their C-terminal tails [6]. GFP-tagged CK1δ/ε kinase domains expressed in RPE-1 cells, over the endogenous protein, largely localize to centrosomes, but at a significantly lower degree than the full length enzyme [6]. This result suggests the C-terminus play a minor role in localizing CK1δ/ε to the centrosome.

A role for CK1δ/ε in the G_2/M-phase transition

The ultimate objective of a cycling cell is to accurately replicate its DNA and to segregate the replicated DNA into two physically distinct, but chromosomally identical, daughter cells. These two objectives are accomplished in S- and M-phase respectively, and are separated by two periods of growth (G_1- and G_2-phase). Coordination between these four phases is critical to the survival of a cell, given the importance of chromosomal separation to occur after DNA replication. Two sets of proteins that help coordinate the cell cycle are cyclins and cyclin-dependent kinases (CDK). Cyclins are a family of proteins that are expressed during discrete periods of the cell cycle (Figure 1-2). Family members form a complex with, and subsequently help activate, different cyclin-dependent kinases (CDKs) [22]. The activity of cyclin-CDK dimers is largely responsible for progression and completion of each phase of the cell cycle by propagating specific signaling pathways.

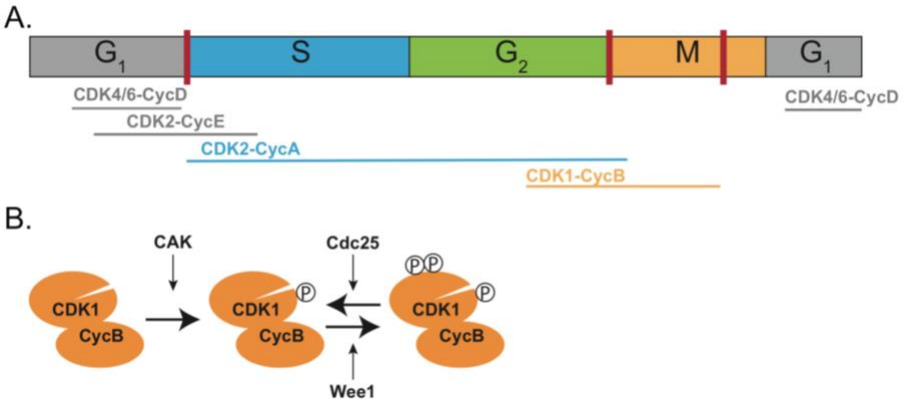

Figure 5-5. Cell cycle control by Cdk-cyclin activity. A. Schematic of different active cyclin-Cdk protein complexes throughout the cell cycle. Red bars correspond to checkpoint. B. Kinases and phosphatase that regulate Cdk1-cyclin B activity.

Cells have multiple checkpoints that mediate proper cell cycle progression. Checkpoints must sense errors in the cell cycle and halt cell-cycle progression until the error(s) has been resolved, after which the cell cycle resumes. These checkpoints are present throughout the cell cycle and are necessary for ensuring fidelity of genomic replication and segregation (Figure 4-4A). The G_2/M checkpoint ensures the cell has accurately duplicated its genomic material and grown sufficiently to enter mitosis. The G_2/M checkpoint is dependent on CDK1 inactivation via a combination of Wee1-dependent phosphorylation of CDK1 and inactivation of Cdc25 (Figure 4-4B) [23, 24]. When the G_2/M checkpoint if alleviated, Cdc25 becomes active, allowing for dephosphorylation of the Wee1 sites on CDK1 [25-27]. The DNA-damage checkpoint can feed into the G_2/M phase transition by inhibiting Wee1 degradation and Cdc25 activation [23].

CK1δ/ε are implicated in control of the G_2/M transition in different ways. CK1δ is reported to inhibit mitotic entry by phosphorylating and activating Wee1 [28]. However, some evidence for this mechanism was obtained using inhibitors at a concentration that also blocks CK1ε activity, making it difficult to interpret. CK1ε is reported to phosphorylate Cdc25A on Ser82 in interphase, and after DNA damage, to keep Cdc25A levels low [29]. However, direct phosphorylation and phospho-mutants were not utilized in this study, bringing into question whether CK1ε directly phosphorylates Cdc25A. Interestingly, although we did not identify Wee1 or Cdc25A as putative substrates in Chapter three, we did identify a negative regulator of Wee1, the F-box protein CDCA3/Tome-1 [30-32]. This raises the possibility that CK1δ/ε may function both directly and indirectly to regulate Wee1. The role of CDCA3 in Wee1 degradation has not been directly tested, but its yeast ortholog, Tome-1, promotes Wee1 degradation at the G_2/M phase transition. After verifying CDCA3 as a CK1δ/ε substrate, I would determine if Wee1 ubiquitination and degradation is affected by CK1δ/ε inhibition. If so, it would provide evidence of a downstream effect of CK1δ/ε inhibition.

A role for CK1δ/ε in mitosis

Cdk1 signaling activates Plk1 and Aurora A [33-38], which then promote centrosome maturation and construction of the mitotic spindle [39-41]. Proper mitotic

spindle assembly and accurate kinetochore-microtubule attachments are necessary for chromosome alignment in metaphase. Proper kinetochore-microtubule attachment generates tension at the centromeres of sister chromatids that is monitored by the chromosomal passenger complex, composed of Aurora B, INCENP, and borealin. Once chromosomes are properly aligned between the spindle poles, the M-phase checkpoint, also known as the spindle assembly checkpoint (SAC), is alleviated. This results in activation of the APC/C, an E3 ubiquitin ligase responsible for initiating the degradation of cyclin B and securin [42, 43]. Cyclin B degradation results in inactivation of Cdk1 and mitotic exit, while degradation of securin allows sister chromatid segregation to opposite poles.

CK1ε is reported to localize to the kinetochore, a significant mitotic signaling hub, in prometaphase [44]. Although we did not observe kinetochore localization in our CK1ε$_{mNG/mNG}$ cell lines, CK1ε-mNG is enriched at the centrosome and has a strong signal throughout the cytoplasm in metaphase (Figure 2-2), which would make it difficult to see kinetochore-specific localization. Consistent with the possibility that CK1ε localizes at the kinetochore, putative kinetochore-associated substrates were identified in Chapter 3. INCENP was identified in the overlap between the SR-treated samples, shugoshin 2 was identified in the SR-1277-treated sample, and CENP-F was identified in the SR-3029-treated sample (Table 3-2 & 3) [45-60]. Additionally, a mitotic pole-associated protein that functions in spindle formation and proper cytokinesis, CSPP1, was identified in the overlap between all three inhibitor-treated samples (Table 3-1) [61]. All four of these putative substrates provide avenues of research for determining how CK1δ/ε may function in mitosis. Each of the proteins could be analyzed for protein mobility using SDS-PAGE and immunoblotting. If they can be produced and purified from bacteria, they could be tested as substrate with *in vitro* assays. If INCENP were verified as a CK1δ/ε substrate, its association with other CPC components could be tested through immunoprecipitation of the protein.

Imaging GFP-tubulin and H2B-mCh cells for shorter periods of time could provide insight into the severity of the chromosome alignment defect and whether it disrupts chromosome segregation and cytokinesis. Future experiments would include

incorporation of CENP-E inhibition to replicate the rescue experiment in a shorter time-frame.

CK1δ/ε network connections

The experiments described in Chapters 2 and 3 provide a broad view of the relationships CK1δ/ε have with several signaling pathways. Although there are few proteins that overlap between the two data-sets, such as GAPVD1 and HUWE1, proteins from each of the data-sets function in the same pathways. Determining the connections between CK1δ/ε interacting partners and substrates would contribute to a mechanistic view of CK1δ/ε's roles in these pathways. For example, ch-TOG, a CK1δ/ε-associated protein (Table 2-1), and CLASP1, a putative CK1δ/ε-substrate (Table 3-2), both function at the kinetochore in mitosis to mediate chromosome alignment [12, 13, 62-68]. Loss of ch-TOG or CLASP1 and CLASP2 results in severe multipolarity and chromosome alignment defects [63, 69-71]. Both proteins localize to the mitotic spindle poles, kinetochores, and kinetochore microtubules (K-MT). The precise importance of these individual localizations to chromosome alignment is unclear. Depletion of D-TACC3, an interacting partner of ch-TOG in cultured cells [72], results in a near complete loss of the kinetochore and K-MT, but not centrosomal, localization of ch-TOG [71]. This affects mitosis by producing small mitotic spindles and reducing kinetochores tension [71]. These phenotypes are in contrast to depleting ch-TOG, which causes small spindles, but also increase multipolarity characterized by a loss of connection between K-MTs and centrosomes [71]. The spindle poles of multipolar cells depleted of ch-TOG, similar to CLASP1/2-depleted cells, have a high percentage of pericentriolar material with no centrioles [63, 71, 73]. The spindle-pole cohesion defect associated with loss of ch-TOG or CLASP1/2 is not seen in cells depleted of TACC3, suggesting that ch-TOG's interaction with TACC3 is most important for its function at the kinetochore, not the centrosome. Although ch-TOG and CLASP1/2 are not reported to interact, it is possible they function in a similar pathway to promote spindle-pole integrity. CK1δ/ε may function in this pathway as well.

Importantly, CK1δ/ε inhibition results in phenotypes that are reminiscent of ch-TOG, and CLASP1/2 depletion [63, 74-76]. If ch-TOG, and CLASP1 interact with and

are phosphorylated by CK1δ/ε, it would more likely have a direct influence on their kinetochore rather than centrosomal function. There are three reasons for this conclusion. Phenotypes associated with long-term kinase inhibition are more likely to produce indirect phenotypes. Secondly, CK1δ/ε inhibition starting in G_2 did not result in a spindle polarity or spindle-pole defect, but it did result in a chromosome alignment defect (Figure 4-3). A first step would be to verify CLASP1 as a CK1δ/ε substrate. First, probe CLASP1 protein mobility with SDS-PAGE of lysate from cells treated with DMSO or CK1δ/ε inhibitors. Second, *in vitro* kinase assays using recombinant CLASP1 and wild-type (WT) and kinase dead (K38R) CK1δ/ε. If I was successful at determining the binding regions between CK1δ/ε and ch-TOG, I could investigate whether CLASP phosphorylation is prevented, or generally affected. This would begin by SDS-PAGE and immunoblotting WT cells and where CK1δ/ε-ch-TOG interaction is ablated. Immunofluorescence analysis of CLASP1 localization would also provide information on whether it is affected by an interaction between CK1δ/ε and ch-TOG.

Reduced γ-tubulin levels at the spindle poles observed in Chapter four may arise from defects in protein trafficking to the centrosome [38, 77-79]. Similar defects are associated with depletion of ch-TOG, which is reported to traffic to the centrosome with the help of clathrin [62]. I would begin by analyzing the localization pattern of ch-TOG in cells treated with CK1δ/ε inhibitors. I would also analyze the protein levels of centrosomal scaffolding proteins that could affect γ-tubulin recruitment. Because CK1δ/ε function in endocytosis in coordination with GAPVD1, ch-TOG localization could be analyzed in GAPVD1$^{-/-}$ and GAPVD1 mutant cell lines.

A role for CK1 in DNA replication and DNA-damage repair

Although the exact role of CK1δ/ε in DNA-damage signaling is not known, there are several lines of evidence that they are necessary for the repair process. Initial evidence for the importance of CK1 proteins in DNA-damage repair was that the yeast strains, *hrr25*Δ, *hhp1*Δ, and *hhp2*Δ were sensitive to DNA-damaging agents [80, 81]. Pulse field gel analysis of *hhp1*Δ and *hhp2*Δ strains demonstrated a defect in DNA repair as compared to wild-type cells, with a more sustained defect in the *hhp1*Δ strain [81]. Importantly, introduction of the human enzymes, CK1δ/ε, rescued the growth

defect and sensitivity to DNA-damaging agents associated with loss of Hrr25, suggesting that CK1δ/ε are also involved in DNA repair [82]. More recently, it was shown that CK1δ deletion from cultured mouse fibroblasts resulted in decreased proliferation and an increase in the average number of γH2A.X foci, consistent with the idea that without CK1δ, DNA damage cannot be repaired [83].

In support of the hypothesis that CK1δ/ε function in cell proliferation and DNA-damage repair, inhibition of these enzymes with highly specific small molecule inhibitors has an anti-proliferative effect (Figure 4-7A) [84]. Cell treatment for 8-16 hours results in a gradual increase in the average nuclear fluorescence intensity of the DNA-damage marker γH2A.X (Figure 4-7B). This data indicates CK1δ/ε inhibition results in an accumulation of DNA-damage, similar to what was seen in mouse fibroblasts where CK1δ was deleted. There are at least two possible reasons for an accumulation of DNA damage after CK1δ/ε inhibition. First, CK1δ/ε may have a direct role in DNA replication. Inhibiting the enzymes may lead to stalled replication forks that gradually lead to replication fork collapse and thus DNA damage [85]. In Chapter 3, we identified the catalytic subunit of DNA polymerase epsilon (Table 3-1) and subunit B of DNA polymerase alpha (Table 3-2) as potential CK1δ/ε substrates. Future experiments should focus on determining if these are true substrates. If so, determining the effect of CK1δ/ε inhibition on DNA replication using DNA combing assays would be beneficial in investigating if CK1δ/ε functions in DNA replication. Cell would be synchronized in S-phase and allowed to grow in inhibitor-free media for 2 hours. Thymidine analogs could be pulsed into cells before, during and after treatment with DMSO or CK1δ/ε inhibitors [86, 87]. Fluorescence imaging techniques would be used to determine the length of analog incorporation in nascent DNA. If CK1δ/ε function in DNA replication, you would expect to see shorter track lengths in samples collected from CK1δ/ε inhibitor-treated cells. Second, CK1δ/ε may have a direct role in DNA-damage repair, and the observed accumulation of DNA damage is due to an inability to repair damage associated with regular levels of replication stress. These two possibilities are not mutually exclusive. Several DNA-damage repair proteins were identified as potential CK1δ/ε substrates in Chapter 3, including XRCC1, ERCC6, and MDC1 (Table 3-1). All three proteins are

phospho-regulated [88-101]. XRCC1 [102] and MDC1 [103-106] interact with centrosomal proteins and localize to sites of DNA damage during mitosis. Although a mitotic function of ERCC6 has not been reported, loss of the protein results in chromosome fragility in metaphase at four specific loci [107]. To begin validating XRCC1, ERCC6, and MDC1 as CK1δ/ε I would analyze protein mobility in cell lysates arrested at different stages of the cell cycle in the presence and absence of CK1δ/ε-inhibitors. A PhosTag reagent can be incorporated into polyacrylamide gels to enhance changes in mobility. If a change in mobility is observed. Ultimately, the goal will be to determine how CK1δ/ε-specific phosphorylation may affect the function of XRCC1, ERCC6, and MDC1.

Several DNA-damage repair proteins were identified in Chapter 3 as putative substrates, and Chapter 4 describes experiments implicating CK1 in DNA damage repair. XRCC1, ERCC6 and MDC1 are great candidates, but so are some proteins identified in the overlap in only the 'SR'-treated sample, such as 53BP1 and LIG1. Future experiments could determine if CK1δ/ε inhibition effects the localization pattern of these DNA damage repair proteins. 53BP1 is of particular interest because, as the name indicates, it interacts with p53 [108-110], a known CK1δ/ε substrate [111]. Additionally, 53BP1 interacts with MDC1 and is involved in promoting non-homologous end-joining during double-stranded break repair [112-114]. After verifying these candidates are true CK1δ/ε substrates using methods described earlier (SDS-PAGE and immunoblotting), we could immunoprecipitate of 53BP1 and MDC1 from cells treated with and without CK1δ/ε inhibitor, and assay for co-purification. Results from these experiments would provide insight into the function of CK1δ/ε in DNA damage repair.

As described in the past, the CK1 family of enzymes is highly complex. Two family members in particular, CK1δ/ε, are remarkably similar and largely redundant pleiotropic enzymes. In this thesis, I have described to you my efforts to study these enzymes. I produced cellular tools used to visualize the localization of the endogenous proteins and identify their interacting partners. I used small molecular inhibitors and quantitative mass spectrometry to identify candidate mitotic substrates. Lastly, I described several

cellular defects associated with inhibiting CK1δ/ε under varying conditions. I hypothesize that the most critical function of CK1δ/ε is to regulate DNA damage repair. It is currently unclear if this function is direct, through phosphorylation of one of the DNA damage repair proteins identified in Chapter 3, or indirect, through interaction and phosphorylation of GAPVD1, Per, and Cry to influence circadian rhythm genes. These are not mutually exclusive. I am confident that future experiments that utilize the two catalogs of proteins I've produced will further our knowledge regarding the mechanism by which CK1δ/ε influence mitosis and DNA damage repair.

Appendix

Materials and methods

Molecular biology methods

GAPVD1 cDNA encoding isoform 6 was purchased from Dharmacon (Cat#: MHS6278-211690496). Because this isoform lacks amino acids 1057-1074 relative to the previously studied isoform 1 [170] and also has an insertion at amino acid 810 (DFLYILQPKQHFQHIEAEADMRIQLSSS), a geneBlock™ fragment from Integrated DNA Technology (IDT) was used to construct the longer isoform. GAPVD1 plasmids were constructed using Gateway cloning, in the case of $Flag_3$-V5-ccdB (Addgene #87064). Gibson cloning was used for construction of peGFP-C2-GAPVD1

The ORF of CK1δ was amplified by PCR from a plasmid (CK1δ pGEX-6p-2) kindly provided by Fanni Gergely (University of Cambridge). The CK1ε ORF was amplified by PCR from GST-CK1ε. Each PCR product was cloned into pMAL-C2, and the correct sequence was validated by DNA sequencing.

For CRISPR/Cas9 gene editing, single guide RNAs (gRNA) were designed using the algorithm designed by the Zhang lab [190] at crispr.mit.edu. The gRNAs were cloned into pSpCas9(BB)-2A-Puro (Addgene, PX459). Repair plasmids for knock-in gene editing were constructed using pUC19 as a backbone, with restriction sites BamHI and EcoRI. The regions flanking the tags were amplified using purified genomic DNA from HEK293 cells using the Qiagen DNeasy blood and tissue kit (Qiagen, Venlo, Netherlands). Repair plasmids were constructed using Gibson cloning, with at least 25 base pairs of overlapping sequence between each of the adjacent fragments. For insertion of the blasticidin resistance gene, a geneBlock™ fragment consisting of a ribosomal skip sequence followed by the blasticidin resistance gene was purchased from IDT.

Cell culture and gene editing

HeLa and HEK293 cells were cultured in Dulbeco's modified eagle medium (DMEM) supplemented with 10% fetal bovine serum (FBS) and 1%

penicillin/streptomycin (Pen/Strep). For CRISPR-mediated gene-editing, cells were transfected with gene editing reagents as described previously [190]. Briefly, for knock-in cell line generation, 6 $X10_5$ cells were transfected with 300 ng of CRISPR/sgRNA plasmid and 1.5 µg of repair plasmid using Lipofectamine 3000. 24 hours after transfection, 5 µg/mL of puromycin was added for an additional 48 hours. For creating knock-out cell lines, cells were further treated with 5 µg/mL blasticidin for 48 hours. Following selections, cells were transferred to a 10-cm dish without selection for 24 hours. Cells were then single-cell sorted through the Vanderbilt Flow Cytometry core facility into 10 96-well plates for each knock-in cell line and a single 96-well plate was filled for the knock-out cell lines. Clones were validated through analysis of whole-cell lysates via immunoblotting and PCR amplification of genomic DNA. Genomic DNA was extracted using the Qiagen DNeasy blood and tissue kit, following the manufacturer's instructions.

For gene rescue experiments, cells were transfected with 2 µg of plasmid DNA using the Nucleofection R kit according to manufacturer's instructions (Lonza) using an AMAXA instrument with their program I-013.

Cell cycle synchronization

HeLa and HEK293 cells were synchronized using a sequential thymidine (Sigma-Aldrich) and aphidicolin (Tocris Bioscience) block-and-release protocol with drugs used at 2.5 mM and 5 µg/mL, respectively. To capture metaphase cells, cells were released from the second block for eight hours, then treated with 25 µM proTAME (R&D Systems) and 100 µM Apcin (R&D Systems) for four hours. Mitotic enrichment was verified by analyzing cells using phase-contrast microscopy and measuring the percent of rounded cells. For G1 synchronization, cells were released from the metaphase arrest for 3-4 hours.

Protein Methods

Cell lysates were prepared as previously described [61]. Briefly, cell pellets were lysed in 1% NP-40 buffer containing 6mM Na_2HPO_4, 4mM NaH_2PO_4, 1% Nonidet P40, 150mM NaCl, 2mM EDTA, 50mM NaF, 0.1mM Na_3VO_4 and supplemented with 1mM PMSF, benzamidine, sodium orthovanadate, β-glycerophosphate, sodium fluoride, and

sodium pyrophosphate. For immunoblotting, IP samples or ~40 µg of WCL was resolved by SDS-PAGE on 4-12% or 3-8% gels and transferred by electroblotting to PVDF membrane (Immobilon P; Millipore, Bedford, MA). Proteins were immunoprecipitated with anti-GAPVD1 (Bethyl Laboratoy; 2µg), anti-FLAG (M2; Sigma-Aldrich) or a serum raised and purified against GST-CK1δ (amino acids 1-415, VU477, Cocalico Biologicals, 2µg) or serum raised against GST-CK1ε (amino acids 1-416, VU473, Cocalico Biologicals, 2µg). Antibody

Antisera were raised against recombinant GST-CK1δ or GST-CK1ε (Cocalico), and their specificity was verified by immunoblotting. The anti-CK1δ/ε serum was further purified by ammonium sulfate precipitation. The serum was cleared by centrifugation and then precipitated with 0.5 volumes of saturated ammonium sulfate added dropwise and incubated overnight at 4°C. The precipitate was cleared from the serum by centrifugation and then the serum was precipitated with an additional 0.5 volumes of saturated ammonium sulfate added dropwise and incubated overnight at 4°C. The precipitate was pelleted by centrifugation, resuspended in 0.4 volumes phosphate-buffered saline (PBS), and dialyzed three times in PBS.

For multifunctional affinity purifications (MAPS), CK1δ/ε were purified as described previously [174]. Briefly, twenty 10 cm plates of HEK293 cells at ~80% confluence were released from plates with trypsin and washed three times with ice cold PBS. Cell pellets were then lysed in 3 mL of lysis buffer containing 50mM Tris-HCl pH7.5, 150mM NaCl, 0.5% Triton X-100, 5% glycerol, 1 mM EDTA, and protease and phosphatase inhibitors (1mM PMSF, benzamindine, sodium othrovanadate, β-glycerophosphate, sodium fluoride, and sodium pyrophosphate). Lysates containing ~35 mg of protein were incubated at 4°C on a nutator for 20 minutes, followed by centrifugation at 16,000xg for 15 minutes at 4°C. Lysate was incubated with 150 µL of anti-Flag magnetic beads (Sigma-Aldrich) at 4°C for 2 hours. The magnetic beads were washed three times with wash buffer (50mM Tris-HCl, pH7.5, 250mM NaCl, 0.05% NP-40). Bait protein was then eluted using 300 µg/mL of 3X-Flag peptide (Sigma-Aldrich) in 2 mL of lysis buffer. The eluted sample was then incubated in 300 µL of streptavidin-coated beads for 2 hours at 4°C. The beads were washed two times with wash buffer,

transferred to a 10 mL column and washed once with elution buffer (25mM Tris-HCl, pH 7.5, 125mM NaCl). Proteins were eluted two times with 1 mL of 2.5 mM biotin in elution buffer. The eluates were TCA precipitated by adjusting them to 25% TCA with 100% TCA, placing them on ice for 30 min with periodic vortexing, and spinning at maximum speed for 30min at 4°C. The TCA pellets were washed once with cold (-20°C) acetone containing 0.05 N HCl and spun for 7 min at maximum speed at 4 °C. They are then washed once with cold (-20 °C) acetone and spun for 7 min at maximum speed at 4 °C. The supernatant was removed and the pellets dried in a speed-vac.

Endocytosis assay

Endocytosis assays were performed as described previously [187]. Specifically, cells were washed with PBS and then serum starved with DMEM supplemented with 0.5% FBS, 1% Pen/Strep (low-serum media) for two hours at 36°C, 5% CO_2. Cells were incubated with 30 µg/uL transferrin-594 (Tfn-594, Thermo Fisher Sci, cat# T13343) or 100 ng/mL epidermal growth factor-488 (EGF-488 Thermo Fisher Sci, cat# E13345) in low serum media for 30 minutes on ice and covered with tin foil. Cells were washed twice with PBS, once with low-serum media, and incubated in low-serum media with 300 µg/mL Tfn or 200 ng/mL EGF (Sigma-Aldrich, cat# T8158) for 10 minutes at 36°C, 5% CO_2. Cells were then acid washed four times for one minute per wash. Cells were washed with PBS twice and fixed with 4% PFA.

Fixation and antibody staining

For methanol fixation, cells were washed once with cold PBS and once with 100% cold methanol, followed by fixation with 100% cold methanol for 15 minutes at -20°C. Cells were then washed 3X with 1x phosphate buffered saline + 0.1% Tween-20 (0.1% PBST) at room temperature, followed by blocking with 2% normal goat serum (NGS) in 0.1% Triton X100 in 1x PBS for 10 minutes. For paraformaldehyde (PFA) fixation, cells were washed twice with PBS, once with 4% PFA, then fixed with 4% PFA for 15 minutes at room temperature. Cells were incubated with antibodies against γ-tubulin (Sigma-Aldrich, GTU88; 1:500), Flag M2 (Sigma-Aldrich, 1:1500) clathrin heavy-chain (CLHC; Cell signaling technology, 1:100), or MKLP1 (Bethyl laboratory, 1:1000). Cells were then incubated with DAPI and secondary antibodies (Alexa Fluor® Goat-anti

Mouse or Rabbit IgG (H+L), ThermoFisher; 1:500) for 45 minutes at 22˚C. Coverslips were mounted on slides using Prolong™ Gold antifade mounting media.

Microscopy methods

Fixed-cell images of HeLa and HEK293 cells were acquired using a personal DeltaVision microscope system (Applied Precision) that includes an Olympus IX71 microscope, 60× NA 1.42 PlanApo and 100× NA 1.40 UPlanSApo objectives, a Photometrics CoolSnap HQ2 camera, and softWoRx imaging software. Images in figures are maximum intensity projections of z-sections spaced at 0.2 µm. Images were deconvolved with 10 iterations. Quantitative analysis of microscopy data was performed using Fiji (a version of ImageJ software) available at: https://fiji.sc/[191]. The mean number of Tfn-594 particles per cell was determined by first setting an intensity threshold for each of the control cells. This threshold was then used in the '3D object counter' plug-in for all of the images. At least 40 cells were analyzed per sample, per experiment.

In vitro kinase assays

Bacterial expression of MBP-CK1 fusion proteins were performed in terrific broth (TB) media at an OD_{595} of ~1.2 and 0.4 µM Isopropyl β-D-1-thiogalactopyranoside (IPTG). MBP-CK1 fusion proteins were purified on amylose beads (New England Biolabs) in column buffer (20 mM Tris [pH 7.0], 150 mM NaCl, 2 mM EDTA, 1 mM DTT and 0.1% NP40) and eluted with maltose (10mM). Kinase reactions were performed with 1000 ng kinase, 1000 ng GAPVD1, 10 µM ATP plus 1 µCi γ-[^{32}P]-ATP in kinase buffer (50 mM Tris [pH 7.5], 10 mM $MgCl_2$, and 5 mM DTT) in 20 µl at 30°C for 45 minutes. Reactions were quenched by adding SDS-PAGE sample buffer and proteins were separated by SDS-PAGE. Phosphorylated proteins were visualized by autoradiography and relative protein quantities were assessed by Coomassie blue staining relative to known standards utilizing Odyssey software (LI-COR Biosciences)**.** Phosphorylated proteins were visualized and quantitated using an FLA7000IP Typhoon Storage Phosphorimager (GE Healthcare Life Sciences).

Two-hybrid analyses

Two-hybrid experiments were performed as described previously (Vo et al., 2016). GAPVD1, CK1δ and CK1ε, cloned into pDEST DB and pDEST AD vectors, respectively, were generously provided by Haiyuan Yu (Cornell University). These were co-transformed into *S. cerevisiae* strain PJ69-4A. Leu+ and Trp+ transformants were selected and then scored for positive interactions by streaking onto synthetic dextrose plates lacking tryptophan, leucine, and histidine. β-Galactosidase reporter enzyme activity in the two-hybrid strains was measured using the Galacto-Star chemiluminescent reporter assay system according to the manufacturer's instructions (Applied Biosystems, Foster City, CA), except that cells were lysed by glass bead disruption. Each experiment was performed in triplicate. Reporter assays were recorded on a Multi-Detection Microplate Reader (Bio-TEK Instruments).

Mass spectrometry analysis

TCA-precipitated proteins MAP purifications were subjected to mass spectrometric analysis on an LTQ velos by 3-phase multidimensional protein identification technology (MudPIT) as previously described (McDonald et al., 2002; Chen et. al. 2013) with modifications. Proteins were re-suspended in 8M urea buffer (8M urea in 100 mM Tris, pH 8.5), reduced with Tris (2-carboxyethyl) phosphine, alkylated with 2-chloro acetamide, and digested with trypsin or chymotrypsin. The resulting peptides were desalted by C-18 spin column (Pierce). Raw mass spectrometry data were filtered with Scansifter and searched by SEQUEST algorithm. Scaffold (version 4.4.8 or version 4.2.1) and Scaffold PTM (version 3.0.1) (both were from Proteome Software, Portland. OR) were used for data assembly and filtering. The following filtering criteria were used: minimum of 90.0% peptide identification probability, minimum of 99% protein identification probability, and minimum of two unique peptides.

References

1. The Gene Ontology C: **The Gene Ontology Resource: 20 years and still GOing strong**. *Nucleic Acids Res* 2019, **47**(D1):D330-D338.
2. Ashburner M, Ball CA, Blake JA, Botstein D, Butler H, Cherry JM, Davis AP, Dolinski K, Dwight SS, Eppig JT *et al*: **Gene ontology: tool for the unification of biology. The Gene Ontology Consortium**. *Nat Genet* 2000, **25**(1):25-29.
3. Wloga D, Joachimiak E, Fabczak H: **Tubulin Post-Translational Modifications and Microtubule Dynamics**. *Int J Mol Sci* 2017, **18**(10).
4. Vu LD, Gevaert K, De Smet I: **Protein Language: Post-Translational Modifications Talking to Each Other**. *Trends Plant Sci* 2018, **23**(12):1068-1080.
5. Czuba LC, Hillgren KM, Swaan PW: **Post-translational modifications of transporters**. *Pharmacol Ther* 2018, **192**:88-99.
6. Pyerin W, Taniguchi H: **Phosphorylation of hepatic phenobarbital-inducible cytochrome P-450**. *EMBO J* 1989, **8**(10):3003-3010.
7. Koch JA, Waxman DJ: **Posttranslational modification of hepatic cytochrome P-450. Phosphorylation of phenobarbital-inducible P-450 forms PB-4 (IIB1) and PB-5 (IIB2) in isolated rat hepatocytes and in vivo**. *Biochemistry* 1989, **28**(8):3145-3152.
8. Martinez A, Haavik J, Flatmark T, Arrondo JL, Muga A: **Conformational properties and stability of tyrosine hydroxylase studied by infrared spectroscopy. Effect of iron/catecholamine binding and phosphorylation**. *J Biol Chem* 1996, **271**(33):19737-19742.
9. Sharma K, D'Souza RC, Tyanova S, Schaab C, Wisniewski JR, Cox J, Mann M: **Ultradeep human phosphoproteome reveals a distinct regulatory nature of Tyr and Ser/Thr-based signaling**. *Cell Rep* 2014, **8**(5):1583-1594.
10. Manning G, Whyte DB, Martinez R, Hunter T, Sudarsanam S: **The protein kinase complement of the human genome**. *Science* 2002, **298**(5600):1912-1934.
11. Adam K, Hunter T: **Histidine kinases and the missing phosphoproteome from prokaryotes to eukaryotes**. *Lab Invest* 2018, **98**(2):233-247.
12. De Verdier CH: **Isolation of phosphothreonine from bovine casein**. *Nature* 1952, **170**(4332):804-805.
13. Kennedy EP, Smith SW: **The isolation of radioactive phosphoserine from phosphoprotein of the Ehrlich ascites tumor**. *J Biol Chem* 1954, **207**(1):153-163.
14. Venerando A, Cesaro L, Pinna LA: **From phosphoproteins to phosphoproteomes: a historical account**. *FEBS J* 2017, **284**(13):1936-1951.
15. Boyle WJ, van der Geer P, Hunter T: **Phosphopeptide mapping and phosphoamino acid analysis by two-dimensional separation on thin-layer cellulose plates**. *Methods Enzymol* 1991, **201**:110-149.
16. Sefton BM, Hunter T, Beemon K, Eckhart W: **Evidence that the phosphorylation of tyrosine is essential for cellular transformation by Rous sarcoma virus**. *Cell* 1980, **20**(3):807-816.

17. Hunter T, Sefton BM: **Transforming gene product of Rous sarcoma virus phosphorylates tyrosine**. *Proc Natl Acad Sci U S A* 1980, **77**(3):1311-1315.
18. Wei YF, Matthews HR: **Identification of phosphohistidine in proteins and purification of protein-histidine kinases**. *Methods Enzymol* 1991, **200**:388-414.
19. Glenney JR, Jr., Zokas L, Kamps MP: **Monoclonal antibodies to phosphotyrosine**. *J Immunol Methods* 1988, **109**(2):277-285.
20. Heffetz D, Fridkin M, Zick Y: **Antibodies directed against phosphothreonine residues as potent tools for studying protein phosphorylation**. *Eur J Biochem* 1989, **182**(2):343-348.
21. Fuhs SR, Meisenhelder J, Aslanian A, Ma L, Zagorska A, Stankova M, Binnie A, Al-Obeidi F, Mauger J, Lemke G *et al*: **Monoclonal 1- and 3-Phosphohistidine Antibodies: New Tools to Study Histidine Phosphorylation**. *Cell* 2015, **162**(1):198-210.
22. Rix U, Superti-Furga G: **Target profiling of small molecules by chemical proteomics**. *Nat Chem Biol* 2009, **5**(9):616-624.
23. Zhang J, Yang PL, Gray NS: **Targeting cancer with small molecule kinase inhibitors**. *Nat Rev Cancer* 2009, **9**(1):28-39.
24. Hanks SK: **Homology probing: identification of cDNA clones encoding members of the protein-serine kinase family**. *Proc Natl Acad Sci U S A* 1987, **84**(2):388-392.
25. Hanks SK, Quinn AM, Hunter T: **The protein kinase family: conserved features and deduced phylogeny of the catalytic domains**. *Science* 1988, **241**(4861):42-52.
26. Kamps MP, Sefton BM: **Neither arginine nor histidine can carry out the function of lysine-295 in the ATP-binding site of p60src**. *Mol Cell Biol* 1986, **6**(3):751-757.
27. De Bondt HL, Rosenblatt J, Jancarik J, Jones HD, Morgan DO, Kim SH: **Crystal structure of cyclin-dependent kinase 2**. *Nature* 1993, **363**(6430):595-602.
28. Gould KL, Moreno S, Owen DJ, Sazer S, Nurse P: **Phosphorylation at Thr167 is required for Schizosaccharomyces pombe p34cdc2 function**. *EMBO J* 1991, **10**(11):3297-3309.
29. Fleig UN, Gould KL: **Regulation of cdc2 activity in Schizosaccharomyces pombe: the role of phosphorylation**. *Semin Cell Biol* 1991, **2**(4):195-204.
30. Shoji S, Ericsson LH, Walsh KA, Fischer EH, Titani K: **Amino acid sequence of the catalytic subunit of bovine type II adenosine cyclic 3',5'-phosphate dependent protein kinase**. *Biochemistry* 1983, **22**(15):3702-3709.
31. Hanks SK: **Genomic analysis of the eukaryotic protein kinase superfamily: a perspective**. *Genome Biol* 2003, **4**(5):111.
32. Graves PR, Haas DW, Hagedorn CH, DePaoli-Roach AA, Roach PJ: **Molecular cloning, expression, and characterization of a 49-kilodalton casein kinase I isoform from rat testis**. *J Biol Chem* 1993, **268**(9):6394-6401.
33. Flotow H, Graves PR, Wang AQ, Fiol CJ, Roeske RW, Roach PJ: **Phosphate groups as substrate determinants for casein kinase I action**. *J Biol Chem* 1990, **265**(24):14264-14269.
34. Flotow H, Roach PJ: **Role of acidic residues as substrate determinants for casein kinase I**. *J Biol Chem* 1991, **266**(6):3724-3727.
35. Johnson AE, Chen JS, Gould KL: **CK1 is required for a mitotic checkpoint that delays cytokinesis**. *Curr Biol* 2013, **23**(19):1920-1926.

36. Venerando A, Marin O, Cozza G, Bustos VH, Sarno S, Pinna LA: **Isoform specific phosphorylation of p53 by protein kinase CK1**. *Cell Mol Life Sci* 2010, **67**(7):1105-1118.
37. Dumaz N, Milne DM, Meek DW: **Protein kinase CK1 is a p53-threonine 18 kinase which requires prior phosphorylation of serine 15**. *FEBS Lett* 1999, **463**(3):312-316.
38. DeMaggio AJ, Lindberg RA, Hunter T, Hoekstra MF: **The budding yeast HRR25 gene product is a casein kinase I isoform**. *Proc Natl Acad Sci U S A* 1992, **89**(15):7008-7012.
39. Meggio F, Perich JW, Reynolds EC, Pinna LA: **Phosphotyrosine as a specificity determinant for casein kinase-2, a growth related Ser/Thr-specific protein kinase**. *FEBS Lett* 1991, **279**(2):307-309.
40. Shinohara Y, Koyama YM, Ukai-Tadenuma M, Hirokawa T, Kikuchi M, Yamada RG, Ukai H, Fujishima H, Umehara T, Tainaka K *et al*: **Temperature-Sensitive Substrate and Product Binding Underlie Temperature-Compensated Phosphorylation in the Clock**. *Mol Cell* 2017, **67**(5):783-798 e720.
41. Luxenburger A, Schmidt D, Ianes C, Pichlo C, Kruger M, von Drathen T, Brunstein E, Gainsford GJ, Baumann U, Knippschild U *et al*: **Design, Synthesis and Biological Evaluation of Isoxazole-Based CK1 Inhibitors Modified with Chiral Pyrrolidine Scaffolds**. *Molecules* 2019, **24**(5).
42. Garcia-Reyes B, Witt L, Jansen B, Karasu E, Gehring T, Leban J, Henne-Bruns D, Pichlo C, Brunstein E, Baumann U *et al*: **Discovery of Inhibitor of Wnt Production 2 (IWP-2) and Related Compounds As Selective ATP-Competitive Inhibitors of Casein Kinase 1 (CK1) delta/epsilon**. *J Med Chem* 2018, **61**(9):4087-4102.
43. Ursu A, Illich DJ, Takemoto Y, Porfetye AT, Zhang M, Brockmeyer A, Janning P, Watanabe N, Osada H, Vetter IR *et al*: **Epiblastin A Induces Reprogramming of Epiblast Stem Cells Into Embryonic Stem Cells by Inhibition of Casein Kinase 1**. *Cell Chem Biol* 2016, **23**(4):494-507.
44. Schehr M, Ianes C, Weisner J, Heintze L, Muller MP, Pichlo C, Charl J, Brunstein E, Ewert J, Lehr M *et al*: **2-Azo-, 2-diazocine-thiazols and 2-azo-imidazoles as photoswitchable kinase inhibitors: limitations and pitfalls of the photoswitchable inhibitor approach**. *Photochem Photobiol Sci* 2019, **18**(6):1398-1407.
45. Xu RM, Carmel G, Sweet RM, Kuret J, Cheng X: **Crystal structure of casein kinase-1, a phosphate-directed protein kinase**. *EMBO J* 1995, **14**(5):1015-1023.
46. Long A, Zhao H, Huang X: **Structural basis for the interaction between casein kinase 1 delta and a potent and selective inhibitor**. *J Med Chem* 2012, **55**(2):956-960.
47. Long AM, Zhao H, Huang X: **Structural basis for the potent and selective inhibition of casein kinase 1 epsilon**. *J Med Chem* 2012, **55**(22):10307-10311.
48. Longenecker KL, Roach PJ, Hurley TD: **Three-dimensional structure of mammalian casein kinase I: molecular basis for phosphate recognition**. *J Mol Biol* 1996, **257**(3):618-631.
49. Cristina-Maria Cruciat CD, Reinoud E. A. de Groot, Bisei Ohkawara,, Carmen Reinhard HCK, Christof Niehrs: **RNA Helicase DDX3 Is a Regulatory Subunit of Casein Kinase 1 in Wnt−β-Catenin Signaling**. *Science* 2013, **339**(6126):1436-1441.
50. Jiang S, Zhang M, Sun J, Yang X: **Casein kinase 1alpha: biological mechanisms and theranostic potential**. *Cell Commun Signal* 2018, **16**(1):23.

51. Gorss S.D. ARA: **Casein Kinase I: Spatial organization and positioning of a multifunctional protein kinase family Review.pdf**. *Cell Signal* 1998, **10**(10):699-711.
52. Gross SD, Anderson RA: **Casein kinase I: spatial organization and positioning of a multifunctional protein kinase family**. *Cell Signal* 1998, **10**(10):699-711.
53. Vancura A, Sessler A, Leichus B, Kuret J: **A prenylation motif is required for plasma membrane localization and biochemical function of casein kinase I in budding yeast**. *J Biol Chem* 1994, **269**(30):19271-19278.
54. Wang PC, Vancura A, Mitcheson TG, Kuret J: **Two genes in Saccharomyces cerevisiae encode a membrane-bound form of casein kinase-1**. *Mol Biol Cell* 1992, **3**(3):275-286.
55. Babu P, Bryan JD, Panek HR, Jordan SL, Forbrich BM, Kelley SC, Colvin RT, Robinson LC: **Plasma membrane localization of the Yck2p yeast casein kinase 1 isoform requires the C-terminal extension and secretory pathway function**. *J Cell Sci* 2002, **115**(Pt 24):4957-4968.
56. Zhai L, Graves PR, Robinson LC, Italiano M, Culbertson MR, Rowles J, Cobb MH, DePaoli-Roach AA, Roach PJ: **Casein kinase I gamma subfamily. Molecular cloning, expression, and characterization of three mammalian isoforms and complementation of defects in the Saccharomyces cerevisiae YCK genes**. *J Biol Chem* 1995, **270**(21):12717-12724.
57. Graves PR, Roach PJ: **Role of COOH-terminal phosphorylation in the regulation of casein kinase I delta**. *J Biol Chem* 1995, **270**(37):21689-21694.
58. Budini M, Jacob G, Jedlicki A, Perez C, Allende CC, Allende JE: **Autophosphorylation of carboxy-terminal residues inhibits the activity of protein kinase CK1alpha**. *J Cell Biochem* 2009, **106**(3):399-408.
59. Rivers A, Gietzen KF, Vielhaber E, Virshup DM: **Regulation of casein kinase I epsilon and casein kinase I delta by an in vivo futile phosphorylation cycle**. *J Biol Chem* 1998, **273**(26):15980-15984.
60. Cegielska A, Gietzen KF, Rivers A, Virshup DM: **Autoinhibition of casein kinase I epsilon (CKI epsilon) is relieved by protein phosphatases and limited proteolysis**. *J Biol Chem* 1998, **273**(3):1357-1364.
61. Elmore ZC, Guillen RX, Gould KL: **The kinase domain of CK1 enzymes contains the localization cue essential for compartmentalized signaling at the spindle pole**. *Mol Biol Cell* 2018:mbcE18020129.
62. Fish KJ, Cegielska A, Getman ME, Landes GM, Virshup DM: **Isolation and characterization of human casein kinase I epsilon (CKI), a novel member of the CKI gene family**. *J Biol Chem* 1995, **270**(25):14875-14883.
63. Hoekstra MF, Liskay RM, Ou AC, DeMaggio AJ, Burbee DG, Heffron F: **HRR25, a putative protein kinase from budding yeast: association with repair of damaged DNA**. *Science* 1991, **253**(5023):1031-1034.
64. Petronczki M, Matos J, Mori S, Gregan J, Bogdanova A, Schwickart M, Mechtler K, Shirahige K, Zachariae W, Nasmyth K: **Monopolar attachment of sister kinetochores at meiosis I requires casein kinase 1**. *Cell* 2006, **126**(6):1049-1064.
65. Ho Y, Mason S, Kobayashi R, Hoekstra M, Andrews B: **Role of the casein kinase I isoform, Hrr25, and the cell cycle-regulatory transcription factor, SBF, in the transcriptional response to DNA damage in Saccharomyces cerevisiae**. *Proc Natl Acad Sci U S A* 1997, **94**(2):581-586.

66. Johnson AL, Barker DG, Johnston LH: **Induction of yeast DNA ligase genes in exponential and stationary phase cultures in response to DNA damaging agents**. *Curr Genet* 1986, **11**(2):107-112.
67. Toyn JH, Toone WM, Morgan BA, Johnston LH: **The activation of DNA replication in yeast**. *Trends Biochem Sci* 1995, **20**(2):70-73.
68. Elledge SJ, Davis RW: **Identification and isolation of the gene encoding the small subunit of ribonucleotide reductase from Saccharomyces cerevisiae: DNA damage-inducible gene required for mitotic viability**. *Mol Cell Biol* 1987, **7**(8):2783-2793.
69. Elledge SJ, Davis RW: **Two genes differentially regulated in the cell cycle and by DNA-damaging agents encode alternative regulatory subunits of ribonucleotide reductase**. *Genes Dev* 1990, **4**(5):740-751.
70. Wang J, Davis S, Menon S, Zhang J, Ding J, Cervantes S, Miller E, Jiang Y, Ferro-Novick S: **Ypt1/Rab1 regulates Hrr25/CK1delta kinase activity in ER-Golgi traffic and macroautophagy**. *J Cell Biol* 2015, **210**(2):273-285.
71. Lord C, Bhandari D, Menon S, Ghassemian M, Nycz D, Hay J, Ghosh P, Ferro-Novick S: **Sequential interactions with Sec23 control the direction of vesicle traffic**. *Nature* 2011, **473**(7346):181-186.
72. Peng Y, Grassart A, Lu R, Wong CC, Yates J, 3rd, Barnes G, Drubin DG: **Casein kinase 1 promotes initiation of clathrin-mediated endocytosis**. *Dev Cell* 2015, **32**(2):231-240.
73. Peng Y, Moritz M, Han X, Giddings TH, Lyon A, Kollman J, Winey M, Yates J, 3rd, Agard DA, Drubin DG *et al*: **Interaction of CK1delta with gammaTuSC ensures proper microtubule assembly and spindle positioning**. *Mol Biol Cell* 2015, **26**(13):2505-2518.
74. Jendretzki A, Ciklic I, Rodicio R, Schmitz HP, Heinisch JJ: **Cyk3 acts in actomyosin ring independent cytokinesis by recruiting Inn1 to the yeast bud neck**. *Mol Genet Genomics* 2009, **282**(4):437-451.
75. Korinek WS, Bi E, Epp JA, Wang L, Ho J, Chant J: **Cyk3, a novel SH3-domain protein, affects cytokinesis in yeast**. *Curr Biol* 2000, **10**(15):947-950.
76. Onishi M, Ko N, Nishihama R, Pringle JR: **Distinct roles of Rho1, Cdc42, and Cyk3 in septum formation and abscission during yeast cytokinesis**. *J Cell Biol* 2013, **202**(2):311-329.
77. Devrekanli A, Foltman M, Roncero C, Sanchez-Diaz A, Labib K: **Inn1 and Cyk3 regulate chitin synthase during cytokinesis in budding yeasts**. *J Cell Sci* 2012, **125**(Pt 22):5453-5466.
78. Wang M, Nishihama R, Onishi M, Pringle JR: **Role of the Hof1-Cyk3 interaction in cleavage-furrow ingression and primary-septum formation during yeast cytokinesis**. *Mol Biol Cell* 2018, **29**(5):597-609.
79. Meitinger F, Petrova B, Lombardi IM, Bertazzi DT, Hub B, Zentgraf H, Pereira G: **Targeted localization of Inn1, Cyk3 and Chs2 by the mitotic-exit network regulates cytokinesis in budding yeast**. *J Cell Sci* 2010, **123**(Pt 11):1851-1861.
80. Baro B, Queralt E, Monje-Casas F: **Regulation of Mitotic Exit in Saccharomyces cerevisiae**. *Methods Mol Biol* 2017, **1505**:3-17.
81. Moritz M, Agard DA: **Gamma-tubulin complexes and microtubule nucleation**. *Curr Opin Struct Biol* 2001, **11**(2):174-181.

82. Farache D, Emorine L, Haren L, Merdes A: **Assembly and regulation of gamma-tubulin complexes**. *Open Biol* 2018, **8**(3).
83. Ghalei H, Schaub FX, Doherty JR, Noguchi Y, Roush WR, Cleveland JL, Stroupe ME, Karbstein K: **Hrr25/CK1delta-directed release of Ltv1 from pre-40S ribosomes is necessary for ribosome assembly and cell growth**. *J Cell Biol* 2015, **208**(6):745-759.
84. Lusk CP, Waller DD, Makhnevych T, Dienemann A, Whiteway M, Thomas DY, Wozniak RW: **Nup53p is a target of two mitotic kinases, Cdk1p and Hrr25p**. *Traffic* 2007, **8**(6):647-660.
85. Rabitsch KP, Petronczki M, Javerzat JP, Genier S, Chwalla B, Schleiffer A, Tanaka TU, Nasmyth K: **Kinetochore recruitment of two nucleolar proteins is required for homolog segregation in meiosis I**. *Dev Cell* 2003, **4**(4):535-548.
86. Toth A, Rabitsch KP, Galova M, Schleiffer A, Buonomo SB, Nasmyth K: **Functional genomics identifies monopolin: a kinetochore protein required for segregation of homologs during meiosis i**. *Cell* 2000, **103**(7):1155-1168.
87. Katis VL, Lipp JJ, Imre R, Bogdanova A, Okaz E, Habermann B, Mechtler K, Nasmyth K, Zachariae W: **Rec8 phosphorylation by casein kinase 1 and Cdc7-Dbf4 kinase regulates cohesin cleavage by separase during meiosis**. *Dev Cell* 2010, **18**(3):397-409.
88. Ishiguro T, Tanaka K, Sakuno T, Watanabe Y: **Shugoshin-PP2A counteracts casein-kinase-1-dependent cleavage of Rec8 by separase**. *Nat Cell Biol* 2010, **12**(5):500-506.
89. Dhillon N HM: **Characterization of two protein kinases from S. pombe involved in the regulation of DNA repair.pdf**. *EMBO J* 1994, **13**(12):2777-2788.
90. Fantes PA: **Control of cell size and cycle time in Schizosaccharomyces pombe**. *J Cell Sci* 1977, **24**:51-67.
91. Russell P, Nurse P: **cdc25+ functions as an inducer in the mitotic control of fission yeast**. *Cell* 1986, **45**(1):145-153.
92. Mahyous Saeyd SA, Ewert-Krzemieniewska K, Liu B, Caspari T: **Hyperactive Cdc2 kinase interferes with the response to broken replication forks by trapping S.pombe Crb2 in its mitotic T215 phosphorylated state**. *Nucleic Acids Res* 2014, **42**(12):7734-7747.
93. Tanaka H, Tanaka K, Murakami H, Okayama H: **Fission yeast cdc24 is a replication factor C- and proliferating cell nuclear antigen-interacting factor essential for S-phase completion**. *Mol Cell Biol* 1999, **19**(2):1038-1048.
94. Johnson AE, McCollum D, Gould KL: **Polar opposites: Fine-tuning cytokinesis through SIN asymmetry**. *Cytoskeleton (Hoboken)* 2012, **69**(10):686-699.
95. Johnson AE, Gould KL: **Dma1 ubiquitinates the SIN scaffold, Sid4, to impede the mitotic localization of Plo1 kinase**. *EMBO J* 2011, **30**(2):341-354.
96. Sudakin V, Chan GK, Yen TJ: **Checkpoint inhibition of the APC/C in HeLa cells is mediated by a complex of BUBR1, BUB3, CDC20, and MAD2**. *J Cell Biol* 2001, **154**(5):925-936.
97. Hagting A, Den Elzen N, Vodermaier HC, Waizenegger IC, Peters JM, Pines J: **Human securin proteolysis is controlled by the spindle checkpoint and reveals when the APC/C switches from activation by Cdc20 to Cdh1**. *J Cell Biol* 2002, **157**(7):1125-1137.

98. Tang Z, Shu H, Oncel D, Chen S, Yu H: **Phosphorylation of Cdc20 by Bub1 provides a catalytic mechanism for APC/C inhibition by the spindle checkpoint**. *Mol Cell* 2004, **16**(3):387-397.
99. Sudakin V, Yen TJ: **Purification of the mitotic checkpoint complex, an inhibitor of the APC/C from HeLa cells**. *Methods Mol Biol* 2004, **281**:199-212.
100. Diaz-Martinez LA, Yu H: **Running on a treadmill: dynamic inhibition of APC/C by the spindle checkpoint**. *Cell Div* 2007, **2**:23.
101. Jia L, Kim S, Yu H: **Tracking spindle checkpoint signals from kinetochores to APC/C**. *Trends Biochem Sci* 2013, **38**(6):302-311.
102. Guertin DA, Venkatram S, Gould KL, McCollum D: **Dma1 prevents mitotic exit and cytokinesis by inhibiting the septation initiation network (SIN)**. *Dev Cell* 2002, **3**(6):779-790.
103. Johnson AE, Collier SE, Ohi MD, Gould KL: **Fission yeast Dma1 requires RING domain dimerization for its ubiquitin ligase activity and mitotic checkpoint function**. *J Biol Chem* 2012, **287**(31):25741-25748.
104. Rowles J, Slaughter C, Moomaw C, Hsu J, Cobb MH: **Purification of casein kinase I and isolation of cDNAs encoding multiple casein kinase I-like enzymes**. *Proc Natl Acad Sci U S A* 1991, **88**(21):9548-9552.
105. Fish K.J. CA, Getman M.E., Landes G.M., Virshup D.M.: **Isolation and characterization of human casein kinase I epsilon (CKI), a novel member of the CKI gene family.pdf**. *J Biol Chem* 1995, **270**(25):14875-14883.
106. Bibian M, Rahaim RJ, Choi JY, Noguchi Y, Schurer S, Chen W, Nakanishi S, Licht K, Rosenberg LH, Li L *et al*: **Development of highly selective casein kinase 1delta/1epsilon (CK1delta/epsilon) inhibitors with potent antiproliferative properties**. *Bioorg Med Chem Lett* 2013, **23**(15):4374-4380.
107. Etchegaray JP, Machida KK, Noton E, Constance CM, Dallmann R, Di Napoli MN, DeBruyne JP, Lambert CM, Yu EA, Reppert SM *et al*: **Casein kinase 1 delta regulates the pace of the mammalian circadian clock**. *Mol Cell Biol* 2009, **29**(14):3853-3866.
108. Yang Y, Xu T, Zhang Y, Qin X: **Molecular basis for the regulation of the circadian clock kinases CK1delta and CK1epsilon**. *Cell Signal* 2017, **31**:58-65.
109. Fulcher LJ, Bozatzi P, Tachie-Menson T, Wu KZL, Cummins TD, Bufton JC, Pinkas DM, Dunbar K, Shrestha S, Wood NT *et al*: **The DUF1669 domain of FAM83 family proteins anchor casein kinase 1 isoforms**. *Sci Signal* 2018, **11**(531).
110. Inuzuka H, Tseng A, Gao D, Zhai B, Zhang Q, Shaik S, Wan L, Ang XL, Mock C, Yin H *et al*: **Phosphorylation by casein kinase I promotes the turnover of the Mdm2 oncoprotein via the SCF(beta-TRCP) ubiquitin ligase**. *Cancer Cell* 2010, **18**(2):147-159.
111. Zhao B, Li L, Tumaneng K, Wang CY, Guan KL: **A coordinated phosphorylation by Lats and CK1 regulates YAP stability through SCF(beta-TRCP)**. *Genes Dev* 2010, **24**(1):72-85.
112. Alsheich-Bartok O, Haupt S, Alkalay-Snir I, Saito S, Appella E, Haupt Y: **PML enhances the regulation of p53 by CK1 in response to DNA damage**. *Oncogene* 2008, **27**(26):3653-3661.

113. Zemp I, Wandrey F, Rao S, Ashiono C, Wyler E, Montellese C, Kutay U: **CK1delta and CK1epsilon are components of human 40S subunit precursors required for cytoplasmic 40S maturation**. *J Cell Sci* 2014, **127**(Pt 6):1242-1253.
114. Penas C, Ramachandran V, Simanski S, Lee C, Madoux F, Rahaim RJ, Chauhan R, Barnaby O, Schurer S, Hodder P *et al*: **Casein kinase 1delta-dependent Wee1 protein degradation**. *J Biol Chem* 2014, **289**(27):18893-18903.
115. Piao S, Lee SJ, Xu Y, Gwak J, Oh S, Park BJ, Ha NC: **CK1epsilon targets Cdc25A for ubiquitin-mediated proteolysis under normal conditions and in response to checkpoint activation**. *Cell Cycle* 2011, **10**(3):531-537.
116. Sakanaka C: **Phosphorylation and regulation of beta-catenin by casein kinase 1 epsilon**. *Journal of Biochemistry* 2002, **132**(5):697-703.
117. Vielhaber E, Eide E, Rivers A, Gao ZH, Virshup DM: **Nuclear entry of the circadian regulator mPER1 is controlled by mammalian casein kinase I epsilon**. *Mol Cell Biol* 2000, **20**(13):4888-4899.
118. Clevers H: **Wnt/beta-catenin signaling in development and disease**. *Cell* 2006, **127**(3):469-480.
119. Kim CJ, Song JH, Cho YG, Kim YS, Kim SY, Nam SW, Yoo NJ, Lee JY, Park WS: **Somatic mutations of the beta-TrCP gene in gastric cancer**. *APMIS* 2007, **115**(2):127-133.
120. Liu F, Millar SE: **Wnt/beta-catenin signaling in oral tissue development and disease**. *J Dent Res* 2010, **89**(4):318-330.
121. Greer YE, Rubin JS: **Casein kinase 1 delta functions at the centrosome to mediate Wnt-3a-dependent neurite outgrowth**. *J Cell Biol* 2011, **192**(6):993-1004.
122. Gao ZH, Seeling JM, Hill V, Yochum A, Virshup DM: **Casein kinase I phosphorylates and destabilizes the beta-catenin degradation complex**. *Proc Natl Acad Sci U S A* 2002, **99**(3):1182-1187.
123. Kishida M, Hino S, Michiue T, Yamamoto H, Kishida S, Fukui A, Asashima M, Kikuchi A: **Synergistic activation of the Wnt signaling pathway by Dvl and casein kinase Iepsilon**. *J Biol Chem* 2001, **276**(35):33147-33155.
124. Grammer TC, Liu KJ, Mariani FV, Harland RM: **Use of large-scale expression cloning screens in the Xenopus laevis tadpole to identify gene function**. *Dev Biol* 2000, **228**(2):197-210.
125. McKay RM, Peters JM, Graff JM: **The casein kinase I family in Wnt signaling**. *Dev Biol* 2001, **235**(2):388-396.
126. Colwell CS: **Linking neural activity and molecular oscillations in the SCN**. *Nat Rev Neurosci* 2011, **12**(10):553-569.
127. Lee C, Weaver DR, Reppert SM: **Direct association between mouse PERIOD and CKIepsilon is critical for a functioning circadian clock**. *Mol Cell Biol* 2004, **24**(2):584-594.
128. Kategaya LS, Hilliard A, Zhang L, Asara JM, Ptacek LJ, Fu YH: **Casein kinase 1 proteomics reveal prohibitin 2 function in molecular clock**. *PLoS One* 2012, **7**(2):e31987.
129. Aryal RP, Kwak PB, Tamayo AG, Gebert M, Chiu PL, Walz T, Weitz CJ: **Macromolecular Assemblies of the Mammalian Circadian Clock**. *Mol Cell* 2017, **67**(5):770-782 e776.

130. Kim JY, Kwak PB, Gebert M, Duong HA, Weitz CJ: **Purification and analysis of PERIOD protein complexes of the mammalian circadian clock**. *Methods Enzymol* 2015, **551**:197-210.
131. Keesler GA, Camacho F, Guo Y, Virshup D, Mondadori C, Yao Z: **Phosphorylation and destabilization of human period I clock protein by human casein kinase I epsilon**. *Neuroreport* 2000, **11**(5):951-955.
132. Eide EJ, Vielhaber EL, Hinz WA, Virshup DM: **The circadian regulatory proteins BMAL1 and cryptochromes are substrates of casein kinase Iepsilon**. *J Biol Chem* 2002, **277**(19):17248-17254.
133. Shirogane T, Jin J, Ang XL, Harper JW: **SCFbeta-TRCP controls clock-dependent transcription via casein kinase 1-dependent degradation of the mammalian period-1 (Per1) protein**. *J Biol Chem* 2005, **280**(29):26863-26872.
134. Eide EJ, Woolf MF, Kang H, Woolf P, Hurst W, Camacho F, Vielhaber EL, Giovanni A, Virshup DM: **Control of mammalian circadian rhythm by CKIepsilon-regulated proteasome-mediated PER2 degradation**. *Mol Cell Biol* 2005, **25**(7):2795-2807.
135. Partch CL, Green CB, Takahashi JS: **Molecular architecture of the mammalian circadian clock**. *Trends Cell Biol* 2014, **24**(2):90-99.
136. Ralph MR, Menaker M: **A mutation of the circadian system in golden hamsters**. *Science* 1988, **241**(4870):1225-1227.
137. Lowrey PL, Shimomura K, Antoch MP, Yamazaki S, Zemenides PD, Ralph MR, Menaker M, Takahashi JS: **Positional syntenic cloning and functional characterization of the mammalian circadian mutation tau**. *Science* 2000, **288**(5465):483-492.
138. Xu Y, Padiath QS, Shapiro RE, Jones CR, Wu SC, Saigoh N, Saigoh K, Ptacek LJ, Fu YH: **Functional consequences of a CKIdelta mutation causing familial advanced sleep phase syndrome**. *Nature* 2005, **434**(7033):640-644.
139. Toh KL, Jones CR, He Y, Eide EJ, Hinz WA, Virshup DM, Ptacek LJ, Fu YH: **An hPer2 phosphorylation site mutation in familial advanced sleep phase syndrome**. *Science* 2001, **291**(5506):1040-1043.
140. Chen Z, Yoo SH, Park YS, Kim KH, Wei S, Buhr E, Ye ZY, Pan HL, Takahashi JS: **Identification of diverse modulators of central and peripheral circadian clocks by high-throughput chemical screening**. *Proc Natl Acad Sci U S A* 2012, **109**(1):101-106.
141. Meng QJ, Maywood ES, Bechtold DA, Lu WQ, Li J, Gibbs JE, Dupre SM, Chesham JE, Rajamohan F, Knafels J *et al*: **Entrainment of disrupted circadian behavior through inhibition of casein kinase 1 (CK1) enzymes**. *Proc Natl Acad Sci U S A* 2010, **107**(34):15240-15245.
142. Virshup DM, Eide EJ, Forger DB, Gallego M, Harnish EV: **Reversible protein phosphorylation regulates circadian rhythms**. *Cold Spring Harb Symp Quant Biol* 2007, **72**:413-420.
143. Narasimamurthy R, Hunt SR, Lu Y, Fustin JM, Okamura H, Partch CL, Forger DB, Kim JK, Virshup DM: **CK1delta/epsilon protein kinase primes the PER2 circadian phosphoswitch**. *Proc Natl Acad Sci U S A* 2018, **115**(23):5986-5991.
144. Qi ST, Wang ZB, Huang L, Liang LF, Xian YX, Ouyang YC, Hou Y, Sun QY, Wang WH: **Casein kinase 1 (alpha, delta and epsilon) localize at the spindle poles, but may**

not be essential for mammalian oocyte meiotic progression. *Cell Cycle* 2015, **14**(11):1675-1685.
145. Behrend L, Stoter M, Kurth M, Rutter G, Heukeshoven J, Deppert W, Knippschild U: **Interaction of casein kinase 1 delta (CK1delta) with post-Golgi structures, microtubules and the spindle apparatus**. *Eur J Cell Biol* 2000, **79**(4):240-251.
146. Hutchins JR, Toyoda Y, Hegemann B, Poser I, Heriche JK, Sykora MM, Augsburg M, Hudecz O, Buschhorn BA, Bulkescher J *et al*: **Systematic analysis of human protein complexes identifies chromosome segregation proteins**. *Science* 2010, **328**(5978):593-599.
147. Russell P, Nurse P: **Negative regulation of mitosis by wee1+, a gene encoding a protein kinase homolog**. *Cell* 1987, **49**(4):559-567.
148. Coleman TR, Tang Z, Dunphy WG: **Negative regulation of the wee1 protein kinase by direct action of the nim1/cdr1 mitotic inducer**. *Cell* 1993, **72**(6):919-929.
149. Parker LL, Walter SA, Young PG, Piwnica-Worms H: **Phosphorylation and inactivation of the mitotic inhibitor Wee1 by the nim1/cdr1 kinase**. *Nature* 1993, **363**(6431):736-738.
150. Tang Z, Coleman TR, Dunphy WG: **Two distinct mechanisms for negative regulation of the Wee1 protein kinase**. *EMBO J* 1993, **12**(9):3427-3436.
151. Gould KL, Nurse P: **Tyrosine phosphorylation of the fission yeast cdc2+ protein kinase regulates entry into mitosis**. *Nature* 1989, **342**(6245):39-45.
152. Lange BM: **Integration of the centrosome in cell cycle control, stress response and signal transduction pathways**. *Curr Opin Cell Biol* 2002, **14**(1):35-43.
153. Doxsey S, Zimmerman W, Mikule K: **Centrosome control of the cell cycle**. *Trends Cell Biol* 2005, **15**(6):303-311.
154. Kramer A, Mailand N, Lukas C, Syljuasen RG, Wilkinson CJ, Nigg EA, Bartek J, Lukas J: **Centrosome-associated Chk1 prevents premature activation of cyclin-B-Cdk1 kinase**. *Nat Cell Biol* 2004, **6**(9):884-891.
155. Mullee LI, Morrison CG: **Centrosomes in the DNA damage response--the hub outside the centre**. *Chromosome Res* 2016, **24**(1):35-51.
156. Vertii A, Hehnly H, Doxsey S: **The Centrosome, a Multitalented Renaissance Organelle**. *Cold Spring Harb Perspect Biol* 2016, **8**(12).
157. Kasbek C, Yang CH, Yusof AM, Chapman HM, Winey M, Fisk HA: **Preventing the degradation of mps1 at centrosomes is sufficient to cause centrosome reduplication in human cells**. *Mol Biol Cell* 2007, **18**(11):4457-4469.
158. Jackman M, Lindon C, Nigg EA, Pines J: **Active cyclin B1-Cdk1 first appears on centrosomes in prophase**. *Nat Cell Biol* 2003, **5**(2):143-148.
159. Pascreau G, Eckerdt F, Churchill ME, Maller JL: **Discovery of a distinct domain in cyclin A sufficient for centrosomal localization independently of Cdk binding**. *Proc Natl Acad Sci U S A* 2010, **107**(7):2932-2937.
160. Knippschild U, Gocht A, Wolff S, Huber N, Lohler J, Stoter M: **The casein kinase 1 family: participation in multiple cellular processes in eukaryotes**. *Cell Signal* 2005, **17**(6):675-689.
161. Cheong JK, Virshup DM: **Casein kinase 1: Complexity in the family**. *Int J Biochem Cell Biol* 2011, **43**(4):465-469.

162. Cesaro L, Pinna LA: **The generation of phosphoserine stretches in phosphoproteins: mechanism and significance**. *Mol Biosyst* 2015, **11**(10):2666-2679.
163. Babu P, Deschenes RJ, Robinson LC: **Akr1p-dependent palmitoylation of Yck2p yeast casein kinase 1 is necessary and sufficient for plasma membrane targeting**. *J Biol Chem* 2004, **279**(26):27138-27147.
164. Davidson G, Wu W, Shen J, Bilic J, Fenger U, Stannek P, Glinka A, Niehrs C: **Casein kinase 1 gamma couples Wnt receptor activation to cytoplasmic signal transduction**. *Nature* 2005, **438**(7069):867-872.
165. Knippschild U, Kruger M, Richter J, Xu P, Garcia-Reyes B, Peifer C, Halekotte J, Bakulev V, Bischof J: **The CK1 Family: Contribution to Cellular Stress Response and Its Role in Carcinogenesis**. *Front Oncol* 2014, **4**:96.
166. Greer YE, Gao B, Yang Y, Nussenzweig A, Rubin JS: **Lack of Casein Kinase 1 Delta Promotes Genomic Instability - The Accumulation of DNA Damage and Down-Regulation of Checkpoint Kinase 1**. *PLoS One* 2017, **12**(1):e0170903.
167. Hunker CM, Galvis A, Kruk I, Giambini H, Veisaga ML, Barbieri MA: **Rab5-activating protein 6, a novel endosomal protein with a role in endocytosis**. *Biochem Biophys Res Commun* 2006, **340**(3):967-975.
168. Lodhi IJ, Bridges D, Chiang SH, Zhang Y, Cheng A, Geletka LM, Weisman LS, Saltiel AR: **Insulin stimulates phosphatidylinositol 3-phosphate production via the activation of Rab5**. *Mol Biol Cell* 2008, **19**(7):2718-2728.
169. Lodhi IJ, Chiang SH, Chang L, Vollenweider D, Watson RT, Inoue M, Pessin JE, Saltiel AR: **Gapex-5, a Rab31 guanine nucleotide exchange factor that regulates Glut4 trafficking in adipocytes**. *Cell Metab* 2007, **5**(1):59-72.
170. Semerdjieva S, Shortt B, Maxwell E, Singh S, Fonarev P, Hansen J, Schiavo G, Grant BD, Smythe E: **Coordinated regulation of AP2 uncoating from clathrin-coated vesicles by rab5 and hRME-6**. *J Cell Biol* 2008, **183**(3):499-511.
171. Sato M, Sato K, Fonarev P, Huang CJ, Liou W, Grant BD: **Caenorhabditis elegans RME-6 is a novel regulator of RAB-5 at the clathrin-coated pit**. *Nat Cell Biol* 2005, **7**(6):559-569.
172. Collinet C, Stoter M, Bradshaw CR, Samusik N, Rink JC, Kenski D, Habermann B, Buchholz F, Henschel R, Mueller MS *et al*: **Systems survey of endocytosis by multiparametric image analysis**. *Nature* 2010, **464**(7286):243-249.
173. Hermle T, Schneider R, Schapiro D, Braun DA, van der Ven AT, Warejko JK, Daga A, Widmeier E, Nakayama M, Jobst-Schwan T *et al*: **GAPVD1 and ANKFY1 Mutations Implicate RAB5 Regulation in Nephrotic Syndrome**. *J Am Soc Nephrol* 2018, **29**(8):2123-2138.
174. Ma H, McLean JR, Gould KL, McCollum D: **An efficient fluorescent protein-based multifunctional affinity purification approach in mammalian cells**. *Methods Mol Biol* 2014, **1177**:175-191.
175. Shaner NC, Lambert GG, Chammas A, Ni Y, Cranfill PJ, Baird MA, Sell BR, Allen JR, Day RN, Israelsson M *et al*: **A bright monomeric green fluorescent protein derived from Branchiostoma lanceolatum**. *Nat Methods* 2013, **10**(5):407-409.
176. Milne DM, Looby P, Meek DW: **Catalytic activity of protein kinase CK1 delta (casein kinase 1delta) is essential for its normal subcellular localization**. *Exp Cell Res* 2001, **263**(1):43-54.

177. Zybailov B, Mosley AL, Sardiu ME, Coleman MK, Florens L, Washburn MP: **Statistical analysis of membrane proteome expression changes in Saccharomyces cerevisiae**. *J Proteome Res* 2006, **5**(9):2339-2347.
178. Jiang J: **CK1 in Developmental Signaling: Hedgehog and Wnt**. *Curr Top Dev Biol* 2017, **123**:303-329.
179. Sillibourne JE, Milne DM, Takahashi M, Ono Y, Meek DW: **Centrosomal anchoring of the protein kinase CK1delta mediated by attachment to the large, coiled-coil scaffolding protein CG-NAP/AKAP450**. *J Mol Biol* 2002, **322**(4):785-797.
180. Hegemann B, Hutchins JR, Hudecz O, Novatchkova M, Rameseder J, Sykora MM, Liu S, Mazanek M, Lenart P, Heriche JK *et al*: **Systematic phosphorylation analysis of human mitotic protein complexes**. *Sci Signal* 2011, **4**(198):rs12.
181. Dephoure N, Zhou C, Villen J, Beausoleil SA, Bakalarski CE, Elledge SJ, Gygi SP: **A quantitative atlas of mitotic phosphorylation**. *Proc Natl Acad Sci U S A* 2008, **105**(31):10762-10767.
182. Olsen JV, Vermeulen M, Santamaria A, Kumar C, Miller ML, Jensen LJ, Gnad F, Cox J, Jensen TS, Nigg EA *et al*: **Quantitative phosphoproteomics reveals widespread full phosphorylation site occupancy during mitosis**. *Sci Signal* 2010, **3**(104):ra3.
183. Zhou H, Di Palma S, Preisinger C, Peng M, Polat AN, Heck AJ, Mohammed S: **Toward a comprehensive characterization of a human cancer cell phosphoproteome**. *J Proteome Res* 2013, **12**(1):260-271.
184. Venerando A, Ruzzene M, Pinna LA: **Casein kinase: the triple meaning of a misnomer**. *Biochem J* 2014, **460**(2):141-156.
185. Kettenbach AN, Schweppe DK, Faherty BK, Pechenick D, Pletnev AA, Gerber SA: **Quantitative phosphoproteomics identifies substrates and functional modules of Aurora and Polo-like kinase activities in mitotic cells**. *Sci Signal* 2011, **4**(179):rs5.
186. Franchin C, Cesaro L, Salvi M, Millioni R, Iori E, Cifani P, James P, Arrigoni G, Pinna L: **Quantitative analysis of a phosphoproteome readily altered by the protein kinase CK2 inhibitor quinalizarin in HEK-293T cells**. *Biochim Biophys Acta* 2015, **1854**(6):609-623.
187. Elkin SR, Bendris N, Reis CR, Zhou Y, Xie Y, Huffman KE, Minna JD, Schmid SL: **A systematic analysis reveals heterogeneous changes in the endocytic activities of cancer cells**. *Cancer Res* 2015, **75**(21):4640-4650.
188. Lerit DA, Poulton JS: **Centrosomes are multifunctional regulators of genome stability**. *Chromosome Res* 2016, **24**(1):5-17.
189. Prosser SL, Pelletier L: **Mitotic spindle assembly in animal cells: a fine balancing act**. *Nat Rev Mol Cell Biol* 2017, **18**(3):187-201.
190. Ran FA, Hsu PD, Wright J, Agarwala V, Scott DA, Zhang F: **Genome engineering using the CRISPR-Cas9 system**. *Nat Protoc* 2013, **8**(11):2281-2308.
191. Schindelin J, Arganda-Carreras I, Frise E, Kaynig V, Longair M, Pietzsch T, Preibisch S, Rueden C, Saalfeld S, Schmid B *et al*: **Fiji: an open-source platform for biological-image analysis**. *Nat Methods* 2012, **9**(7):676-682.